ASSESSMENT OF EROSION AND SEDIMENTATION IN CHITE WATERSHED, MIZORAM

A THESIS SUBMITTED IN PARTIAL FULFILLMENT OF THE REQUIREMENTS FOR THE DEGREE OF DOCTOR OF PHILOSOPHY

PC. LALRINDIKA

MZU REGISTRATION NO.: 1074 OF 2006-07

PH.D. REGISTRATION NO: MZU/Ph.D./1204 of 27.08.2018

DEPARTMENT OF GEOGRAPHY AND RESOURCE MANAGEMENT

SCHOOL OF EARTH SCIENCE AND NATURAL RESOURCE MANAGEMENT

APRIL, 2024

ASSESSMENT OF EROSION AND SEDIMENTATION IN CHITE WATERSHED, MIZORAM

BY

PC. LALRINDIKA

DEPARTMENT OF GEOGRAPHY AND RESOURCE MANAGEMENT

SUPERVISOR

PROF. P. RINAWMA

JOINT SUPERVISOR

DR. R. ZONUNSANGA

SUBMITTED

IN PARTIAL FULFILLMENT OF THE REQUIREMENT OF THE DEGREE OF DOCTOR OF PHILOSOPHY IN GEOGRAPHY OF MIZORAM UNIVERSITY, AIZAWL.

DEPARTMENT OF GEOGRAPHY AND RESOURE MANAGEMENT
MIZORAM UNIVERSITY - 796004

Prof. P. Rinawma

Post Box No. 190
Gram: MZU

Phone: 0389-2331604 (O)
: 0389-2331613 (O)
Mobile: 9436155803
Email: rinawma@yahoo.co.in

CERTIFICATE

This is to certify that the thesis entitled "**Assessment of Erosion and Sedimentation in Chite Watershed, Mizoram**", submitted by PC. Lalrindika, under Registration No: MZU/Ph.D./1204 of 27.08.2018, embodies the record of the original research endeavour carried out by him under my supervision. He has been duly registered and has fulfilled all the requirements laid down in the Ph.D. regulations of Mizoram University. I further certify that the thesis presented is worthy of being considered for the award of the Ph.D. degree. This research has not been submitted for the attainment of any research degree at any other university.

Place: Aizawl

Date:

(PROF. P. RINAWMA)

Supervisor

(DR. R. ZONUNSANGA)

Joint Supervisor

MIZORAM UNIVERSITY

APRIL 2024

DECLARATION

I, PC. Lalrindika, hereby declare that the subject matter of this thesis is the record of work done by me, that the contents of this thesis did not form basis of the award of any previous degree to me or to do the best of my knowledge to anybody else, and that the thesis has not been submitted by me for any research degree in any other University/Institute.

This is being submitted to the Mizoram University for the degree of Doctor of Philosophy in Geography and Resource Management.

(PC. LALRINDIKA)

Candidate

(PROF. CH. UDAYA BHASKARARAO)

Head

(PROF. P. RINAWMA)

Supervisor

ACKNOWLEDGEMENT

First and foremost, I would like to thank almighty God for the guidance and blessings that have enabled me to successfully complete this research work.

I would like to express my deepest gratitude to my Supervisor, Professor P. Rinawma, Professor, Department of Geography and Resource Management, Mizoram University, and my Joint Supervisor Dr. R. Zonunsanga, Centre for Disaster Management, Mizoram University, for their unwavering support, guidance, and mentorship throughout my research journey. Their expertise, patience, and dedication have been invaluable in shaping the outcome of this research.

I wholeheartedly acknowledge the University Grant Commission (UGC) for providing financial assistance through UGC NET-JRF and SRF fellowship during the course of my research work.

I am also indebted to all the faculty and staff of the Department of Geography and Resource Management, Mizoram University, for their assistance and cooperation.

I am deeply grateful to the dedicated laboratory technicians at the State Soil Testing Laboratory, Department of Agriculture, Government of Mizoram, for their invaluable contribution to my research. I am also thankful to Irene Lalnipari Sellate, Research Scholar, Department of Environmental Science, Mizoram University, who guided me in collecting and handling soil data. Their expertise and commitment in soil sample collection and testing the soil samples were pivotal in ensuring the quality and accuracy of the data presented in this thesis.

I extend my sincere appreciation to the State Meteorological Centre, Directorate of Science & Technology, Government of Mizoram, HQ CE (P) Pushpak, Aizawl, and BDO Office, Thingsulthliah, for their invaluable support in providing essential rainfall data for my research. Their contribution has been a valuable asset in understanding the potential impact of rainfall on soil erosion along with the regional variations and trends in rainfall patterns.

I would also like to acknowledge the invaluable assistance and camaraderie of my fellow research scholars. In particular, I would like to mention Dr. Vanlaltanpuia, Assistant Professor, Government Aizawl North College, whose presence significantly enhanced the quality of my academic journey, making it both fulfilling and delightful.

I extend my appreciation to all my friends, especially Saurabh Kumar Sarma, Lalrinmawia, K. Lalruatfela, Ramsiamthara Fanai, Laldinhlua, Lalnunsiama, Lalthanpuia, PC. Lalfakzuala, Lalhriatpuia and others who generously volunteered their time for my extended field surveys and data collection, without whom this study would not have been possible.

I owe a profound debt of gratitude to my parents, P.C. Vanlalhruaia, and Vanlalruali, for instilling the values of perseverance and the importance of education. Your sacrifices and belief in my abilities have been the driving force behind my pursuit of knowledge. To my beloved wife, H. Lalbiakdiki, your unwavering encouragement, understanding, and sacrifices have been the pillars of strength that sustained me during the long hours and demanding schedules of this journey. And to my precious daughter, P.C. Lallawmkimi, who has been my constant motivation and inspiration that helps me to keep pushing forward. I would like to extend my heartfelt appreciation to my brothers, Lalchhandama Pachuau and PC. Vanlalfinga, for their unwavering support and continuous encouragement which have been a source of motivation and strength.

This thesis is a culmination of the efforts and support of many, and I am grateful for each one of you who has played a part in this endeavour.

(PC. LALRINDIKA)

Research Scholar

CONTENTS

List of Figures

List of Tables

List of Plates

Abbreviations

º	Degree
º C	Degree Celsius
%	Percentage
θ	Slope in degrees
a	Area accumulation
a	Soil structure index
a/A	Relative area
A	Drainage basin area in km^2
A	Gross soil erosion
A_s	Upslope contributing area
AHP	Analytical Hierarchy Process
AUC	Area under the ROC curve
b	Soil permeability index
BDO	Block Development Officer
C	Cover management factor
CER	Classified soil erosion rate
CI	Consistency Index
CR	Consistency ratio
C_V	Compound Value
DD	Drainage density
DFS	Distance from streams
EI	Erosion Index
ELE	Elevation
ES	Erosion susceptibility
Et al.	et alia
Etc.	et cetera
ETI	Erosion Tolerance Index
ESA	European Space Agency
EVUs	Erosion Vulnerability Units

Fig	Figure
FP	False positives
GE	Gross Erosion calculated by the RUSLE model
GIS	Geographic Information System
GPS	Global Positioning System
GSI	Geological Survey of India
h	Cumulative elevation range
h/H	Relative height
Ha	Hectare
Hc	Hypsometric curve
Hi	Hypsometric integral
HQ CE (P)	Headquarter of Chief Engineer (Project)
HQP	Headquarter of Chief Engineer (Project)
IDW	Inverse Distance Weighted
IBM SPSS	International Business Machines Corporation, Statistical Package for the Social Sciences
IMD	Indian Meteorological Department
IRDAS	Institute of Resource Development and Social Management
K	Soil erodibility factor
km^2	Square kilometre
km/km^2	Kilometre per square kilometre
LD	Lineament density
LIT	Lithology
LR	Logistic Regression
LS	Slope length and steepness factor
LULC	Land use/land cover
LW	Larger watershed
M	Meters
Mm	Millimetre
M	Soil particle size parameter

MASL	Mean annual soil loss
Max	Maximum
MCDM	Multi-criteria decision-making
Mg h^{-1} y^{-1}	Megagram per hectare per year
M ha	Million hectares
Min	Minimum
MJ.mm/ha^{-1}.h^{-1}.$year^{-1}$	Megajoule millimetre per hectare per hour per year
MLC	Maximum Likelihood Classification
MSL	Mean sea level
NDVI	Normalized Difference Vegetation Index
NGOs	Non-Governmental Organizations
NIR	Near-Infrared Band
O	Organic Matter
P	Support practice factor
Pow	Map algebra expression for Power in the raster calculator
R	Rainfall erosivity factor
R	Red Band of the Sentinel-2 image
RCMs	Regional climate models
RI	Rainfall Intensity
RI	Random Index
ROC	Receiver operating characteristics curves
RS	Remote Sensing
RUSLE	Revised Universal Soil Loss Equation
SAC, ISRO	Space Application Centre, Indian Space Research Organization
SATEEC	Sediment Assessment Tool for Effective Erosion Control
SCS-CN	Soil Conservation Service – Curve Number
SD	Standard deviation
SDR	Sediment Delivery Ratio

SESI	Soil Erosion Susceptibility Index
SLP	Slope
SMC	State Meteorological Centre
SOI	Survey of India
SRTM-DEM	Shuttle Radar Topography Mission Digital Elevation Model
ST	Soil Texture
SW	Smaller watershed
SW	Sub-watershed
SWAT	Soil and Water Assessment Tool
SY	Sediment Yield
SYI	Sediment Yield Index
T	Soil loss tolerance limits
T1	Soil formation rate
T2	Soil sustainability
T3	Soil conservation management
TBDO	Thingsulthliah Block Development Office
TN	True negative
TOL	Tolerance
tons ha^{-1} yr^{-1}	Tons per hectare per year
tons.ha.h.ha^{-1}.MJ^{-1}.mm^{-1}	Metric ton per hectare per hour per hectare per Megajoule per millimetre
tons $year^{-1}$	Tons per year
USDA-NRCS	United States Department of Agriculture, Natural Resources Conservation Service
USGS	United States Geological Survey
USLE	Universal Soil Loss Equation
UTM	Universal Transverse Mercator
VIF	Variance inflation factors
Viz.	Namely
Yr	Year

CHAPTER-1

INTRODUCTION

1.1 Introduction

Soil erosion and sedimentation are recently considered as one of the most significant threats among various environmental problems around the world (Xiaoqing, 2003). Soil erosion occurs naturally when soil or other materials are removed, transported, and deposited elsewhere by various agents like water, wind, and glacier (Lal, 2001). These are termed geological erosion as they are influenced by physical factors like climate, vegetation, terrain, soil properties, etc., and do not pose any remarkable threat to human beings. However, human activities such as deforestation, unsustainable agricultural practice, rapid development of settlements, transport infrastructure, etc., may significantly increase the rate of soil erosion. Such conditions are called accelerated erosion, which may exert both on-site and off-site consequences. The on-site effect refers to the extensive removal of valuable topsoil and vital soil nutrients in situ. Essential soil nutrient like nitrogen, phosphorus, potassium, calcium, and soil organic matter are carried away by erosion (Pimentel, 2006), thus leading to land degradation.

On the other hand, the off-site impact mainly arises from sedimentation downstream. Soil removed from the upper catchments is deposited in the downstream parts of the river. It gives rise to numerous problems, among which sedimentation of reservoirs downstream is reported to be the most prominent (Kothyari, 1996). This has remarkably reduced the reservoir's water storage and hydroelectric power generating capacity. Moreover, sedimentation in the streams has also disrupted the riverine ecosystem and its recreational value, depleting water quality and enhancing the chances of floods (Gelagay, 2016). Hence, sedimentation is the consequence of accelerated soil erosion on the hillslopes, and an increase or decrease in the amount of soil loss will consequently influence the amount of sedimentation in a drainage basin (Toy et al., 2002; Biswas and Pani, 2015; Dewanjan & Ahmad 2020).

Soil erosion is a common problem faced by agricultural land in the tropical and semi-arid regions of the world and is a critical concern for many developing nations in Asia, Africa, and South America (Morgan, 2005; Thapa and Weber, 1991). In a humid subtropical region, India's location renders water erosion a major issue to productive topsoil and landform deformation (Rajbanshi and Bhattacharya, 2020; Bhattacharyya et al., 2015). In addition, the rugged mountainous terrain of these humid climatic zones undergoes significant soil removal (Markose and Jayappa, 2016). The Space Application Centre, Indian Space Research Organization (ISRO) has recently reported that about 97.85 million hectares (M ha) of land areas, constituting 29.77% of the total geographical area of India has experienced land degradation in which water-induced soil erosion occurring on 36.20 M ha of land is the most significant forms (SAC, 2021). Each year, a predicted amount of 5334 million tons of soil is removed by water erosion at an average soil erosion rate of 16.35 tons ha^{-1} yr^{-1}, where 61% of the total sediments detached from the land areas are displaced from their original place, 29% are delivered into the sea, and the remaining 10% are deposited in reservoirs which rapidly reduce the storage capacity. As the country's economy is primarily based on agriculture, the intensified soil erosion rate has been a major setback for the agricultural sector and the reservoirs located around the country are rapidly depleted by the subsequent sediments deposition which are produced from the upper catchments (Narayana and Babu, 1983; Ganasri and Ramesh, 2015).

Water erosion is identically the most significant form of land degradation in the northeastern parts of the country. As the region is characterized by a fragile environmental setup such as rugged hilly terrain, steep slope, abundant supply of rainfall, weak geology, high seismicity, high drainage density, etc., it is highly vulnerable to soil erosion and has promoted a considerable amount of sediment flux from various watershed each year (Mandal and Sharda, 2011; Ahmed and Srinivasa, 2015). Moreover, the vulnerability of the region has been aggravated by the modification of the natural environment through several human activities like the age-old unscientific practice of shifting cultivation on steep slopes, intensive deforestation, urbanization, rapid developmental works like road construction, settlement, mining, quarrying, etc., (Kothyari, 1996). Nevertheless, most of the research studies concurred

that forest degradation constitutes a significant factor contributing to widespread occurrences of soil erosion, removing huge amount of sediment in the northeastern region (Choudhury et al., 2022). In the region, the practice of shifting cultivation and large-scale deforestation has a massive impact on soil health, leading to an enormous loss of 200 tons ha^{-1} yr^{-1}, in which shifting cultivation alone resulted to a mean erosion rate of about 30.2 to 170.2 tons ha^{-1} yr^{-1} (Saha et al., 2012). Furthermore, shifting cultivation has led to severe erosion of about 30 lakh hectares of land, actively promoting heavy sediment loads in the river basins (Narayana and Babu, 1983). Thus, the massive eradication of forest areas and its utilization for shifting cultivation on steep slopes are the significant factors of soil loss, rapidly reducing soil fertility and the deposition of large quantities of sediments in the waterbodies located downstream, developing an imbalanced ecosystem in the region.

Among the northeastern states, Mizoram has been reported to have experienced a more severe water-induced land degradation as the total degraded land accounts for about 34.92% of its total geographical area with an erosion rate accounting to about 10 to 20 tons ha^{-1} yr^{-1} (Choudhury et al., 2022). The Institute of Resource Development and Social Management (IRDAS) reported that 12 watersheds out of 22 watersheds in the entire state of Mizoram have experienced critical problems of soil erosion and land degradation, which further increases run-off rates, resulting in a tremendous amount of sediment yield (IRDAS, 1994; Tiwari and Jha, 1997). Rapid rate of soil erosion and increasing sediment production rate are mainly attributed to the traditional practice of shifting cultivation and the associated clearing of natural vegetation in this vulnerable environmental setup (Zonunsanga and Rao, 2013). Under this conventional form of cultivation, the reduction of time allotted for a fallow duration, which recently lasts for a period of only 1 to 2 years from the past fallowing custom of about 15 to 20 years, has been reported to be the significant reason for inducing accelerated erosion and soil loss (Choudhury et al., 2022; Grogan et al., 2012). Nevertheless, forests conversion into croplands in shifting cultivation and its subsequent burning have also significantly depleted the organic carbon (OC) storage in the soil, which considerably reduced both the fertility and productivity of soil. (Sahoo et al., 2019).

1.2 Statement of the problem

Soil erosion and sedimentation continue to be widespread and significant problems within sustainable land management, water resource planning, and environmental security in the mountainous regions of Mizoram. Despite the apparent repercussions, there has been a lack of adequate research dedicated to conducting comprehensive studies on these phenomena. Therefore, a precise and timely assessment is crucial for better understanding their spatial extension and magnitude to develop effective erosion control measures and sustainable natural resource management.

The conventional methods of determining soil erosion rate and sedimentation in a watershed include field surveys and field measurements based on experimental plots, as well as acquiring run-off and sediment data from stream gauging stations, which require a lot of equipment, capital, time, labour and have limitations in terms of spatial representation for dynamic environments in a wide area (Lu et al., 2004; Pradeep et al., 2015; Ganasri and Ramesh, 2015; Kucuker and Giraldo, 2022). Moreover, actual field measurements are exceptional to mountainous and agricultural land throughout the country, and recorded data for run-off, and sediment flux is not readily available at the watershed level since most of the river basins are still ungauged (Prasannakumar et al., 2012; Rajbhanshi and Bhattacharya, 2020). Due to these limitations, it is difficult to comprehensively evaluate the complex spatial patterns, varying magnitude, and temporal dynamics of soil erosion processes within a watershed (Vijith et al., 2012; Bhat et al., 2017; Kalambukattu and Kumar, 2017). Considering the absence of extensive studies in the region and lack of secondary data, coupled with limitations of conventional methods to comprehend this complex phenomenon, the purpose of the present study is to fill this knowledge gap, generating synoptic information through the application of geospatial technology-based modeling in a watershed.

1.3 Research objectives

The present study was undertaken in the Chite watershed, Mizoram, to develop a systematic framework for assessing soil erosion and sedimentation by applying comprehensive modelling approaches based on remote sensing and Geographic Information System (GIS) techniques. The study aims to achieve the following specific objectives:

1.3.1. To identify the spatial pattern of soil erosion susceptibility.

1.3.2. To evaluate soil erosion rate and soil loss.

1.3.3 To determine the area above the soil loss tolerance limits.

1.3.4 To estimate the amount of sediment yield.

1.3.5 To prioritize critical areas for sustainable watershed management.

1.4 Significance of the study

The research being undertaken encompasses significant implications for sustainable watershed management, soil erosion control and environmental conservation. Recently, the advanced technique of remote sensing and GIS has gained universal approval as a dominant tool for ecological hazard assessment and for developing effective resource conservation and management strategies (Pham et al., 2018; Sujatha and Sridhar, 2018; Halefom and Teshome, 2019; Makaya et al., 2019; Rashid et al., 2020). This advancement in geoinformatics has also successfully ensured an adequate manifestation and modeling of various earth phenomena (Anbazhagan et al. 2011). With remote sensing and GIS technique-based modeling approaches, the present study attempts to assess soil erosion comprehensively. Moreover, this study was intended to provide reliable, cost-effective, and spatially explicit information on erosion and sedimentation in a watershed. This valuable insight into the complex processes and problems will be helpful for sustainable watershed management that focuses on the formulation of feasible erosion and sediment mitigation plans, strategic land use planning, and appropriate land and water management policies.

In addition, this research will showcase the potential advantages of remote sensing and GIS techniques regarding the problems associated with assessing accelerated erosion rate in a hilly watershed. By demonstrating the reliability and applicability of these technologies, this study can help promote wider adoption of geospatial modelling techniques and their practical implications for monitoring and analyzing soil erosion along with its on-site and off-site consequences in the future. Consequently, this will result in a better understanding and improved application of environmental management practices at a watershed scale.

1.5 Scope and Limitations

The most feasible micro-level planning region, i.e., a watershed, has been selected for assessing soil erosion and sedimentation in this research. This study integrated several modeling approaches with extensive field investigations and laboratory analysis data. Various factors that influence soil erosion such as topography, climate, soil properties, land use/land cover, vegetation cover, etc., and their multifaceted interactions are considered through various soil erosion modelling approaches. Besides these, the study will also reflect the selection of different remote sensing data along with their necessary pre-processing works, enhancing the development of a geospatial modelling framework and algorithms for evaluating the spatial pattern of erosion susceptibility, soil loss, soil loss tolerance, and the rate of sediment flux in the study area. Moreover, the comprehensive information generated from various analyses will be integrated for watershed prioritization, identifying critically sensitive areas, which can further enhance the implementation of erosion control and natural resource management measures.

However, certain limitations in this study need to be acknowledged. Validation of soil loss and sediment yield is impossible from field-recorded data as the Chite watershed is an ungauged basin and lacks field-based erosion measurements. The rainfall data are pretty limited in terms of spatial and temporal dimensions. Findings of soil textual analysis may have lower precision as it was done solely based on the procedures of standard manuals without any prior knowledge or expertise. The satellite

imageries are all obtained from an open-source data portal, so the resolutions are not the most desirable. Collection of soil samples at their absolute location was impossible for all the pre-determined sites due to the absence of a road network, steep terrain, and built-up surfaces in settlement areas. Furthermore, many ongoing and scheduled field investigations were terminated for quite a long time due to the outbreak of COVID-19. Despite all these shortcomings, efforts were made to ensure a robust and reliable methodology for the present research work.

1.6 Organization of the Thesis

The whole thesis has been structured into eight chapters to give a coherent framework for the research. Firstly, Chapter 1 presents an introduction, establishing a quick overview of the contextual information, statement of the problem, research objectives, significance of the study, and scope and limitations of the present research work. Chapter 2 provides the study area's various physical and environmental settings, including elevation, slope, hypsometry, geology, geomorphology, drainage, climate, and vegetation. Chapter 3 deals with a comprehensive review of relevant literature from various international, national and regional levels. The detailed research methodology comprising data collection, pre-processing procedures, and preparation of a geospatial modeling framework is described in Chapter 4. Chapter 5 concerns soil erosion susceptibility mapping based on the Analytical Hierarchy Process (AHP) integrated with remote sensing and GIS techniques. Chapter 6 focuses on estimating soil loss and sediment yield using the Revised Universal Soil Loss Equation (RUSLE) model and the Sediment Delivery Ratio (SDR) approach, respectively. Chapter 7 is concerned with prioritizing watersheds to enhance implementation of resource conservation measures and management strategies for soil erosion and sedimentation in the watershed. Lastly, Chapter 8 presents conclusions and recommendations drawn from the research findings.

CHAPTER-2

PHYSICAL AND ENVIRONMENTAL SETTINGS

2.1 Study Area

The Chite Watershed is located in Aizawl District, encompassing a significant portion of the eastern slopes of Aizawl City, specifically in the upper catchment area. It is probably the most urbanized watershed in the state, as Aizawl comprise about one-third of its population. Geographically, the watershed is located between 23º38'29" to 23º45'24" N latitudes and 92º42'54" to 92º47'15" E longitudes (Fig. 2.1). The watershed extends in a North-South direction, covering approximately 52.16 km^2 of land area. The region embraced parts of the Survey of India (SOI) Topographical sheets No. 84A/9, 84A/10 and 84A/14. The study area represents a sub-watershed within the larger Tuirial watershed, which ranked 7^{th} in the severity of soil erosion and land degradation among the 22 Mizoram watersheds. It is also identified as a high-priority zone concerning sediment yield and run-off (IRDAS, 1994; Tiwari and Jha, 1997).

The Chite River holds significance as a vital tributary stream to the Tuirial (Sonai) River in the upper course. Emerging near Bawngkawn in the northern parts of Aizawl, the river originates at an altitude of roughly 875 meters above mean sea level (MSL). Flowing in a North-South direction, the Chite river covers a distance of about 13.68 km. As the river represents the upper course of a larger river system, it has shaped various distinctive features commonly found in the youthful stage of a stream, such as rapids, waterfalls, gorges, V-shaped valleys, etc.

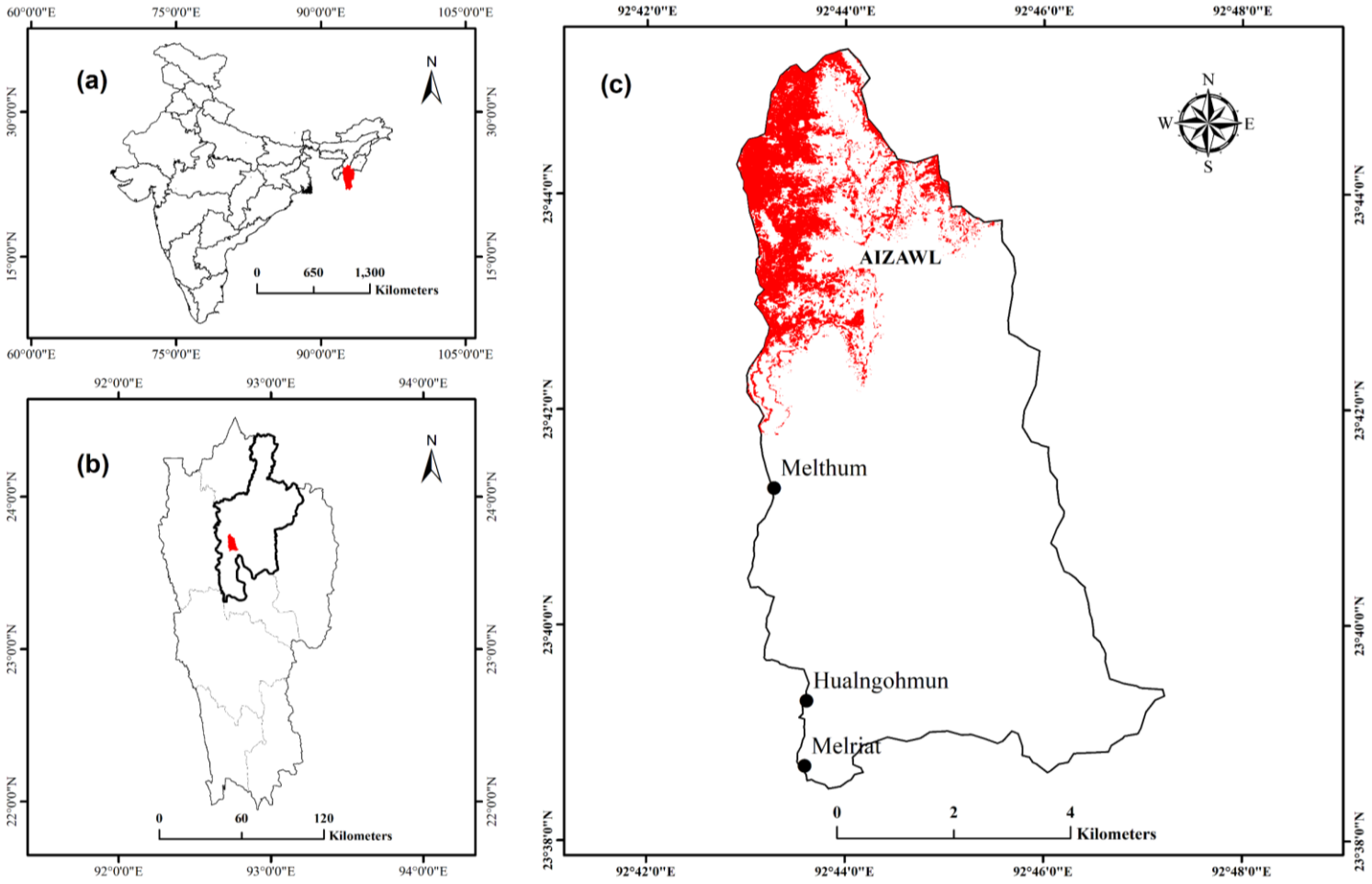

Fig 2.1: Location map of the study area (a) India, (b) Mizoram and (c) Chite watershed.

2.2 Elevation

Elevation represents the height of land with respect to mean sea level. Generally, higher elevation suggests more significant run-off and less infiltration (Vijith and Dodge Wan, 2019). Thus, there will be an increase in chances of soil erosion in areas where elevation is higher (Aslam et al., 2021). As the study area has a mountainous terrain, the highest point within the watershed is 1239 metres, located in the northern part, while the lowest elevation of about 172 meters can be found at the mouth of Chite river in the southeastern parts (Fig. 2.2). There is a noticeable overall pattern of increasing elevation as one moves from the southern sections of the watershed towards the northern areas.

The elevation of the study is classified into five categories as shown in Table 2.1. Elevations up to 300 meters are considered very low and are found in the lower sections of the river valley. It covers an area of approximately 1.23 km^2, which accounts for about 2.35% of the total area. Elevations ranging from 300 to 500 meters are regarded as low class and occupies 10.17 km^2, making up 19.50% of the study area. The moderate class extends from 500 to 700 meters and covers 16.68 km^2, the most extensive spatial coverage, representing 31.97% of the total geographical area. The high class includes elevations extending between 700 and 900 meters and is found along almost all corners of the watershed, covering 16.48 km^2 of land area, constituting 31.58% of the whole area. Elevations above 900 meters are categorized as very high. They are predominantly situated along the watershed's northern, northeastern, and northwestern ridges, encompassing an area of 7.62 km^2, corresponding to 14.60% of the total watershed area.

Table 2.1: Elevation of Chite watershed.

Class	Elevation in metres	Area in km^2	Area in %
Very low	< 300	1.23	2.36
Low	300 - 500	10.17	19.49
Moderate	500 - 700	16.68	31.98
High	700 - 900	16.46	31.56
Very high	> 900	7.62	14.61
Total		52.16	100

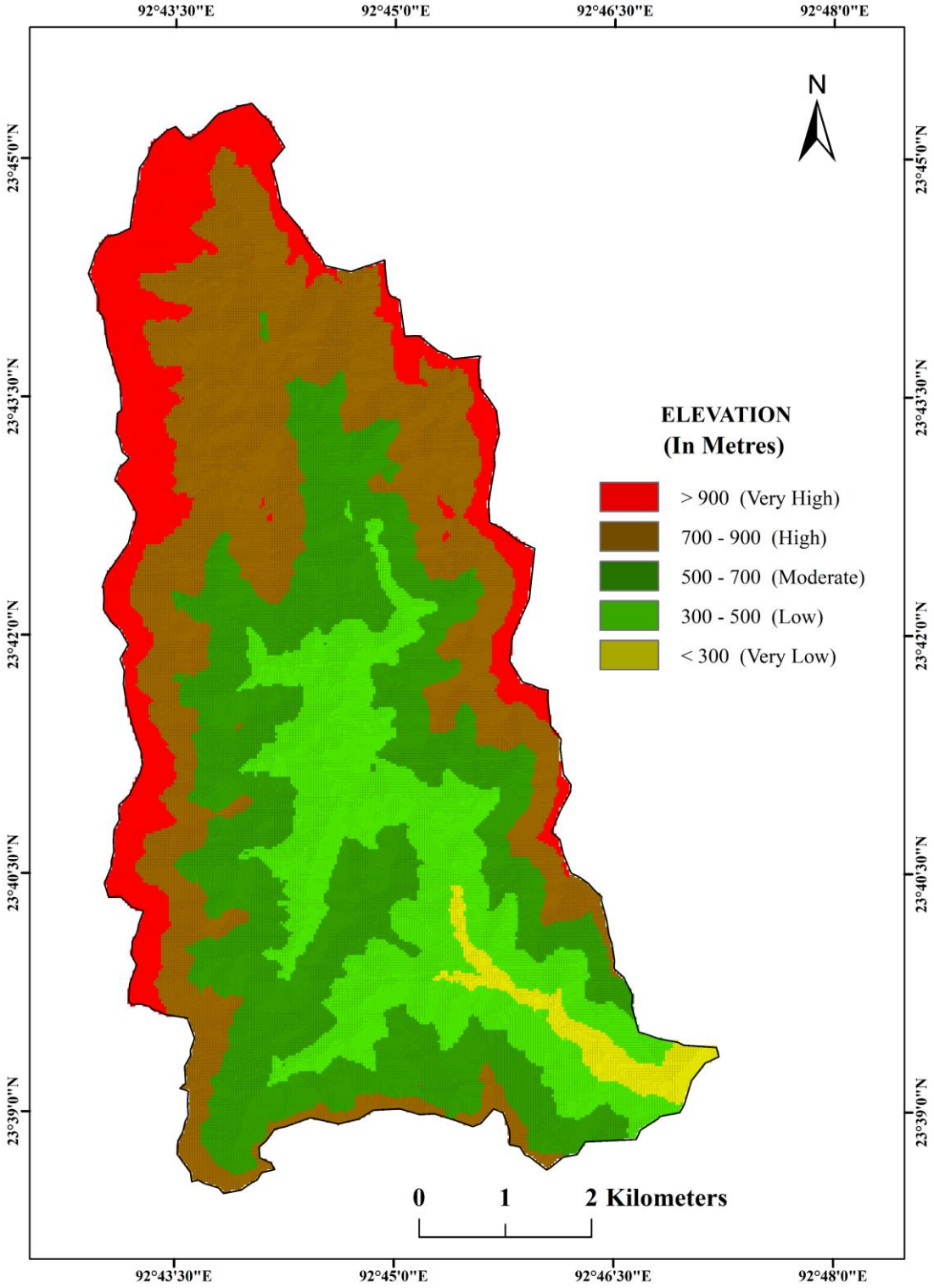

Fig 2.2: Elevation map of Chite watershed.

2.3 Slope

Slope refers to the angle formed between any parts of the earth's surface in relation to the horizontal datum (Sharma and Singh, 2017). It is the most significant derivative of elevation, which measures the extent of elevation change or inclination of the land's surface, and the slope steepness is expressed in degrees or percentages. The slope of the study area is measured in degree, which is the arc tangent of the ratio of rise over run (Chang, 2018). The increase in the steepness of the slope has a corresponding influence on the amount and velocity of run-off and infiltration rate, thus controlling the amount of soil loss, which might be doubled for every four times increase in the slope (Garde, 2006; Tideman, 1996).

The slope of Chite watershed has been categorized into five distinct classes based on their steepness (Fig 2.3). These classes, including very low, low, moderate, high, and very high, are assigned to specific slope degrees: less than 15º, 15º to 25º, 25º to 35º, 35º to 45º degrees, and greater than 45º, respectively (Table 2.2). The very low class encompasses an area of 9.77 km^2, accounting for approximately 18.73% of the total area. These slopes are predominantly observed in the middle and upper parts of the river valley. The low class and moderate class are primarily located adjacent to the very low class, on the lower part of the foothills, covering an area of approximately 17.42 km^2 and 17.37 km^2, respectively. The low-class slopes constitute the most considerable portion, representing 33.40% of the watershed. The very high-class slopes, characterized by an inclination greater than 45 degrees, are mostly found below the high hill ridges and occupy the smallest area, measuring only 0.97 km^2, corresponding to 1.86% of the study area.

Table 2.2: Slope of Chite watershed.

Class	Slope in (Degrees)	Area in km^2	Area in %
Very low	< 15º	9.77	18.73
Low	15º - 25º	17.42	33.40
Moderate	25º - 35º	17.37	33.30
High	35º - 45º	6.63	12.71
Very high	> 45º	0.97	1.86
Total		52.16	100

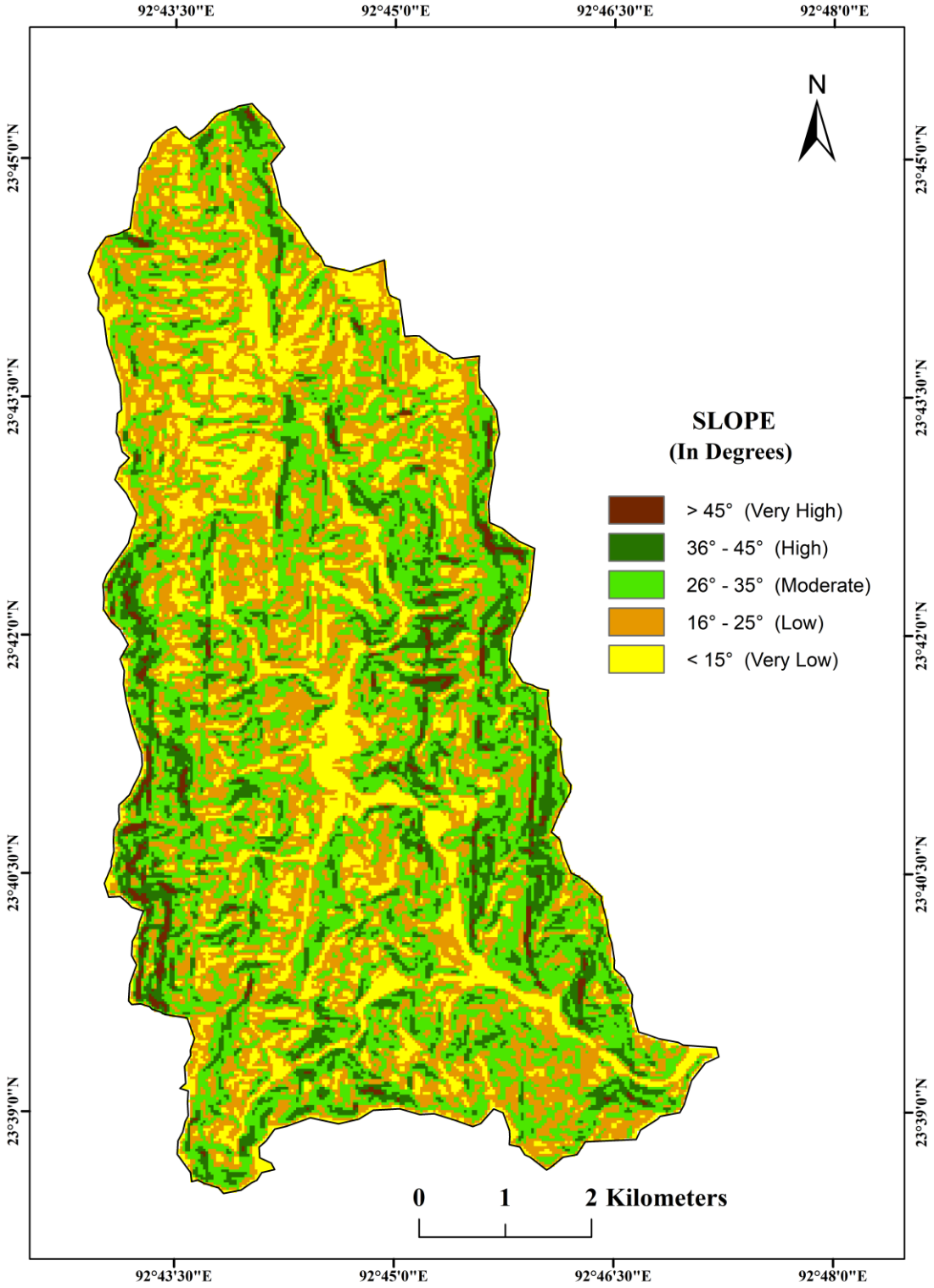

Fig 2.3: Slope map of Chite watershed.

2.4 Hypsometric analysis

Hypsometric analysis plays a significant role in predicting soil erosion and sedimentation processes within the field of study (Strahler, 1952). Langbein et al. (1947) initially introduced this concept, which was further expanded upon by Strahler (1952) to assess the extent of landform dissection and developmental stages by examining the correlation between a basin's elevation and its corresponding area. By employing graphical representations such as the Hypsometric curve (Hc) and a dimensionless quantitative value known as the Hypsometric integral (Hi), the erosional condition of a river basin can be effectively communicated through hypsometric analysis (Ritter et al., 2002).

Strahler (1952) provided an interpretation of hypsometric curves (Hc) and hypsometric integral (Hi) based on their distinctive shapes and values. An upward curve with a convex shape with HI $\geq$ 0.60 signifies a youthful stage of landform development where rapid erosional processes predominate, while an S-shaped curve with concave higher elevations and convex lower elevations of Hi between 0.35 – 0.60 represents landforms in a mature stage with an equilibrium state of landforms development. Conversely, a downward concave-shaped curve with Hi $\leq$ 0.35 represents an older stage, and the concavity of a watershed indicates the stability of the landforms and that accumulation of sediments likely to occur.

The hypsometric curve (Fig 2.4) plotted from the derived hypsometric curve table (Table 2.3), when compared with the hypsometric curve model prepared by Ritter et al. (2002) (Fig 2.5), reveals that the watershed has reached the early maturity stage and that the rate of erosional processes is still more dominant in landforms development. The hypsometric integral (Hi) was also calculated for eight sub-watersheds (SW) in the study area (Table 2.4). Based on the obtained Hi values, SW-8 has already reached the old stage, while SW-1, SW-5, SW-6 and SW-7 and SW-3 and SW-4 have reached their early maturity and maturity stages, respectively (Fig 2.6). This signifies that most of the study area has witnessed an active denudation. Moreover, SW-2 is still in its youthful stage, which indicates the highest susceptibility to soil erosion. The calculated Hi values for the whole watershed also have reached

0.48, which is an early maturity stage. Furthermore, the calculated hypsometric integral (Hi) corresponds well with the study area's hypsometric curve (Hc).

Table 2.3: Derivation of Hypsometric curve (Hc) for Chite watershed.

Elevations (m)	**Area (km^2)**	**'a' Area Accumulation**	**'a / A' Relative Area**	**'h' Cumulative Elevation Range**	**'h / H' Relative Height**
181 - 314	1.47	52.16 **(A)**	1.00	133	0.13
315 - 447	6.11	50.76	0.97	265	0.25
448 - 580	10.53	44.66	0.85	397	0.38
581 - 713	11.03	34.12	0.65	529	0.50
714 - 846	11.76	23.09	0.44	661	0.63
847 - 979	7.39	11.33	0.22	793	0.75
980 - 1112	3.49	3.95	0.08	925	0.88
1113 - 1243	0.46	0.46	0.01	1055 **(H)**	1.00

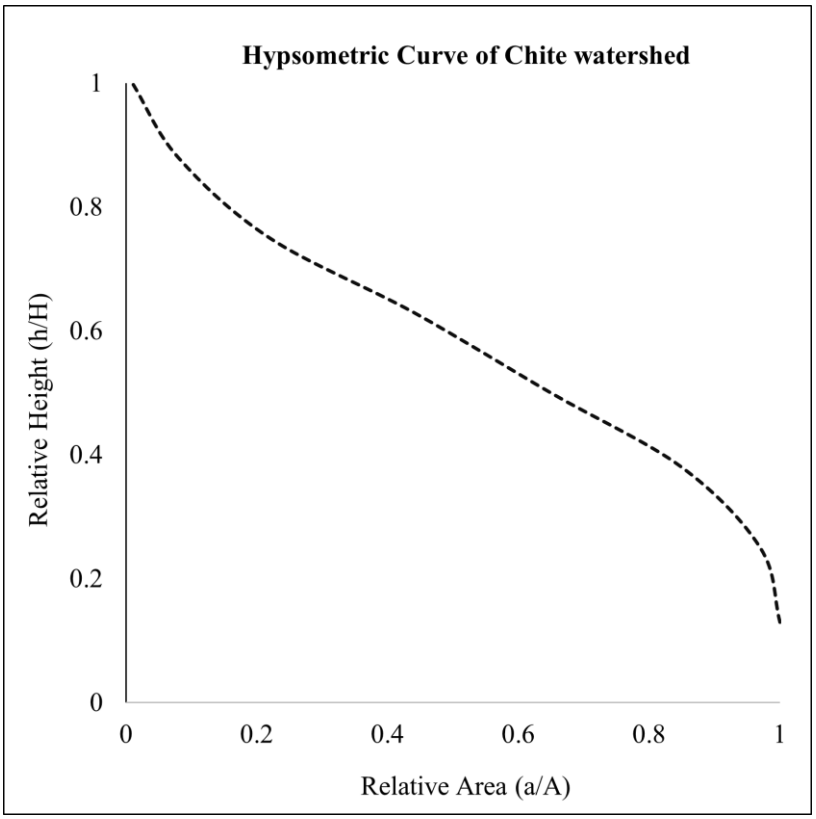

Fig 2.4: Hypsometric curve of Chite watershed.

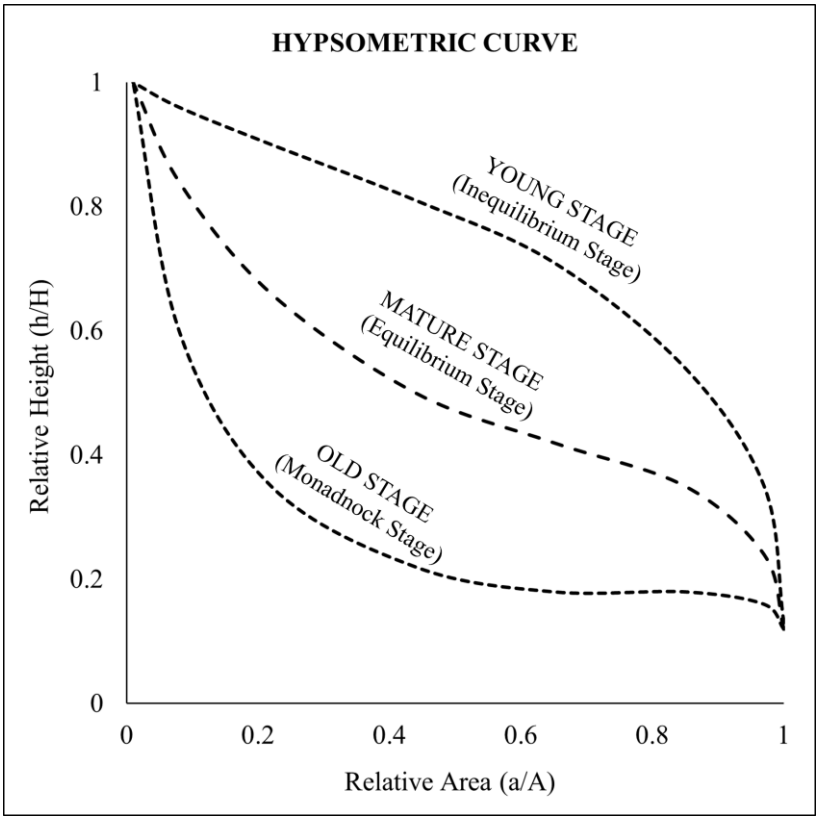

Fig 2.5: Hypsometric curve model (Ritter et al., 2002)

Table 2.4: Calculated Hypsometric integral (Hi) for Chite watershed.

Sub-Watershed		Elevation			Hypsometric Integral (Hi)	Geological Stage
No.	Area (km^2)	Min	Max	Mean		
SW-1	11.10	714.00	846.00	779.48	0.50	Early Maturity
SW-2	3.06	181.00	314.00	270.12	0.67	Youthful
SW-3	8.12	847.00	979.00	904.67	0.44	Maturity
SW-4	3.15	980.00	1112.00	1037.14	0.43	Maturity
SW-5	8.75	448.00	580.00	518.26	0.53	Early Maturity
SW-6	4.76	315.00	447.00	390.06	0.57	Early Maturity
SW-7	10.27	581.00	713.00	644.07	0.48	Early Maturity
SW-8	2.96	1113.00	1243.00	1140.27	0.21	Old Stage
Study Area = 52.16		**Study Area Hi = 0.48 (Early Maturity Stage)**				

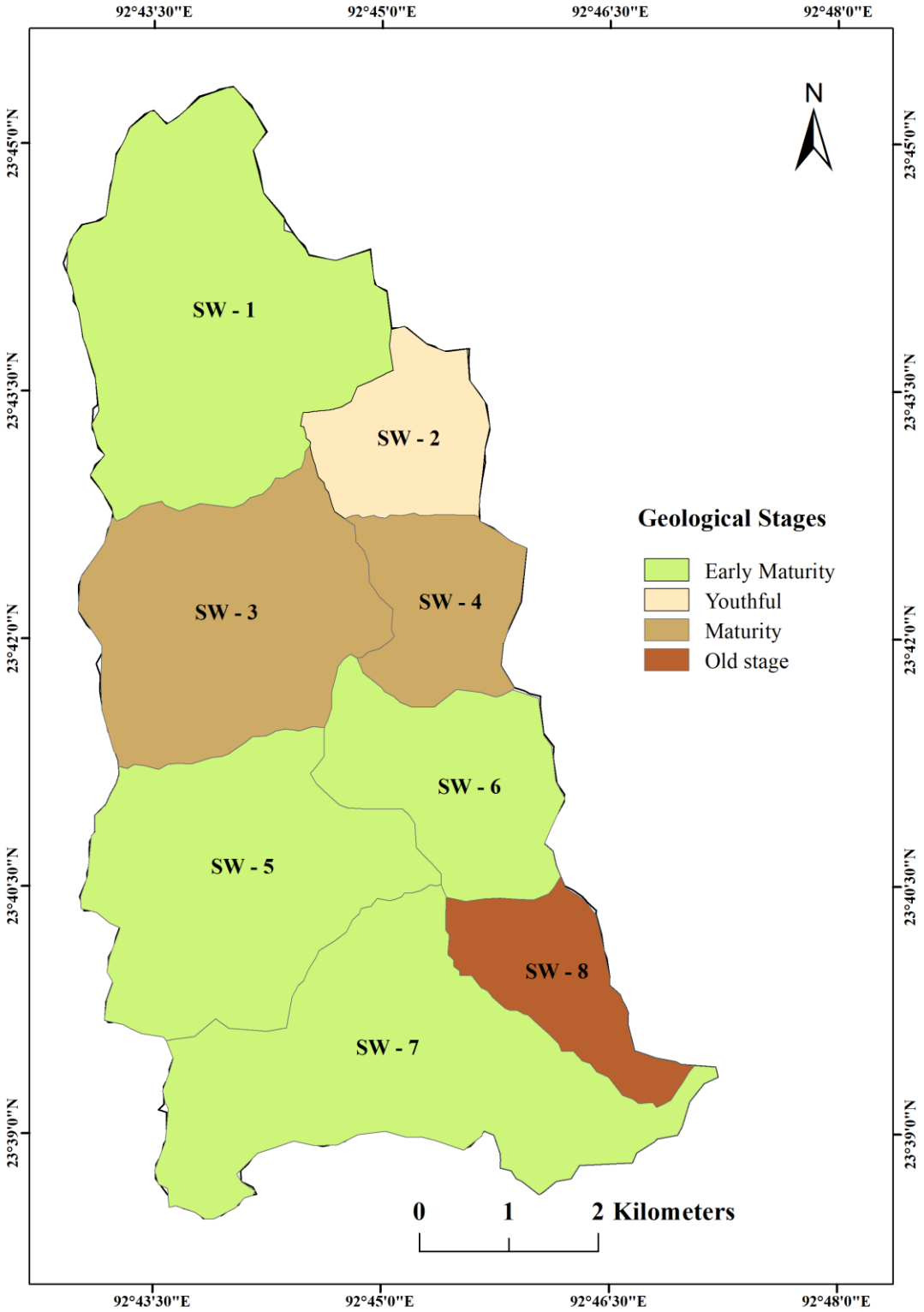

Fig 2.6: Geological stages of different sub-watersheds in Chite watershed.

2.5 Geology

Geologically, the study area comprises a lithological unit that belongs to the Bhuban formation within the Surma Group. Consequently, the predominant rocks in this region comprise sandstone, siltstone, mudstone, and shale, along with their intermixture in varying quantities (Ganju, 1975). Siltstone, mudstone, and shale possess small particle grain sizes, which might result in lower permeability of the rocks. Given the dominant prevalence of siltstone, mudstone, and shale, these rocks may be typically associated with higher surface run-off, leading to higher susceptibility to soil erosion.

The study area consists of two primary rock types: (i) Sandstone subordinate with siltstone, mudstone, and shale and (ii) an admixture of Shale, siltstone, and mudstone (Fig 2.7). The first lithological unit encompasses an area of approximately 2.95 km^2, accounting for 5.66 % of the study area. In contrast, the second unit occupies most of the watershed, representing 94.34 % and covering an area of 49.21 km^2 (Table 2.5).

Table 2.5: Geology of Chite watershed.

Lithologic Unit	**Area in km^2**	**Area in %**
Sandstone with subordinate siltstone, mudstone, shale	2.95	5.66
Grey sandy splintery shale, siltstone and mudstone	49.21	94.34
Total	**52.16**	**100**

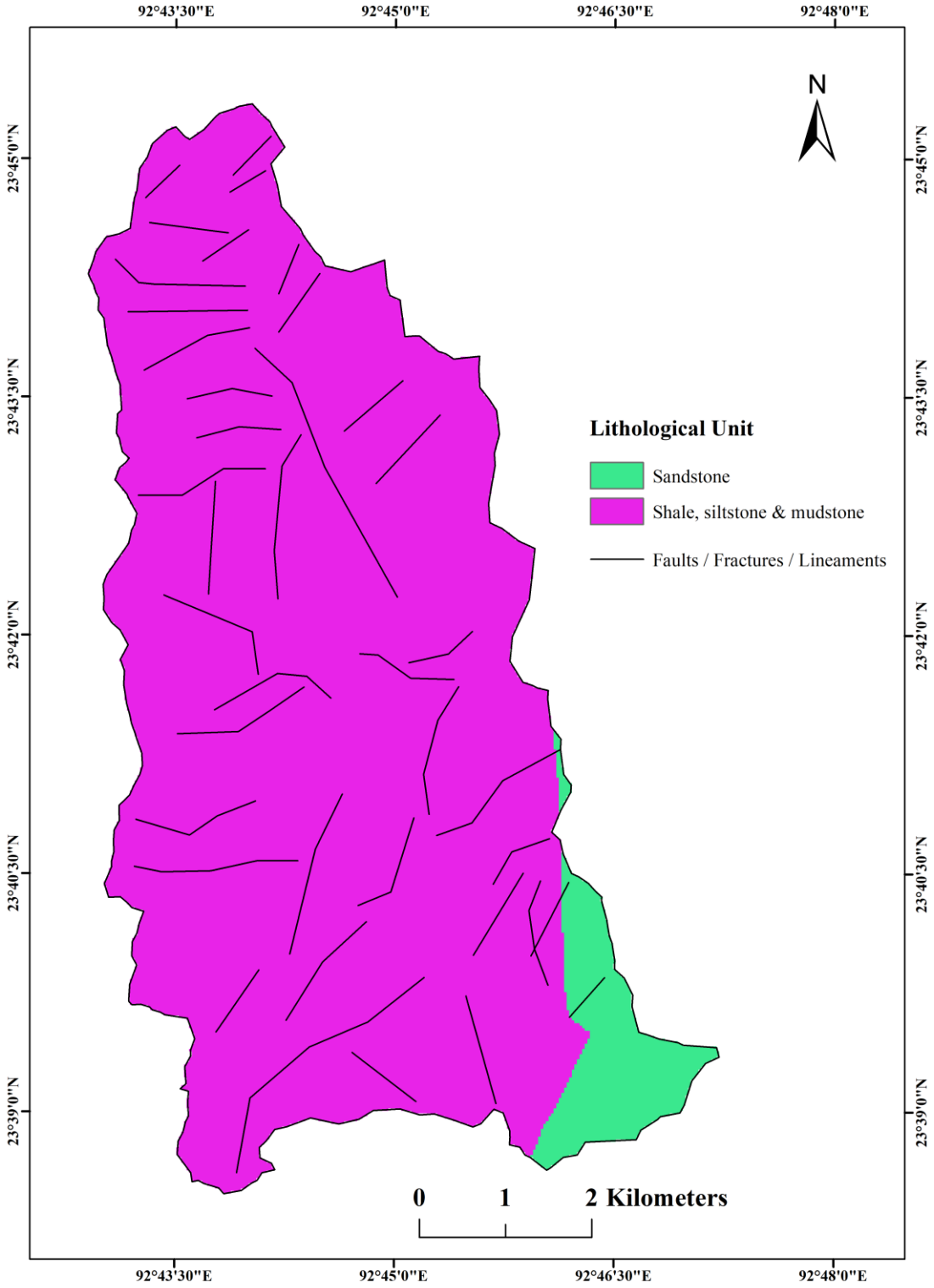

Fig 2.7: Geological map of Chite watershed.

2.6 Geomorphology

According to Bloom (1979), geomorphology is the systematic and analytical description of landscapes and the mechanisms responsible for their transformation. Generally, all landforms in a particular region reflect a close relationship between the underlying lithology and the operating geological processes.

From the geomorphology map (Fig 2.8), it can be observed that most of the study area, i.e., 97.47 %, which covers 50.84 $km^{2,}$ is characterized by highly dissected structural hills and valleys, indicating a high susceptibility of the watershed to erosion (Table 2.6). A prominent structural feature like lineaments can also be found, which depict the surface expression of geological features like faults and fractures on the earth's surface. These linear arrangements mainly result from various morphological features like streams, mountain ridges, etc. (Lillesand et al., 2017).

Table 2.6: Geomorphology of Chite watershed.

Geomorphic Features	**Area in km^2**	**Area in %**
Moderately dissected structural hills & valleys	1.32	2.53
Highly dissected structural hills & valleys	50.84	97.47
Total	**52.16**	**100**

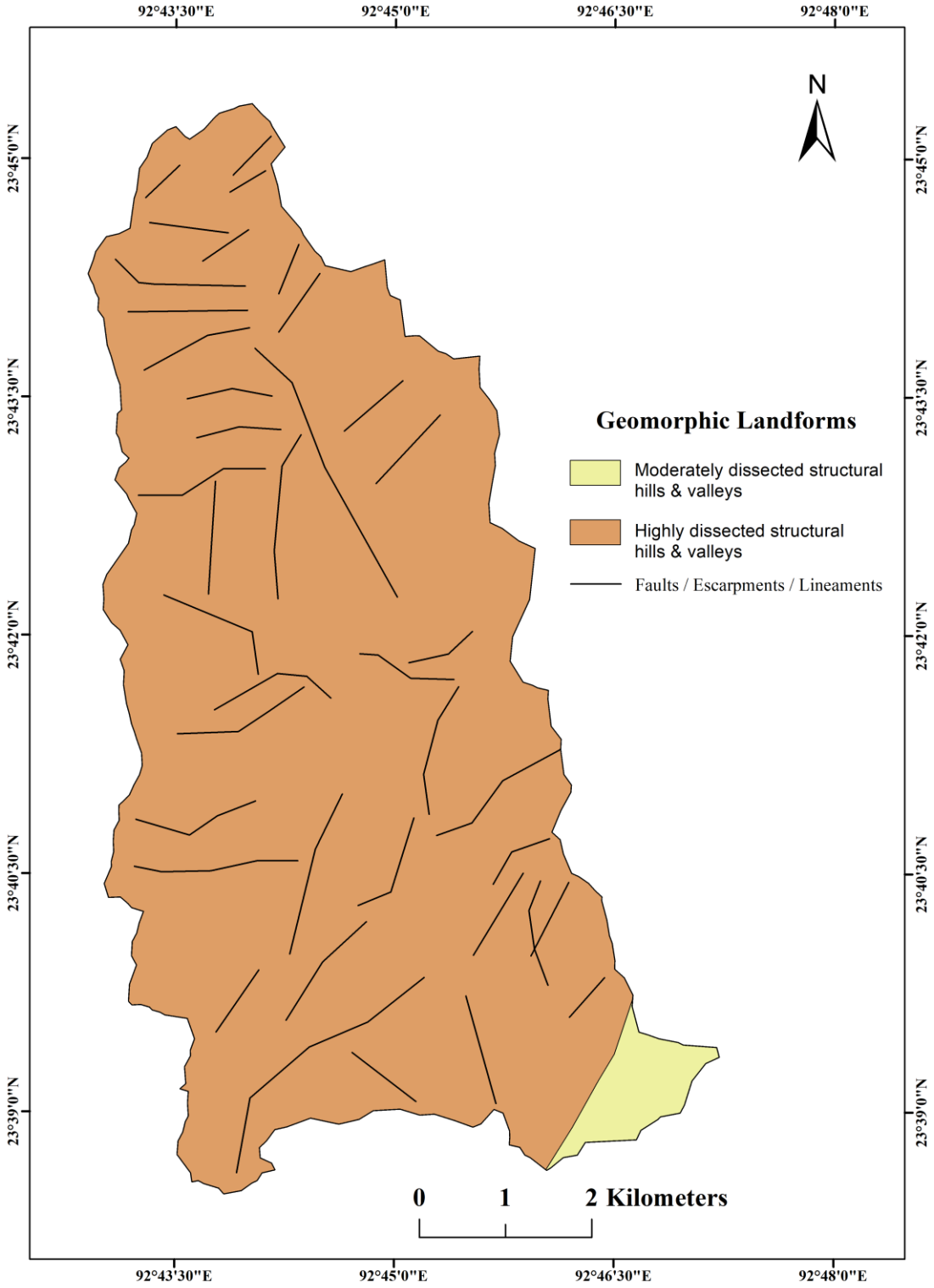

Fig 2.8: Geomorphological map of Chite watershed.

2.7 Drainage

The Chite River originates near Bawngkawn at an elevation of approximately 875 meters above mean sea level (MSL). It flows in a North-South direction, covering a distance of roughly 13.68 km. At an approximate altitude of 200 meters, it drains into the Tuirial (Sonai) River.

According to Strahler's (1957) method, the main river is classified as a 4^{th}-order stream in a basin's hierarchical system of streams (Fig 2.9). Among the various tributary streams, four prominent streams can be classified under 3^{rd}-order streams: Lawibual lui, Tuikhawhthla lui, Paikhai lui and Zangen lui. It was observed that most of the 1st order streams are non-perennial. The drainage system comprises 110 streams, ranging from 1st order to 4th order. There are 82 - 1^{st} order streams, 21 - 2^{nd} order streams, 6 - 3^{rd} order streams and 1 - 4^{th} order streams, and the combined length of these streams measures approximately 85.44 km (Table 2.7). The streams generally follow the linear arrangements of geomorphological features like faults in the watershed.

Table 2.7: Drainage of Chite watershed.

Stream Order	Length of streams (in km)	No. of streams
1^{st} Order	42.32	82
2^{nd} Order	21.10	21
3^{rd} Order	9.89	6
4^{th} Order	12.13	1
Total	**85.44**	**110**

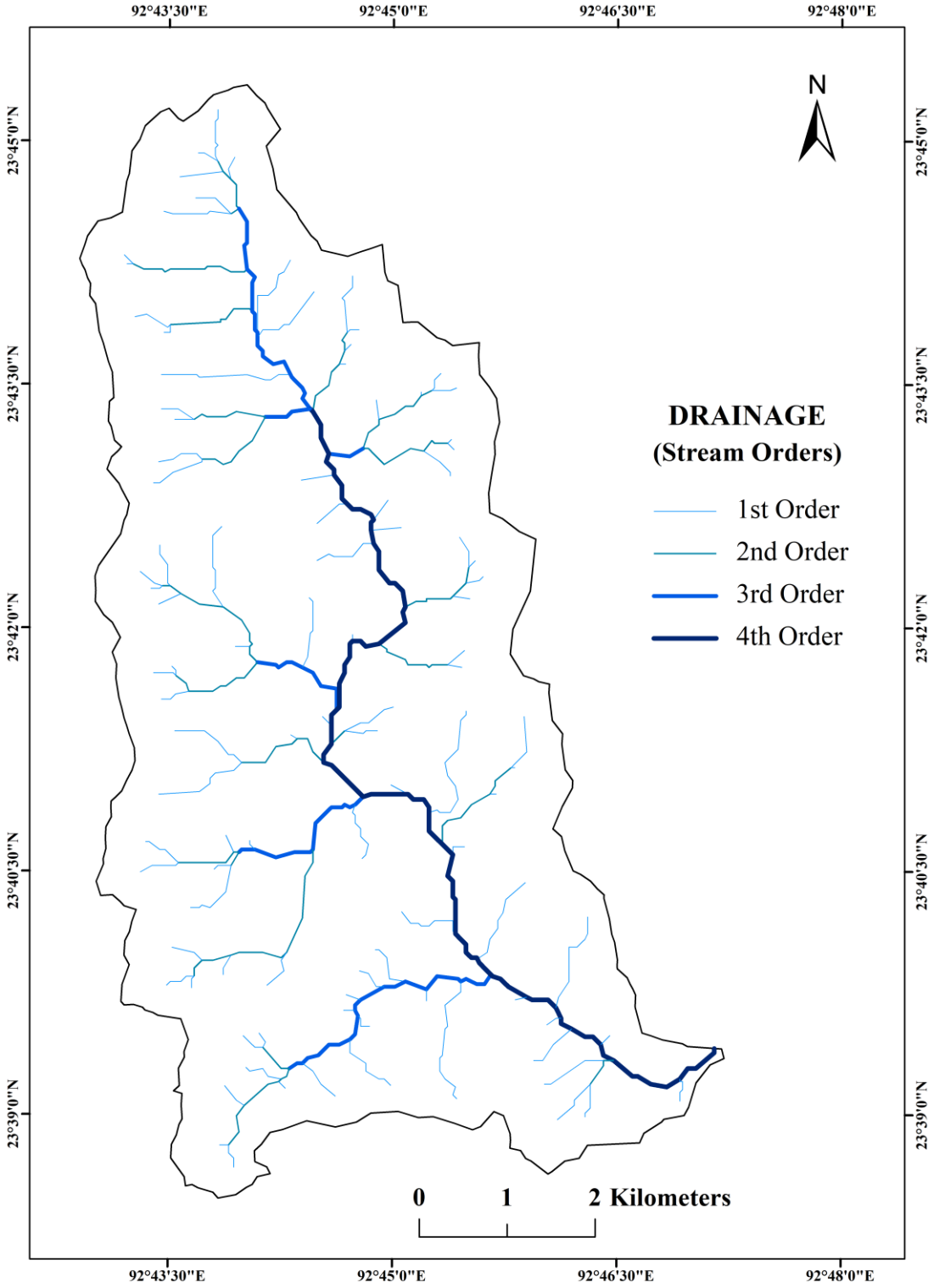

Fig 2.9: Drainage map of Chite watershed.

2.8 Climate

In addition to being located in a tropical region, the study area's mountainous terrain and high elevation plays a crucial role in controlling the temperature, resulting in a consistently moderate climate throughout the year, neither excessively hot nor cold. During summer, the temperature ranges typically between 25º C to 34º C, while it falls to about 11º C to 23º C during winter. The area also receives substantial rainfall annually due to the direct impact of the southwest monsoon. As a result, the study area has a humid tropical climate characterized by a distinct but brief winter season and a long summer season with abundant rainfall (Pachuau, 2009).

Among the different climatic factors, rainfall greatly influences soil erosion. This is primarily because rainfall can detach soil particles and transport them from one location to another via run-off, making it the primary driver of soil erosion (Garde, 2006). Heavy rainfall generally occurs in the region from May to September (Pachuau, 2009). Rainfall analysis of the region showed that the long-term average annual rainfall for a period of 12 years is 2086.60 mm (Table 2.8). From the rainfall map (Fig 2.10), the spatial pattern of rainfall distribution indicates that the central and northern parts received more rainfall with an average annual rainfall above 2100 mm, while there is a declining trend in the amount of rainfall towards the southern parts. The temporal trend of rainfall is also observed to be slightly declining during the 12 years (Fig 2.11).

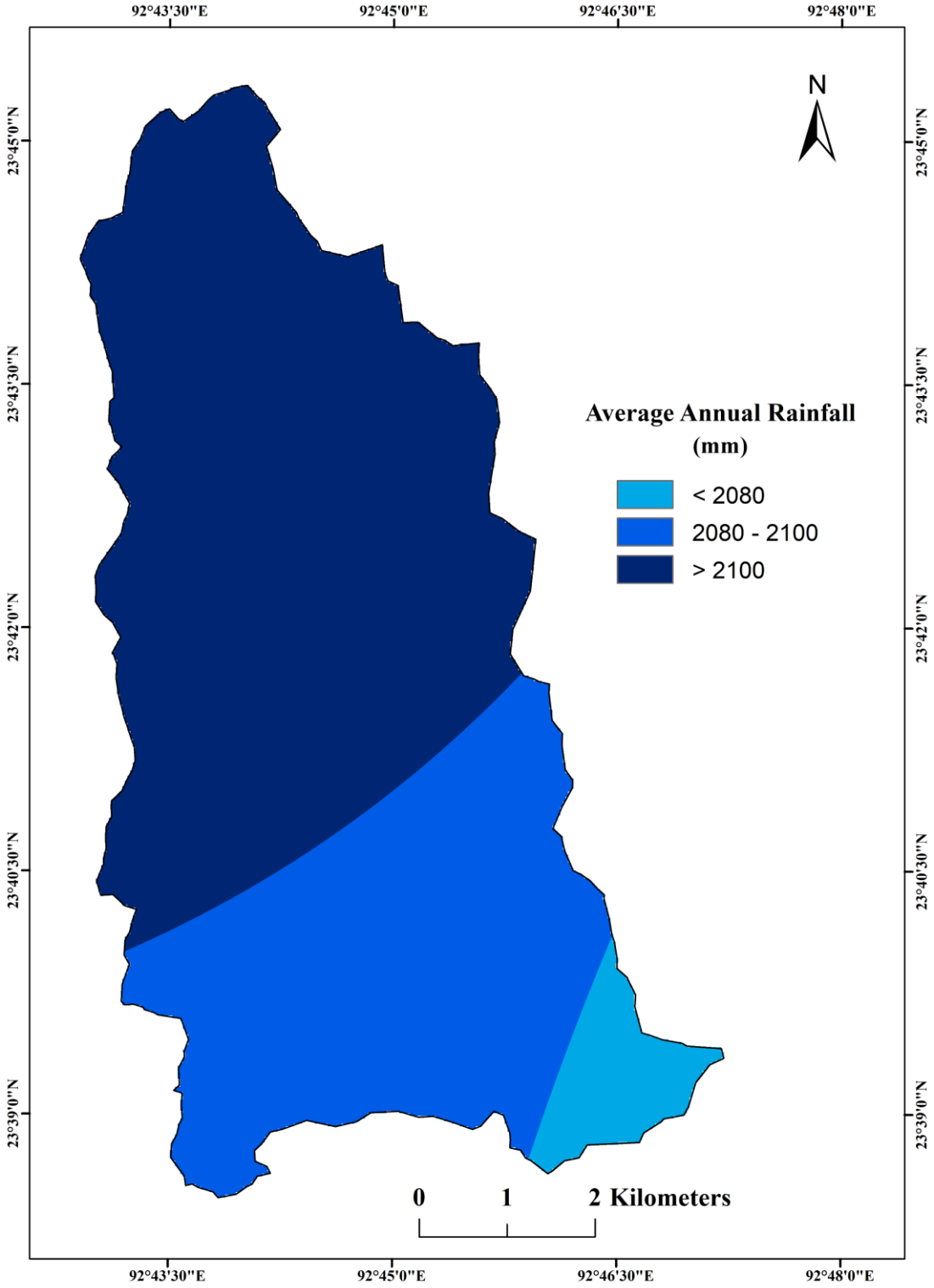

Fig 2.10: Rainfall map of Chite watershed.

Table 2.8: Rainfall data in and around the Chite watershed.

YEARS	Stations rainfall records (mm)		
	Science & Technology	HQ CE (P) Pushpak	Thingsulthliah BDO
2010	2650.8	2659.3	2226
2011	1909.4	1922.5	1578.8
2012	2543.1	2318.5	2236
2013	1920.8	1845	1285
2014	1790.6	1815	1637.8
2015	2412.3	2322.3	2326.5
2016	2161.1	2179.7	2172.5
2017	2686.7	2792.12	2827.4
2018	1749	1860.7	1940
2019	1709.8	1782	2052
2020	1741.5	1766.5	2109
2021	1917.6	2280.6	1989.5
Average rainfall(mm)	**2099.39**	**2128.69**	**2031.71**
Long term Average annual rainfall of Chite watershed = 2086.60 mm			

Source: Directorate of Science & Technology, State Meteorological Centre, Govt. of Mizoram, HQ CE (P), Pushpak and BDO office, Thingsullthliah.

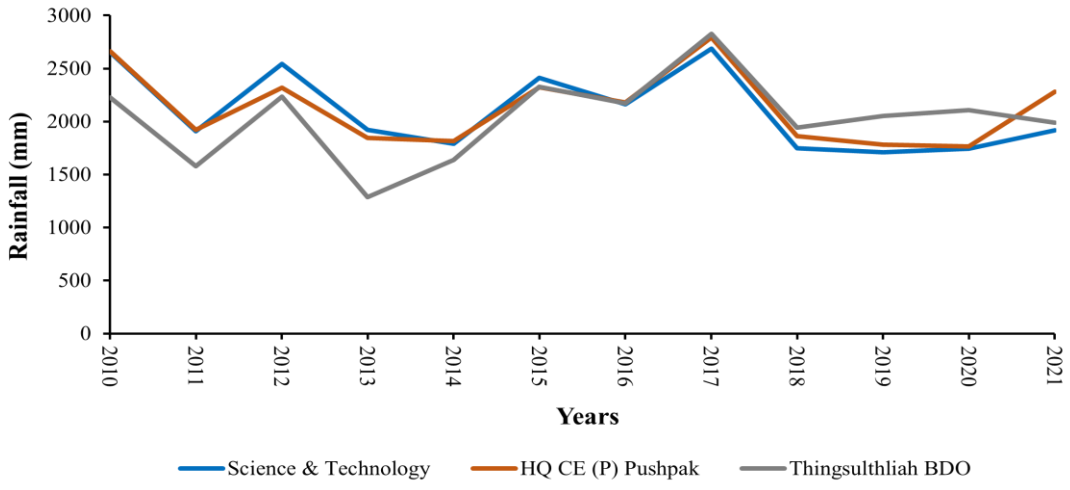

Fig 2.11: Line graph showing average annual rainfall for the three stations.

2.9 Vegetation

The presence of vegetation in an area significantly impacts the susceptibility to soil erosion. Typically, when there is dense vegetation cover, it serves as a robust defence mechanism in reducing the rate of soil erosion by enhancing the infiltration rate and decreasing the volume and velocity of run-off, while the absence of vegetation increases the likelihood of soil loss occurring (Tideman, 1996; Tripathi and Singh, 1993). The vegetation map of the present study has been depicted by the vegetation analysis through the Normalized Difference Vegetation Index (NDVI) (Fig 2.12).

Usually, when the NDVI ranges from approximately 0.6 to 0.8, it signifies the presence of dense and thriving vegetation cover. Conversely, a lower NDVI value of 0.1 or below indicates a scarcity or absence of vegetation, such as in barren land, soil or built-up areas. Moreover, a moderate NDVI value of 0.2 to 0.3 suggests the prevalence of depleted and open forest areas dominated mainly by shrubs and grasslands (Bhandari et al., 2012; Gandhi et al., 2015). Hence, it is evident form the analysis that there is a noticeable absence of substantial vegetation cover in the study area (Fig 2.12). Even the regions classified as having relatively very high or high vegetation class can be considered to have only moderate vegetative growth. Field surveys have also revealed that these areas mainly consist of scattered patches of open forests. Approximately half (around 49.87%) of the study area is occupied by areas with minimal or no vegetation cover, indicating a substantial depletion of the natural vegetation (Table 2.9). These areas are mainly attributed to built-up land and areas cleared away for shifting cultivation.

Table 2.9: Vegetation cover of Chite watershed.

Class	NDVI Values	Area in km^2	Area in %
Very low	0.09 - 0.2	6.89	13.21
Low	0.21 – 0.3	19.12	36.66
Moderate	0.31 – 0.4	17.21	32.99
High	0.41 – 0.5	6.39	12.25
Very high	0.5 – 0.62	2.55	4.89
Total		52.16	100

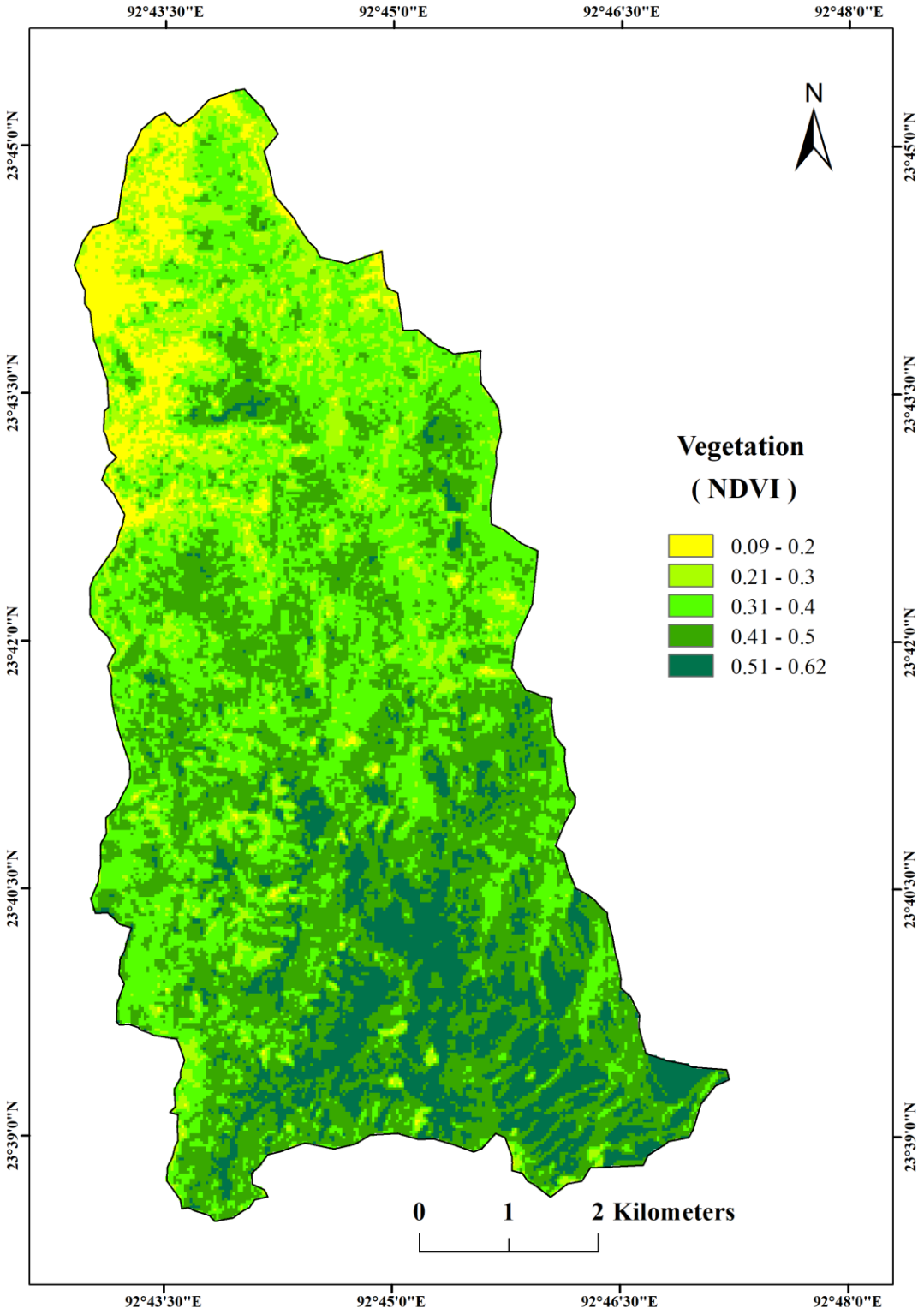

Fig 2.12: Vegetation map of Chite watershed.

CHAPTER-3

REVIEW OF LITERATURE

3.1 Introduction

This chapter provides an essential component of the present research work as it commences the journey towards a comprehensive understanding of soil erosion and sedimentation in a watershed. In this research, an extensive body of research encompassing diverse sources and methodologies were explored to draw insight into the state of knowledge in this critical field. The following sections examined different aspects of the multifaceted approaches, constituting an extensive exploration of erosion and sedimentation assessment literature. Most of the literary analysis in the present chapter includes several contemporary research approaches accomplished through the collaboration of advanced techniques encompassing remote sensing and Geographic Information Systems (GIS).

3.2 General

Through a comprehensive study, Xiaoqing (2003) shows that soil erosion and sedimentation are the most recent and significant threats among various global environmental issues. The study highlighted the importance of identifying the interrelationships between several factors that cause soil erosion and others that minimize soil loss. Soil erosion and sediment yield prediction has been outlined as a relevant means to address soil removal in a watershed. The work has also presented different models and measurements for soil erosion and sediment yield to address such problems for their management in a watershed.

Human-induced accelerated rate of soil erosion is a critical environmental problem. Lal (2001) asserted that this problem will have a continuous impact throughout the 21st century, predominantly among developing countries encompassing the tropical and sub-tropical regions. While addressing the ongoing debate on the precise extent and limitations of erosion modeling, the author strongly suggests field

verification for specific soil types and regions. The study also emphasized the environmental consequences of erosion, including changes in soil carbon dynamics and non-point source water pollution. Furthermore, the study recommended improvements in estimating global soil erosion by applying remote sensing and GIS techniques.

Toy et al. (2002) regard water erosion as the principal geomorphic process that profoundly influences most parts of the world's landscapes. It has been determined by four essential conditioning factors, including climate, terrain, soil, and land use land cover. The study has stated that the on-site effect of accelerated soil erosion produced by human activities on a hillslope resulted in a subsequent off-site sedimentation impact, disrupting both the economy and the ecosystem. Considering its widespread occurrence across different times and locations, the study considered erosion one of the most critical global environmental challenges.

In his studies, Pimentel (2006) acknowledged the emergence of soil erosion as a critical issue affecting a society's environment and health. He described it as one of the most severe challenges for human welfare. It was emphasized that 99.7% of food resources are produced from land that has lost approximately 10 million hectares of fertile cropland yearly through soil erosion. Furthermore, the study also underscores the rapid rate of soil depletion, surpassing the rate of soil regeneration by 10 to 40 times. This perilous trend is reported to threaten future food sufficiency and jeopardise ecological sustainability.

Through his works on river morphology, Garde (2006) claimed that water-induced soil erosion has been a critical issue for mountainous regions and agricultural land in humid and sub-humid areas. It has resulted in a significant decrease in soil fertility, consequently reducing crop productivity. Reflecting the prominence of sediment yield estimation to derive information on erosion rates and soil loss in a watershed, the study also demonstrates the application of various measurements and modeling approaches in a river basin.

Morgan (2005) conducted a study incorporating important soil erosion aspects. The author proclaimed that soil erosion is a common problem faced by agricultural

land in the tropical and semi-arid regions of the world. This study emphasizes the global significance of erosion and the need for localized solutions within the framework of local environmental systems. It shed light on the development of erosion-prediction technologies, specifically erosion models, and the methodologies used in field and laboratory research. This serves as the foundation for understanding erosion-control principles and practices. The author also offers insights into conservation planning, tools utilized in planning, and examples of adapted conservation programs for different land uses.

Narayana and Babu (1983) introduced an approach for obtaining an initial assessment of soil erosion, river sediment loads, and reservoir sedimentation when precise nationwide erosion estimates are unavailable. The study utilizes available information on soil loss, sediment load, annual erosivity of rainfall and reservoir sedimentation from the entire country. Based on this collected information, the study developed a statistical relationship through which the erosion rates, sediment load and deposition are calculated for the whole country.

Kothyari (1996) have prepared India's erosion and sedimentation status, drawing data from several soil erosion and sedimentation studies conducted across the country. The study identified the northeastern Himalayas as the most affected region by soil erosion, mainly due to a fragile environmental setup. Furthermore, human activities such as infrastructure development and economic activities worsened erosion rates, with shifting cultivation significantly contributing. The study has also shown that soil erosion in upper catchments has caused rapid sedimentation of the reservoirs. The study recommended detailed investigations in specific catchment areas to address these issues to identify critical regions for implementing control measures and effective conservation techniques.

The Space Application Centre, Indian Space Research Organization (SAC, 2021) prepared “Desertification and Land Degradation Atlas of India” for 2018 to 2019 based on the application of remote sensing and Geographic Information System (GIS) technology for monitoring land degradation throughout India. The latest report reveals water erosion has been the significant contributor to land degradation, affecting

29.77% of the country, i.e., about 97.85 million hectares of land area. The report has also imparted that water erosion is more dominant in the relatively humid areas of the country.

Tripathi and Singh (1993) have attempted to compile various information regarding the theory and practice of soil erosion control and its conservation, primarily focused on the Indian context. They have prepared an extensive content on soil erosion caused by both wind and water as well as its conservation, embracing the impact and mechanisms of erosion, various principles and measures of erosion control, the influence of erosion on particular problematic regions, and watershed management project on evaluation and management planning for soil and water conservation.

Choudhury et al. (2022) reviewed studies spanning the last three decades focused on soil erosion in Northeastern India. Their review considered various literature to provide an overview of the region's soil erosion status and proposed measures to combat the escalating erosion rates. The analysis highlighted the impact of physical factors like hilly topography, abundant rainfall, and unsustainable agricultural practices as the key contributors to severe soil erosion in the area. They concluded that converting forested land into unsustainable agriculture on steep slopes, especially in areas with heavy rainfall, significantly influenced soil loss and downstream sediment deposition.

A comprehensive study on the degradation of soil quality and soil loss in the Northeastern parts of India has been undertaken by Saha et al. (2012). In this study, shifting cultivation and widespread forest depletion has been attributed to the major cause of impoverished soil health and loss in the region. The study has also highlighted that the traditional practice of shifting cultivation encompasses the rural inhabitants' social, cultural and economy. In this light, the authors have made several recommendations to minimize all sorts of degradation and improve resource sustainability. Besides several recommendations made by them, some of the most significant ones include agroforestry, an integrated farming system, as well as augmented utilization of organic fertilizers in the region.

Grogan et al. (2012) endeavoured to devise a competent remedy for the detrimental effects of shifting cultivation in a sharply inclined slope of Mizoram. Their study underscores the desperate requirement for a unique and specialized approach to manage the likelihood of substantial soil erosion in the region. Through a review of pertinent literature, the study proposes several strategies to improve shifting cultivation and viable options for replacing this unsustainable agricultural practice. The authors further deduced that deliberate utilization of chemical and organic fertilizers could significantly resolve the issue of reduced fallow intervals.

In 1994, the Institute of Resource Development and Social Management (IRDAS) conducted a study to identify and prioritize various watersheds in Mizoram concerning the severity of soil erosion and land degradation. The study emphasized the pressing necessity for soil resource conservation and management in response to the increased runoff and erosion-induced land degradation caused by steep terrain, abundant rainfall, rapid deforestation, common practise of shifting cultivation and weak structure of soil. However, the study has also emphasized that, given limited financial and human resources, these initiatives should primarily target the most critical watersheds.

3.3 Soil Erosion Susceptibility Assessment

Watersheds in tropical regions are very sensitive to the various impacts of soil erosion, embracing topsoil loss, soil fertility reduction, channel erosion, flash floods, sedimentation, etc. Addressing the multiple repercussions of soil erosion in relatively weaker tropical watersheds, Ghosh and Mukhopadhyay (2021) emphasized the essentiality of mapping erosion susceptibility to carry out sustainable resource management and erosion control. The study has highlighted the advantage of applying multi-criteria decision-making (MCDM) approaches in combination with GIS over conventional methods, particularly in areas of developing countries where data is limited.

Harker and Vargas (1987) and Khaira and Dwivedi (2018) featured that the Analytical Hierarchy Process (AHP) has consistently been a highly favoured and

extensively employed technique for multi-criteria decision-making and planning due to its lucidity and flexibility with precise outcomes, its capability to assess qualitative as well quantitative factors, and its ability to detect inconsistency or bias. In addition, Vaidya and Kumar (2006) stated the simple and dependable nature of the AHP for analyzing a complex system, which makes it a well-preferred method, especially among developing nations. Furthermore, Semlali et al. (2019), Vojtek and Vojtekova (2019), and Chakrabortty et al. (2020) enunciated the compatibility of this method with the advanced technique of remote sensing and GIS, which has dramatically increased and improved the application of the AHP for spatial analysis in different studies. This capacity of the Analytic Hierarchy Process (AHP) has further enhanced the method's applicability to soil erosion susceptibility mapping worldwide.

In an attempt to evaluate soil erosion at a catchment scale in Cyprus, Alexakis et al. (2013) unveil the advantage of AHP methods above the RUSLE models for erosion risk modeling. The main benefits of the AHP have been attributed to its ability to relate the collaborative dependency among the erosion conditioning factors. However, with an identical outcome from both methods, the integrated approach was observed to provide a time and cost-efficient methodology for erosion assessment.

Integrating the advanced technique of GIS and the AHP method Aslam et al. (2021) prepared an erosion susceptibility map for the Chitral district in Pakistan. They have selected 10 erosion causative factors which were assigned weights based on their potential impact on soil erosion. The AHP analysis has revealed that steeper slopes of relatively higher elevations are more sensitive to soil erosion. Among the land use land cover classes, barren lands were found to be more prone to soil erosion occurrences, followed by agricultural land. The generated map manifests high erosion susceptibility for the study area, which was attributed to the hilly terrain of the district.

Ebhouma et al. (2022) carried out erosion vulnerability mapping based on AHP technique under the GIS platform to address land degradation. It was ascertained that around 21% of their study area faced a significant risk of soil erosion. Moreover, the relatively higher risk has even constituted 14% of these areas. Higher vulnerability of the area is mainly ascribed to the combined outcome of mainly slopes, vegetation and rainfall. As the predicted model was verified to attain high accuracy, the study was

anticipated as a crucial tool for prioritizing regions in need of soil conservation and erosion control measures.

Haidara et al. (2019) have attempted to establish rapid and cost-effective management to soil erosion. For information to policymakers, erosion vulnerability assessment was executed through a combination of the Fuzzy AHP and GIS. Employing six conditioning factors of soil erosion, the study produced erosion risk areas, confirming the competency of applied integrated approaches.

For designing erosion conservation planning, Kachouri et al. (2015) assessed erosion hazard by developing two models, the AHP and Logistic Regression (LR) with GIS technology. The model's validation through field observation reveals that both models produce a close resemblance. The spatial pattern of erosion hazard depicted by the AHP model highlighted the model's efficiency for a rapid erosion risk assessment.

Mushtaq et al. (2023) utilized GIS and AHP to identify areas at risk of soil erosion in the mountainous regions of Central Kashmir. They have considered various factors, with topography, land use/land cover (LULC), and lithology being the most influential factors. The primary cause of high erosion vulnerability in the study area was unsustainable agriculture practices along the steep slopes and high-altitude regions. They have proclaimed the methodology as an effective way to qualitatively assess erosion susceptibility, which can enhance the implementation of suitable conservation measures.

Pradeep et al. (2014) carried out AHP and GIS-based identification of critical prone zone for soil erosion in the Western Ghats mountainous watershed, dominated by agricultural land use. In this study, the authors integrated various geo-environmental parameters that considerably influence soil erosion processes. Increased susceptibility to erosion is evident in regions characterized by highly elevated land with steep gradient slopes. The extensive alteration of the terrain for agricultural land use, combined with inadequate soil conservation efforts, heightens the watershed's vulnerability to soil erosion.

Erosion prediction by GIS based modeling was utilized by Saini et al. (2015) to address the challenge of soil erosion and limitations of conventional methods for identifying erosion prone areas in the upper Markanda River catchment. In the study, relative weights assigned to the selected erosion causative factors through the AHP

method show that rainfall has the most significant contribution. The findings from this study reveal a critical condition as 60% of their study areas constitute the very high- and high-risk classes of soil erosion. Verifying these findings through field observations and satellite images also confirms the occurrence of erosional features in these critical areas. It was therefore suggested to produce erosion vulnerability maps based on the applied approaches as they are imperative to implement erosion control measures and its conservation planning.

A land degradation vulnerability model can be effectively prepared through dependable satellite data based on integrating the AHP and GIS techniques (Sandeep et al., 2020). In their study, Sandeep et al. (2020) assessed land degradation vulnerability by incorporating several thematic layers representing erosion conditioning factors. These layers were derived from several earth observation satellite datasets and analyzed with the AHP method under GIS environment to identify their relative influence on land degradation. The findings of the study exhibit the capacity of the applied integrated methodologies to provide a robust land degradation model.

Vijith and Dodge-Wan (2019) successfully assessed erosion susceptibility for a watershed based on the AHP analysis in GIS platform. After determining ranks and weights for various variables, the study indicates LULC to be the most influential factor, followed by slope. In this study, the very high and high erosion susceptibility zone occupies 10% and 14% of the study area, respectively, and these areas are confined to higher elevations with steeper slope gradients. Comparison between the generated map and field observations revealed land use changes as the leading causes of erosion vulnerability in the watershed. The authors asserted that the results of their study might represent reliable information on the watershed's erosion status and may assist in land use planning and implementing erosion control measures.

For soil erosion susceptibility mapping, Saha et al. (2019) conducted AHP and fuzzy logic modeling based on GIS separately for a river basin widely utilized for agriculture in eastern India. The study mainly focused on identifying erosion risk caused by agricultural development in the study area. The findings from the two models revealed higher erosion susceptibility in the upper catchment, where anthropogenic activities dominated the land use and where the landforms exhibit steeper slopes and proximity to lineaments. They have validated both the predicted

models using ROC curves and concluded that the generated maps provide a satisfactory result compared to the actual field conditions.

Erosion hazard zonation for a watershed in northeast India was carried out by Das et al. (2020) using geospatial modeling that utilized the AHP method along with the RUSLE model. The AHP analysis has shown that steeper slopes, higher elevation, drainage and lineament density are the most influential variables that enhance the area's vulnerability to erosion. The generated erosion hazard map reveals that more than half of the watershed and about one-fourth of the watershed are under moderate and high erosion vulnerability classes, respectively, showing the higher susceptibility of the regions towards soil erosion. The performed validation of the AHP model indicates a satisfactory result with a high prediction accuracy rate of 84.90%.

Landslide susceptibility mapping has been performed by Pourghasemi et al. (2012), Chen et al. (2016), Myronidis et al. (2016) and Achour et al. (2017) in different parts of the world. All the studies have employed the AHP and other varying methods to generate landslide susceptibility maps. These studies have considered various landslide causative factors prepared and integrated in GIS for spatial analysis. The predicted maps for all the studies were validated using the receiver operating characteristics (ROC) curves, which reveals that the AHP method combined with the GIS techniques is an efficient methodology for carrying out susceptibility maps based on multiple variables.

Daoud (2017) presented studies on multicollinearity, discussing the nature, causes and impacts on the dependability of a regression model. The author addressed the severity of correlation among various predictors, suggesting its solution before a modeling process. The study further stressed the rejection of any model that encounters a multicollinearity problem, as the model’s interpretation is impossible in such a situation.

To produce a reliable gully erosion susceptibility map for Toroud watershed in Iran, Arabameri et al. (2018) compared four different models with GIS technology. In this study, multicollinearity analysis was performed by using diagnostic tools, viz., “Variance inflation factors (VIF) and tolerance (TOL)”, to identify the existence of correlation among various predictors selected for preparing each model. Subsequently, they screened 13 variables from 18 previously considered erosion conditioning factors

for modeling. The generated susceptibility map for all the models were then validated against 26 active gully locations using the "Receiver operating characteristics (ROC)" curves within the watershed. It was observed that each predicted model produced an excellent outcome. However, the modeling based on the AHP has yielded the most precise results and can be effectively employed for soil conservation planning.

In their respective research, Pourghasemi et al. (2013) and Alqadhi et al. (2022) engaged in landslide susceptibility mapping across diverse geographical regions, employing a variety of methodologies. Both studies, however, recognize the importance of conducting multicollinearity analysis when considering numerous variables for susceptibility mapping. To address this, they both utilized well-established diagnostic tools, such as the "Variance Inflation Factor (VIF) and Tolerance (TOL)", to identify and subsequently eliminate highly correlated landslide conditioning factors.

3.4 Soil Loss Evaluation

The "Revised Universal Soil Loss Equation (RUSLE)", developed by Renard et al. (1997) has marked a significant evolution in the realm of soil conservation and erosion control. Building upon its predecessor, the "Universal Soil Loss Equation (USLE)" by Wischmeier and Smith (1978), the RUSLE model has emerged as the cornerstone of empirical models for comprehensively assessing soil loss and erosion rates. Its enduring prominence and widespread use can be attributed to a combination of factors that make it an indispensable tool for researchers, land managers, and policymakers. The widespread adoption of the RUSLE model can be attributed to several key factors, including its relatively modest data requirements, simplicity, cost-effectiveness, compatibility with remote sensing and GIS technologies, and its ability to represent spatial patterns of erosion rates accurately. While the model's original purpose was to predict soil erosion in temperate regions, it has demonstrated remarkable adaptability with minor adjustments for ecologically sensitive areas. This adaptability has been noted by researchers and practitioners alike, with studies by Millward and Mersey (1999), Prasannakumar et al. (2012), Negese et al. (2021), and Petito et al. (2022), showcasing its successful deployment in diverse environments such as mountainous terrain, tropical zones, and subtropical regions. This adaptability

underscores the model's applicability across various climatic and topographic conditions, rendering it an invaluable tool for addressing soil erosion in multiple ecosystems. Furthermore, RUSLE can even be harnessed to forecast soil loss in ungauged watersheds by employing simulations based on knowledge of the watershed's attributes and the prevailing hydro-climatic conditions (Garde and Kothyari in 1990)

To ascertain erosion risk and identify suitable conservation measures within the Kianjuki catchment in central Kenya, Angima et al. (2003) carried out erosion prediction based on the RUSLE, considering regional procured data. The findings revealed that erosion rates differ in various runoff pathways, which mostly surpass the soil loss permissible limits calculated for the area. Alongside the recognized location-specific erosion risks, the study recommended the application of a specific hedge grass to stabilize agricultural terraces.

Addressing the ongoing tasks of forest conservation in the Brazilian Amazonia, Lu et al. (2004) attempt to establish an interrelationship between erosion hazards and various land use/land cover (LULC) classes for managing land degradation. Combining the RUSLE model with RS and GIS techniques, it was observed that pastureland has a high risk of soil erosion, while the fully grown forests are well protected. The study has emphatically approved the capacity of RS and GIS for soil erosion assessment in the study area.

Pradhan et al. (2011) assessed soil erosion in a high erosion and landslide-vulnerable areas of Penang Island in Malaysia. In this study, the authors showcase the application of GIS-based USLE model for quantifying soil loss and spatial erosion hazard analysis. As soil conservation measures are not implemented in the study area, the authors assumed the P-factor as 1. They have related the erosion hazard map with the field-verified landslide inventory map through frequency ratio statistics, which reveals a significant correlation.

In estimating soil loss within a watershed, Chen et al. (2011) employed the RUSLE model under remote sensing and GIS technology within the Miyun Watershed in North China. In this study, the authors applied a uniform P factor value of 1 due to the limited presence of conservation practices in the watershed. The findings manifest an erosion rate of about 9.86 tons ha^{-1} $year^{-1}$ in the upper catchment, where a notable

area of about 47.5 km^2 was under a highly severe risk zone. It was suggested to implement immediate conservation measures for the prioritized areas.

Farhan and Nawaiseh (2015) executed erosion assessments in Wadi Kerak watershed to implement suitable conservation measures. The study has been performed through the RUSLE model in conjunction with GIS platform. With an estimated mean annual erosion rate of 64 tons ha^{-1} $year^{-1}$, about 54.5% of the study area was under critical conditions of soil loss. The results indicate that most relatively higher prone zones are found in cultivated areas, bare lands and rangeland. Integrated RS, GIS and RUSLE model applied in this study was reported to provide a basic and cost-effective methodology in erosion risk modeling for devising appropriate measures for erosion control.

Integrating the USLE and GIS technology, Pham et al. (2018) attempted to evaluate the soil erosion problem in the A Sap basin of Central Vietnam to produce an appropriate solution for reducing future erosion rates. The findings reveal that erosion rates are highest in natural forested areas, followed by plantation and agriculture. Such anomalies have been attributed to the location of these natural forests on steeper slopes. They have observed that the alteration of farming schedule and intercropping practices are significant methods to safeguard soil loss in agricultural land. Additionally, the most efficient approach for reducing soil erosion in mountainous areas within the A Sap basin involves the introduction of broadleaf trees.

Koirala et al. (2019) calculated soil loss throughout Nepal, considering the necessity of erosion conservation in this agriculture-based economy. Utilizing the GIS-based RUSLE modeling, the study identified erosion risk in about 56% of the area, mostly concentrated in barren lands and agricultural fields of the middle Himalayas. The authors acknowledge the applied methodology as a viable approach for countries like Nepal, which has a shortage of consistent and long-term erosion hazard monitoring.

Belayneh et al. (2019) estimated potential soil loss for watershed prioritization using GIS-based RUSLE modeling in the Gumara watershed of Ethiopia. Water erosion was observed to be a severe issue in the watershed, generating annual soil loss of 9.68 million tons with a mean erosion rate of 42.67 tons ha^{-1} $year^{-1}$. The study reveals that erosion processes are primarily controlled by slope and land use/land

covers, and the higher erosion rates are mostly confined to agricultural land use. The rate of soil loss was also found to exceed the soil loss tolerance for about 71.7% of their study area. Hence, the very severe categories of prioritized sub-watersheds cover more than 3000 ha of the total area.

Moore and Burch 1986(a) developed a physically based equation for the LS-factor, which determines the sediment transport through sheet and rill erosion by overland flow. These theoretically derived equations have been obtained from the unit stream power theory. While comparing the derived equations with the original length-slope factors in the USLE, the authors concluded that these two factors produce more or less similar results. They have even recommended the applications of their derived physically based factor over the original factor of the USLE, which is an empirically developed relation.

Mitasova et al. 1996 formulated a new method to derive topographic factors for large areas with dynamic landscapes, enhancing the authentic digital representation of complex topographic characteristics by applying a digital elevation model (DEM) in a GIS environment. They have developed a vector-grid algorithm to assemble flow lines and calculate the upslope areas that contribute to the flow. Using unit stream power, they have modelled the transporting capacity of the sediments through the arrangement of various topographic features favouring erosion or deposition in the area concerned. Thus, in this new approach, emphasis was placed mainly on the appropriate representation of those complex topographic features that have a significant role in modelling purposes relating to soil erosion or deposition.

Performing RUSLE modeling in a GIS environment, Millward & Mersey (1999) presents a modification of LS and R factors to enhance the compatibility of the soil erosion model in a tropical mountainous watershed. They have utilized the upslope drainage area to calculate a semi-distributed LS factor value, considering the combined impact of both the overland flow and rainfall erosivity, which is difficult and impracticable for mountainous terrain using manual calculation. This study also assigned a P-factor value of 1 to correspond to the absence of soil conservation support practices in the study area. Hence, the study aims to develop a model that requires minimal data for its application, mainly in developing countries.

Ram Babu et al. (2004) updated their previous work from 1987 on the "Rainfall Erosivity and Iso-erodent Map of India." They aimed to improve the accuracy and detail of the Erosion Index (EI) values. To achieve this, they used meteorological data from 31 previous stations and incorporated data from 92 new stations, totalling 123 stations. The rainfall erosivity was determined using the Wischmeier and Smith 1978 method. They then established a linear relationship between rainfall data from both annual and seasonal records and the Erosion Index values. This allowed them to estimate additional Erosion Index values for 500 evenly distributed stations across India. The result was a refined iso-erodent map covering the entire country based on rainfall erosivity values from 623 stations.

Kayet et al. (2018) estimated soil loss in a hilly mining area of Jharkhand, India, through geospatial modeling that combines the RUSLE model with the Soil Conservation Service – Curve Number (SCS-CN) method. The study observed a high relationship between the estimated soil loss and the amount of rainfall and runoff. From their findings, the authors concluded the necessity of accurate soil loss estimation to identify erosion impact in the mining sites of hilly areas throughout the country.

For assessing soil erosion in the Baraker river of Jharkhand, Biswas and Pani (2015) have applied the RUSLE model in GIS environment. This study has observed a high negative correlation between the spatial distribution and quantity of soil loss. Hence, a smaller portion of the study area contributes most of the basin's soil loss. Erosion has been mainly caused by the relatively higher LS and K factor in upstream, and the sediments generated from these areas have further degraded the reservoir located downstream.

Based on RS and GIS tools, Devatha et al. (2015) conducted erosion modeling with USLE to estimate soil loss in the Kulhan watershed, Chattisgarh. Their findings reveal that most of the study area experienced only a slight erosion because of the gentle slope throughout the watershed. However, the study also observed the occurrence of very severe erosion along the main river of the watershed, which has been ascribed to the high LS factor in the river channel.

Ganasri and Ramesh (2015) have prepared erosion potential modeling for the Nethravathi basin, a tropical watershed in the western ghats, by integrating RUSLE

and GIS. In addition, the study has also attempted to examine the influence of alternating land use/land cover (LULC) change on soil erosion rate. Their findings showed that the erosion rate was significantly changed with the change in topography and LULC. The results reveal that agricultural practice in the basin has a remarkable influence on the rate of soil erosion. Erosion risk for the study area substantially increases with the increase in agricultural land. The authors have also discussed that decision-makers can effectively employ their results to advance appropriate erosion control and erosion hazard management measures in the study area.

Emphasizing the problems of soil erosion potential in tropical humid mountainous regions coupled with data scarcity, Markose and Jayappa (2016) highlighted the significance of modeling techniques. This study has attempted to evaluate soil loss and prioritise sub-watersheds in the Kali River basin of Karnataka. The authors performed a quantitative erosion assessment using the RUSLE model under the GIS platform. The high rate of soil loss in the study area is primarily attributed to several anthropogenic activities such as deforestation, rapid urban development, dam construction, etc., in the study area. The study has further advocated that the research findings may be valuable for implementing effective site-specific watershed management plans in the river basin.

To assess the suitability of utilizing the RUSLE methods along with RS and GIS technology for predicting soil loss, Prasannakumar et al. (2011) carried out studies in the Attapady valley of Kerala which lies in the western ghats. Through spatial analysis, it was revealed that the extensive changes in terrain, unsustainable agricultural methods such as shifting cultivation, and the degradation of the forested areas have resulted to a significant soil erosion rate. The study demonstrated the proficient capacity of the applied combined approach with a regionally derived dataset in enhancing soil conservation strategies.

Prasannakumar et al. (2012) estimated soil loss in a forest covering mountainous regions of Kerala, the Pamba sub-watershed, using the widely recognized RUSLE model. The research revealed that within the sub-watershed, regions characterized by virgin forests in the upper catchment exhibited minimal soil erosion rates. At the same time, areas subjected to human activities showed a significantly higher soil erosion rate, exceeding 5 tons ha^{-1} $year^{-1}$. This higher erosion rate has been

attributed to the modifications in terrain, elevated LS-factor values, and increased precipitation in these areas. The study also regards the anticipated erosion rate and their spatial pattern, providing valuable implications for watershed prioritization to execute integrated watershed management.

For generating a conservation-oriented priority map, Uddin et al. (2016) identified the temporal change in erosion rate in the Koshi basin using RUSLE, RS and GIS. The study indicated that about 87% of erosion risk in the basin persisted without change, while the increasing and decreasing trend constituted 9% and 3.8% of the study area, respectively. Based on the results, the study prioritized those areas with relatively higher erosion potential for conservation management.

Zonunsanga and Rao (2013) exhibited their findings on the impact of shifting cultivation on land degradation in the Teirei watershed, Mizoram. They have carried out their studies through the RUSLE model in GIS environment. In this study, soil erosion has been attributed to be the most dominant form of land degradation in Mizoram's fragile environmental set-up. The study has revealed that the extensive practice of shifting cultivation has generated serious soil erosion, contributing to about 60% of the land degradation in the study area. They have also recommended executing improved shifting cultivation practices rather than abolishing the prevailing system.

3.5 Soil Loss Tolerance Limits

According to Morgan (2005), “the aim of soil conservation is to reduce erosion to a level at which the maximum sustainable level of agricultural production, grazing or recreational activity can be obtained from an area of land without unacceptable environmental damage. Since soil erosion is a natural phenomenon, it cannot be prevented. But it can be reduced to a maximum acceptable level or soil loss tolerance”. This literature also reveals that T-values development in different parts of the world is grounded exclusively on agricultural concerns. Hence, it is widely used for identifying the risk of soil erosion wherever the limit is exceeded. It is effectively utilized for executing suitable erosion control measures and sustainable land use planning. It is, therefore, necessary to recognize a specific tolerance limit for a particular region depending on the conditions specific to the region and objectives established at the local level instead of relying on a generalized value.

Recognizing the implications of scientifically evaluated soil loss tolerance limits for identifying erosion risk zones, soil fertility loss, sedimentation, etc., Li et al. (2009) outlined various studies towards establishing T-values. Based on their assessment, the study recommends the consideration of three significant criteria, embracing soil formation rate (T1), soil sustainability (T2) and conservation management (T3), for determining soil loss tolerance of any region.

Mandal et al. (2010) emphasize the significance of examining soil's economic and ecological sustainability for generating threshold limits to soil erosion for soil conservation initiatives. The study was conducted in Doon valley, India and T-values were developed using two methods. The first method relies on evaluating an acceptable rate of declining soil productivity and a sustainable land use planning period. In contrast, the second method takes into account the existing soil conditions. Comparing both methods, the study proclaimed the second method more rational as the data required for its determination are easily available for all regions.

Bhattacharya et al. (2008), Lakaria et al. (2008), and Lenka et al. (2014) have attempted to produce a method for quantitatively estimating soil loss tolerance limits (T) in India, encompassing the Shivalik-Himalayas, Central parts of India, and West Bengal respectively. They have performed T-value estimation to recommend appropriate soil conservation strategies. At the same time, Mandal and Sharda (2011(a)) estimated the T-values integrating pertinent factors based on biophysical models covering the entire country. In all these studies, various properties of soil were incorporated for evaluating soil quality that influences the soil’s ability to resist erosion. For estimating the T-value, these studies adhered to a standard recommendation made by USDA-NRCS, making some adjustments. Their findings reveal that the T-values of all the regions range between 2.5 and 12.5 Mg h^{-1} y^{-1} in contrast to the previously employed fixed value of 11.2 Mg h^{-1} y^{-1} for the whole country. The observed values were considered to assist the process of generating conservative strategies for specific sites and determine priority areas for watershed management initiatives in India.

For the assessment of soil erosion risk in the Eastern Himalayan region, Mandal and Sharda (2011(b)) developed a methodology by incorporating the rates of soil loss with T-values. The spatial data for both the soil data and the permissible

values were prepared under a GIS environment to identify the soil erosion risk zone. Based on the methodology developed, it was found that about 29.70 per cent of the study area falls under a very critical zone of soil erosion risk which is mainly the result of continuous deforestation, faulty methods of farming, and overgrazing, and thus, required instant consideration for soil conservation. The estimated T-values in the northeastern region were observed to be relatively uniform, ranging between 7.5 and 12.5 Mg ha^{-1} yr^{-1}. The study further recommended the application of the erosion risk map as an input for executing various conservation measures and land use planning.

3.6 Sediment Yield Estimation

In the sedimentation handbook, USDA-SCS (1972) demonstrated the reciprocal influence of watershed size on the amount of sediment yield. As sediment travels less distances in a smaller watershed (SW), the chances of balancing varying generated sediments are reduced compared to a relatively larger watershed (LW). Moreover, SW typically exhibits limited land use, higher average slope, steeper channel gradients, etc., than their larger counterparts. Consequently, SW tends to have a higher sediment yield rate and more significant variability than LW. Therefore, sediment yields are estimated mainly based on the size of a particular watershed. However, the study also considered distinct variables like climate, vegetation, soil texture and land use to estimate sediment yield in a given area.

In a comprehensive work on sedimentation engineering, Vanoni (1975) presents broad guidelines covering sediment concerns and the procedures linked to its utilization, preservation and management of land and water resources. The study has discussed that the previous studies based on relationship evaluation indicate the close association of the watershed size with the sediment delivery ratio (SDR) parameters. Hence, a generalized SDR curve was established by deriving an exponential function from various data compiled by studying 300 watersheds.

Walling (1983) emphasized the need for thorough research in erosion and sedimentation, mainly through augmented apprehension on soil loss and sediment delivery processes. The study addressed concerns regarding aggregating spatial and temporal data and identified shortcomings of the sediment delivery ratio (SDR) concept. It discussed contemporary developments in modeling the sediment delivery

system but noted the lack of comprehensive empirical research. The article also stressed the importance of including nutrients and pollutants in sediment delivery research, highlighting the need for further investigation.

Identifying an appropriate model for determining sediment delivery ratio (SDR) in a watershed, Quyang et al. (1997) analyzed various SDR prediction models under a GIS environment. Sediment data, which encompasses information from monitoring stations such as those operated by the US Geological Survey, are employed for validating these models. The study reveals that prediction based on watershed size is the most commonly accepted approach for estimating the SDR among different methods. Based on their assessment, it was observed that drainage area-based SDR produced satisfactory results for the area under consideration. They have further discussed that larger watersheds are generally characterized by lower SDR, as larger areas offer increased opportunities to retain the sediments, reducing sediment yield chances.

To identify gross soil erosion and pollution produced by sediment discharge from the Gediz River basin in Turkey, Fistikoglu and Harmancioglu (2002) carried out modeling based on an integrated USLE-GIS approach. Soil loss was calculated using the USLE model, while sediment yield from the study area was calculated from the product of gross soil erosion through USLE and the SDR. In this study, the authors have also highlighted the challenges associated with implementing the methodology in situations where there is a lack of sufficient and high-quality data related to land use, soil characteristics and vegetation, a common issue in many developing nations.

Lim et al. (2005) enhanced the "Sediment Assessment Tool for Effective Erosion Control (SATEEC)" under the GIS platform for calculating the rate of soil erosion and the subsequent sediment production anywhere in the basin by applying the RUSLE along with the geographically dispersed SDR. The study highlighted a few SDR curves that were developed based on the watershed size and mentioned their wide application due to their simple nature. The authors emphasize using a distinct SDR obtained from an inherent watershed characteristic. However, the study suggested users rely on Vanoni's (1975) SDR equation in case of limited experience as acquiring such specific watershed SDR can be challenging.

Generally, it is commonly assumed that there is an inverse relationship between the amount of sediment yield and the size of a basin. This straightforward concept is often used when estimating sediment yield in an ungauged basin due to its simplicity. In this context, a study by de Vente et al. (2007) reviewed explanations and observations from various authors. The study found that sediment yield generally decreases as the basin area increases. However, this decreasing trend may not be consistent across all regions or delayed depending on local environmental factors such as topography, climate, land use, and geological characteristics. Furthermore, the trends can vary significantly over different periods. Therefore, predicting sediment yield based solely on basin size may be complex and should be cautiously approached.

Gelagay (2016) applied the combination of the Revised Universal Soil Loss Equation model and sediment delivery ratio (RUSLE-SDR) method for preparing the sediment yield map of the Koga watershed in Ethiopia, where there is no sufficient data. The advanced remote sensing and GIS techniques were applied to assess the watershed characteristics and the predicted rate of soil erosion and sediment yield. He estimated the amount of soil loss with the RUSLE model, while the sediment delivery ratio (SDR) was prepared from the slope of the main river channel. The spatial distribution of sediment yield was then prepared by considering the raster layer product of the estimated sediment delivery ratio and the predicted rate of soil erosion cell-wise.

Wu et al. (2017) have examined various research works concerning the global advancement of SDR (Sediment Delivery Ratio), with a primary emphasis on methodologies employed in China. The authors asserted that SDR equations developed empirically using data from a specific region cannot be readily applied to diverse river basins. Consequently, the study suggests creating a regional SDR model that incorporates exceptionally precise regional data, achieved through enhanced high-resolution remote sensing data development.

To investigate the impact of changes in land use and land cover on soil loss and sediment yield, Kidane et al. (2019) utilized the RUSLE-SDR model within a GIS framework. They conducted this assessment for three distinct periods: 1973, 1995, and 2015. Their findings indicated a strong correlation between soil loss and sediment yield in the study area. Notably, the alteration of natural forest on the relatively steeper slopes of the basin into vast farmland was identified as a major contributor to increased

soil loss. This significant shift in land use was recognized as the primary driver of heightened sediment yield downstream. Consequently, the study recommended implementing watershed conservation measures in these critical areas to mitigate soil erosion and its associated issues.

Using GIS, Kothyari & Jain (1997) developed a method for estimating sediment yield in the Karso catchment in Bihar. The USLE parameters, spatial discretization of the watershed, and the estimation of soil erosion and sediment yield were all prepared through the ILWIS package in a GIS environment. For determining the sediment yield at the basin outlet, they have applied the sediment delivery ratio concept for routing the soil loss amount for each cell. They devised an equation for estimating the sediment delivery ratio based on the basin area and slope. By applying the proposed method, they have predicted sediment yield for multiple storm events in the watershed selected for the study and achieved reasonable results. Moreover, they have also recommended the application of this method for various ungauged watersheds with similar characteristics.

To estimate soil loss and sediment yield in a small basin of South India, Magesh and Chandrasekar (2016) applied the RUSLE-SY (sediment yield) modeling approach in the GIS platform. In this study, soil loss was computed by the RUSLE model while the sediment yield was estimated based on the sediment delivery ratio (SDR) formulated by the USDA-SCS, considering its simplicity and viability. The present study revealed that integrating the RUSLE-SY model with GIS produced adequate information for the study area and considered the current approach a promising methodology for comparable regions.

Swarnkar et al. (2018) proposed a methodology to evaluate and disseminate uncertainties for the estimated soil loss, sediment delivery ratio and the sediment yield based on first-order uncertainty analysis to enhance soil erosion and sediment yield estimates. The study utilized the RUSLE-SDR approach and uncertainty estimates to identify erosion distribution, sediment yield, and possible uncertainties from the Garra River basin. Despite numerous constraints, the study discusses the applicability of the suggested approach for verifying uncertainties in soil erosion and sediment yield estimation, especially for the ungauged basins where sheet and rill erosion predominates.

Rajbanshi & Bhattacharya (2021) have studied the potential influence of temporal climatic characteristics for estimating soil erosion and sediment yield of the Konar catchment in the upper Damodar basin, based on the integrated model of RUSLE-SDR. Among the climatic variables, the rainfall erosivity factor (R factor) was mainly selected to relate to various regional climate models (RCMs) where the bias data were corrected to derive future erosivity of rainfall and its impact on the rate of soil erosion and sediment yield. The spatiotemporal results of their predicted rainfall show a positive trend, which implies the possibility of increasing rainfall erosivity and, thus, a higher chance of soil erosion and sediment yield in the study area and the subsequent course of time.

For soil erosion assessment in a mountainous river basin of India highly influenced by monsoon, Thomas et al. (2018) have undertaken quantification of soil loss and sediment yield along with erosion risk mapping. This study computed soil loss using the RUSLE model while sediment yield was estimated through the RUSLE and basin area-based SDR curves RUSLE-SDR approach. Among various land use/land cover classes, it was found that those bearing anthropogenic activities manifest significant sediment sources due to higher SDR values. Besides showcasing the practical use of remote sensing and GIS techniques, the quantified soil loss and sediment yields are anticipated to offer valuable insights for improving watershed management in the study area.

3.7 Watershed Prioritization

In 2016, Farhan and Anaba delineated a small sub-basin of Wadi Shueib in Jordan into fourteen smaller sub-watersheds to conduct a prioritization. Within this research, the authors examined the morphological attributes and susceptibility to erosion for each of these sub-watersheds. To perform these analyses, they took into account a total of twenty-five morphometric parameters and sixteen parameters related to erosion susceptibility. The findings from both assessments were arranged based on their respective values using the compound value method, resulting in priority rankings for each of the sub-watersheds.

To prioritize sub-watersheds concerning sediment loss, Ayele et al. (2020) utilized both the RUSLE and Sediment Yield Index (SYI) models in the Ethiopian

highlands. These two models were used to establish a robust methodology by comparing them rather than relying on a single model. To address the issue of depending solely on one model, the study calculated the average values from both models to determine rankings. However, the obtained results from these models yielded a consistent result, which indicates a significant relationship between the landscape's topography and erosion rates in the study area. As a result, the study recommended the immediate implementation of soil conservation measures in the identified high-priority areas.

Sinshaw et al. (2021) conducted a prioritization of erosion in the Ribb watershed, Ethiopia, to facilitate the implementation of effective soil and water conservation plans. They used the fuzzy Analytical Hierarchy Process (AHP) model, a multi-criteria decision-making tool, to assess the potential risk of soil erosion. The projected soil erosion was categorized into levels ranging from very low to very high susceptibility to erosion. Subsequently, prioritization focused on areas within the high and very high erosion susceptibility zones. This approach aimed to align with the changing climate conditions in the watershed and address the resulting sedimentation concerns downstream in the reservoir.

Utilizing Remote Sensing and GIS techniques, Thakkar and Dhiman (2007) conducted a morphometric analysis considering nine parameters and prioritize the eight sub-watersheds within the Mohr watershed in India. Compound values were computed for each parameter, and prioritized ratings for all the delineated sub-watersheds were established in the study area. The highest priority was then assigned to the sub-watershed, which exhibited a lower compound value, indicating a greater risk of soil erosion. As a result, immediate conservation measures were recommended to those critical areas.

Sudhishri et al. (2014) prioritised a Himalayan watershed to pursue sustainable management. Their study involved the combination of the RUSLE model with locally established thresholds for permissible soil loss (referred to as T), resulting in the creation of an Erosion Tolerance Index (ETI) for the study region, which made use of remote sensing (RS) and geographic information system (GIS) techniques. Their findings underscore the importance of the applied methodology in maintaining soil loss within acceptable limits in the designated areas. This emphasizes the critical role

of soil loss tolerance thresholds in achieving watershed sustainability for the watershed.

Gajbhiye et al. (2013) utilized RS and GIS techniques to examine the geomorphic attributes of the Manot watershed in India. The research aimed to prioritize this watershed by subdividing it into fourteen smaller sub-watersheds. They determined the relative importance of these sub-watersheds by calculating compound values for various morphometric parameters and assigning them ranks. The study's findings were validated in the field within the same area, and it was found that the predicted erosion vulnerability of the watershed closely matched the actual conditions observed.

Mhaske et al. (2021) assessed soil erosion in the mining regions of Jharkhand, India, intending to prioritize watershed management. The study utilized two distinct methods, the RUSLE and AHP models, to calculate the extent of soil loss and assess erosion risk. Their analysis revealed that the hilltop mining areas within the watershed experienced significant soil erosion. In this study, the authors have divided the watershed into smaller segments for prioritization and determined the most heavily impacted areas by combining the outcomes of both methods.

Using the GIS-based USLE model to estimate soil loss, Chatterjee et al. (2013) conducted a prioritization of watersheds in a small section of the Chhotanagpur plateau in India. The study involved the creation of Erosion Vulnerability Units (EVUs) by assessing soil loss in numerous micro-watersheds within the watershed boundaries. These micro-units, each reflecting varying degrees of soil erosion, were intended to facilitate sustainable watershed management and planning in the research area. The authors also recommended applying this methodology to other watersheds with similar conditions to promote the sustainability of watersheds and to support improved planning and conservation strategies.

In 2016, Markose and Jayappa attempted to prioritize sub-watersheds within the Kali River basin in India, by estimating soil loss using the RUSLE model. During their research, the authors partitioned the river basin into 165 sub-watersheds and calculated the extent of soil loss for each unit. They then utilized the estimated erosion rates to assign rankings, categorizing the basin into four levels of erosion risk. They

noted that the assessed soil erosion rates and the resulting prioritization map could be valuable for developing an improved management plan for the study area.

Chowdary et al. (2013) defined specific objectives for prioritizing watershed areas in the Mayurakshi watershed of Jharkhand to implement conservation management. They employed a multi-criteria decision-making (MCDM) approach and the sediment delivery ratio (SDR) model to achieve this. The research involved the delineation of 276 sub-watersheds; among them, 100 sub-watersheds received high priority for implementing watershed management measures. A substantial agreement level of approximately 78% was observed by comparing the outputs of the two models. As a result, the study concluded that watershed prioritization based on spatial data layers is highly dependable.

Altaf et al. (2014) have prioritised sub-watersheds in the Rembiara basin, situated in the western Himalayas, to assess susceptibility to soil erosion. Their study successfully manifested the application of integrated remote sensing and field data to evaluate erosion vulnerability. This assessment was performed through a multi-criteria assessment method, the Compound Value (C_V) within a GIS framework. The research incorporated morphometric and land cover characteristics into the C_V method to determine watershed prioritization based on varying degrees of susceptibility to soil erosion. Moreover, the results were categorized into different levels of erosion susceptibility, spanning from low to very high susceptibility classes for each sub-watershed. Finally, the study prepares a comprehensive prioritization map based on the findings and its classification for different sub-watersheds to initiate suitable actions to reduce soil erosion within the research area.

Bhattacharya et al. (2020) compared the effectiveness of two approaches for prioritizing sub-watersheds in the Kangsabati basin, India. They employed a multi-criteria decision-making (MCDM) method incorporating fifteen morphometric parameters. Also, they used the Soil and Water Assessment Tool (SWAT) model, which relied on five parameters: rainfall, slope, land use, land cover, and soil properties. The results, after validation, demonstrated that the MCDM methods outperformed the SWAT model in terms of prediction accuracy, providing a relatively higher level of precision for sub-watershed prioritization considering erosion susceptibility, reduction in soil fertility and reservoir sedimentation.

CHAPTER-4

METHODOLOGY

4.1 Introduction

The present study deals with assessing soil erosion and sedimentation through a detailed analysis of various influencing factors. It mainly focused on applying qualitative and quantitative models to understand the watershed status comprehensively. The advanced technology of remote sensing and Geographic Information Systems (GIS) has been primarily utilized with these models for producing beneficial insights into the process of soil erosion and sedimentation in the study area, as this technique provides a potent tool for spatial analysis. This chapter presents the various materials and methodologies adopted in the present research.

4.2 Data Acquisition

In the context of this research, information comprising primary and secondary data has been obtained through multiple sources and extensive field surveys as given below: -

(1) Topographical maps provided by the Survey of India, 84 A/9, 84 A/10 and 84 A/14, with a scale of 1:50,0000, have been utilized to create the base map.

(2) Sentinel-2 Satellite Imagery was obtained from Copernicus, European Space Agency (ESA), featuring an image resolution of 10m on 9th March 2022.

(3) Shuttle Radar Topography Mission Digital Elevation Model (SRTM-DEM) with 30m spatial resolution was acquired on 5th August 2021 from the United States Geological Survey (USGS) Earth Explorer.

(4) Lithology and geomorphology map was downloaded from the Geological Survey of India online data portal, Bhukosh-GSI.

(5) Rainfall data were collected from 3 stations, viz., the State Meteorological Centre, Directorate of Science & Technology, Govt. of Mizoram, HQ CE (P) Pushpak, Aizawl and BDO Office, Thingsulthliah.

(6) An extensive field survey was conducted for erosion inventory, and various location of erosional and non-erosional features were identified and marked with handheld GPS.

(7) Ground truthing was also done substantially for visual observation and verification to check the accuracy of various thematic layers produced.

(8) Ninety soil sampling sites were prepared at regular intervals of 1 km following the systematic sampling method. Through field surveys, composited soil samples were collected to improve the replication in each site from a V-shaped cut soil from a depth of 15 cm. The collected soil samples were mixed thoroughly and keep in a clean plastic bag. These samples were dried in a room temperature and then sifted with a 2 mm sieve. Two separate bags of soil samples were gathered for every sites. One of each two samples were then taken to the State Soil Testing Laboratory, Aizawl, to determine the Organic Carbon content, while the other samples were used for soil textural analysis.

4.3 Preparation of Physical and Environmental settings

The Base map for Chite Watershed was first prepared using Survey of India Topographical Map No. 84A/9, 84A/10 and 84A/14. Most of the works, including digitization, georeferencing and preparation of thematic layers, were executed through ArcGIS software.

Elevation, slope, drainage, lineaments, and hypsometric analysis were all produced from the SRTM-DEM. The elevation and slope maps were generated through symbology and 3D Analyst Tools. For extracting the drainage network, flow accumulation made from the DEM image was classified into two classes with a threshold value of 200 in break values so that even the smallest tributary streams are visible. Stream ordering was then computed based on Strahler's (1964) Hierarchical

Rank method. Ground truthing was also performed, and it was observed that most of the 1st-order streams are non-perennial. The lineament features were obtained from the DEM image, where various linear features, excluding the artificial features, were derived through visual interpretation. The DEM imagery was also used to analyse the watershed's hypsometric curve and hypsometric integral using Strahler's (1952) method. The hypsometric curve was prepared graphically by plotting relative area (a/A) and relative relief (h/H) on the horizontal and vertical axes, while the hypsometric integral was computed by the given formula (Pike and Wilson, 1971):

Hi = (Mean Elevation-Min Elevation) / (Max elevation-Min elevation)

Where, Hi refers to the hypsometric integral

Lithological Units obtained from Bhukosh-GSI and Lineaments extracted from DEM imagery represent the geological map. Similarly, the geomorphological map was also outlined by utilizing the downloaded geomorphological map. Lineament features were also added to the geomorphological map, representing various linear structural features of the earth's surface like faults, fractures, etc.

The climate of the study area was spatially represented by rainfall distribution. As the watershed has only one rainfall recording station, the other two stations were selected from nearby areas, which were found to have an impact through the Thiessen polygon. Long-term average rainfall was calculated for 12 years based on the data collected from the 3 stations. The spatial distribution of rainfall was then generated by interpolating the station records using the Inverse Distance Weighted (IDW) method in Spatial Analyst Tools (Fig 4.1).

The vegetation map was represented through the Normalized Vegetation Index (NDVI) prepared from radiometrically corrected Sentinel-2 imagery. For deriving NDVI values for the study area, satellite imagery captured on 9th March 2022 was deliberately chosen, as the months of February and March are considered suitable for studying natural forests and vegetation in the moist evergreen and semi-evergreen regions of North-East India (Ranganath et al., 2000). The method given by Rouse et al. (1974) was used to calculate the NDVI values using a raster calculator:

NDVI = (NIR - R) / (NIR + R)

Where, NIR refers to the Near-Infrared Band

R denotes the Red Band of the Sentinel-2 image.

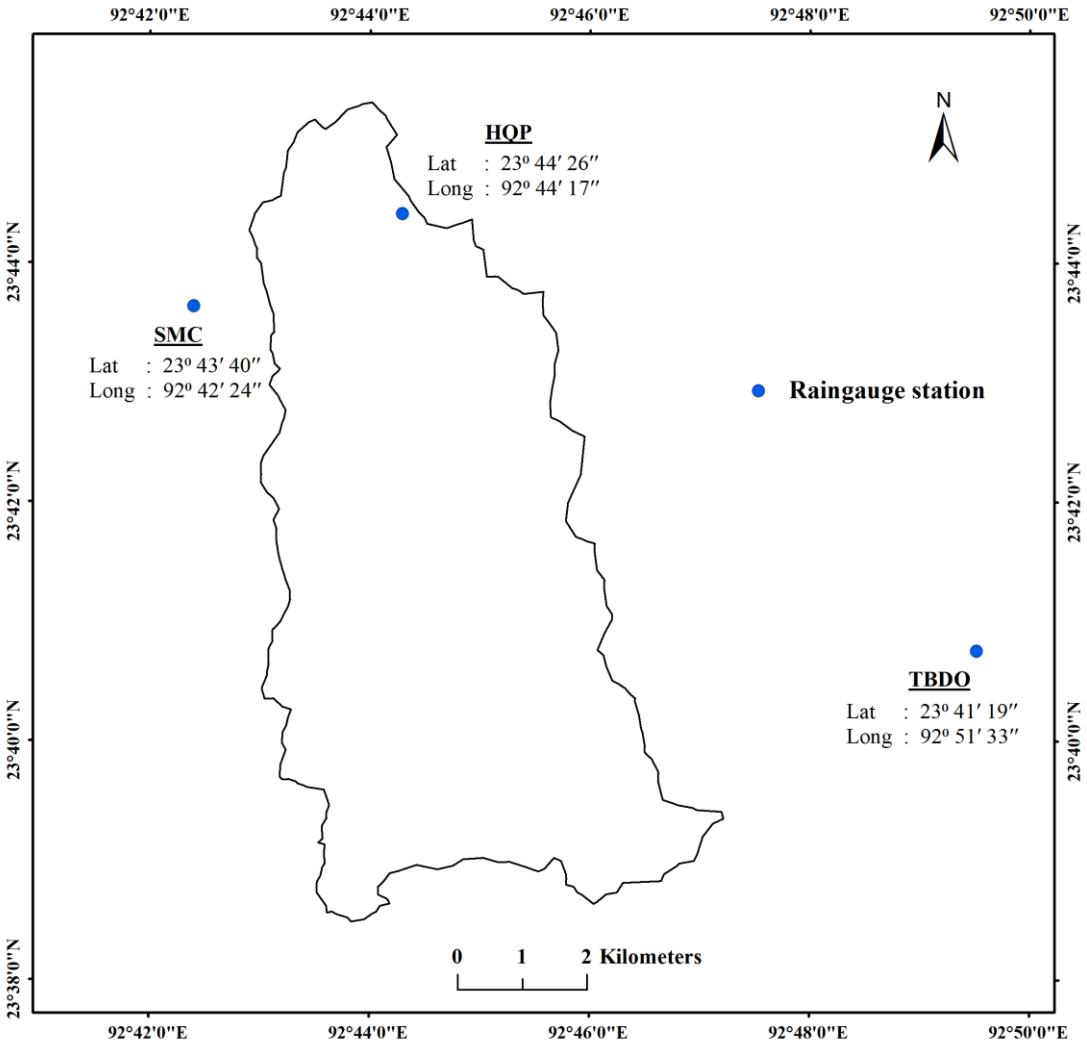

Fig 4.1: Location of rainfall recording stations.

4.4 Assessment of Soil Erosion Susceptibility

4.4.1 Introduction

To ensure the successful application of erosion control and resource conservation measures, it is essential to identify region's susceptibility to the potential effects of soil erosion (Gelagay and Minale, 2016). Ideally, this should be done through erosion susceptibility mapping, preferably on a watershed level. As soil erosion is a dynamic phenomenon, evaluating erosion susceptibility can be quite complex and challenging since it demands a thorough comprehension of intricate relationships among different influencing factors. However, Multi-criteria decision-making (MCDM) method is valuable for addressing complicated issues because it provides a structured framework for evaluating and making decisions when multiple parameters or factors are involved. Hence, different models have been developed based on MCDM approach in various fields. The Analytical Hierarchy Process (AHP), introduced by Saaty (1980), has consistently been a highly favoured and extensively employed technique for multi-criteria decision-making and planning since its inception, mainly because of its lucidity and flexibility with precise outcomes, its capability to assess qualitative as well quantitative factors, its ability to detect inconsistency or bias opinion, etc. (Harker and Vargas, 1987; Khaira and Dwivedi, 2018). Moreover, the method is well compatible with advanced technique of Remote Sensing and GIS, which has dramatically improved its application for spatial analysis (Kachouri et al., 2015; Haidara et al., 2019; Semlali et al., 2019; Vojtek and Vojtekova, 2019; Chakrabortty et al., 2020). This capacity of the AHP has further enhanced its applicability to soil erosion susceptibility mapping worldwide (Sandeep et al., 2020; Aslam et al., 2021; Neji et al., 2021; Mushtaq et al., 2023). The simple and dependable nature of the AHP has also made the technique a particular recommendation for analysing a complex system, especially among developing nations (Vaidya and Kumar, 2006). Hence, erosion susceptibility mapping for the study area was undertaken by integrating the AHP method with the Remote Sensing and GIS techniques, following a systematic methodology, as shown in Fig 4.2.

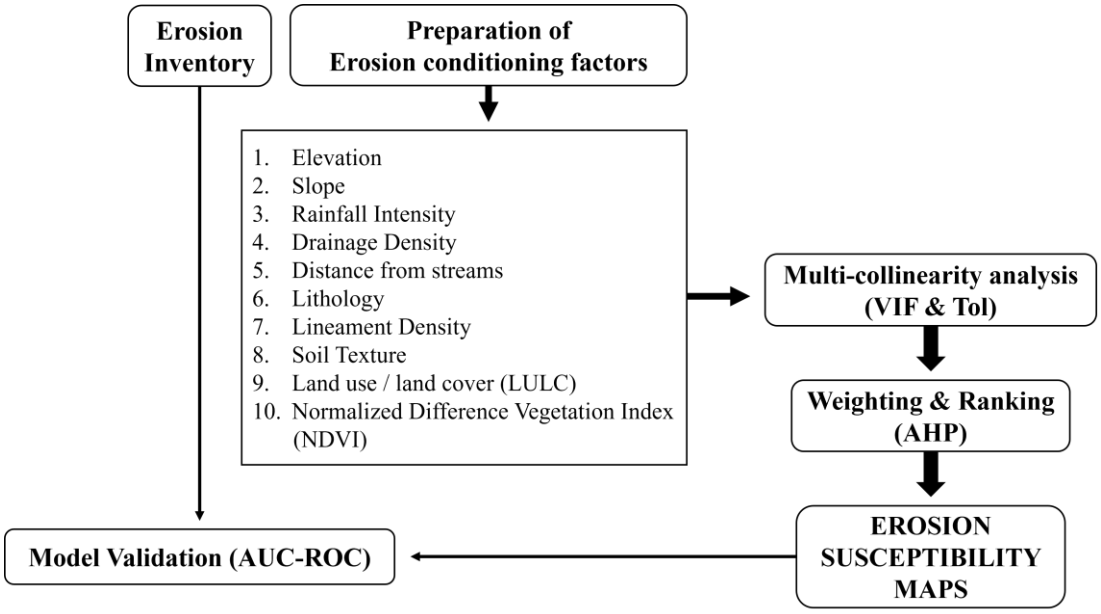

Fig 4.2: Methodological flowchart for erosion susceptibility mapping.

4.4.2 Erosion Inventory

Erosion inventory is essential to prepare an inventory map for validating the soil erosion susceptibility model. Specific sites with active erosional features and those areas found to be relatively safe or less affected by the erosion process were observed through extensive field surveys, and the location details were recorded with handheld GPS. A total of 223 location points were collected for erosion (133 points) and non-erosion sites (90 points) throughout the watershed. The erosion Inventory map was then prepared by integrating the geographical locations of erosion and non-erosion points with the base map (Fig 4.3).

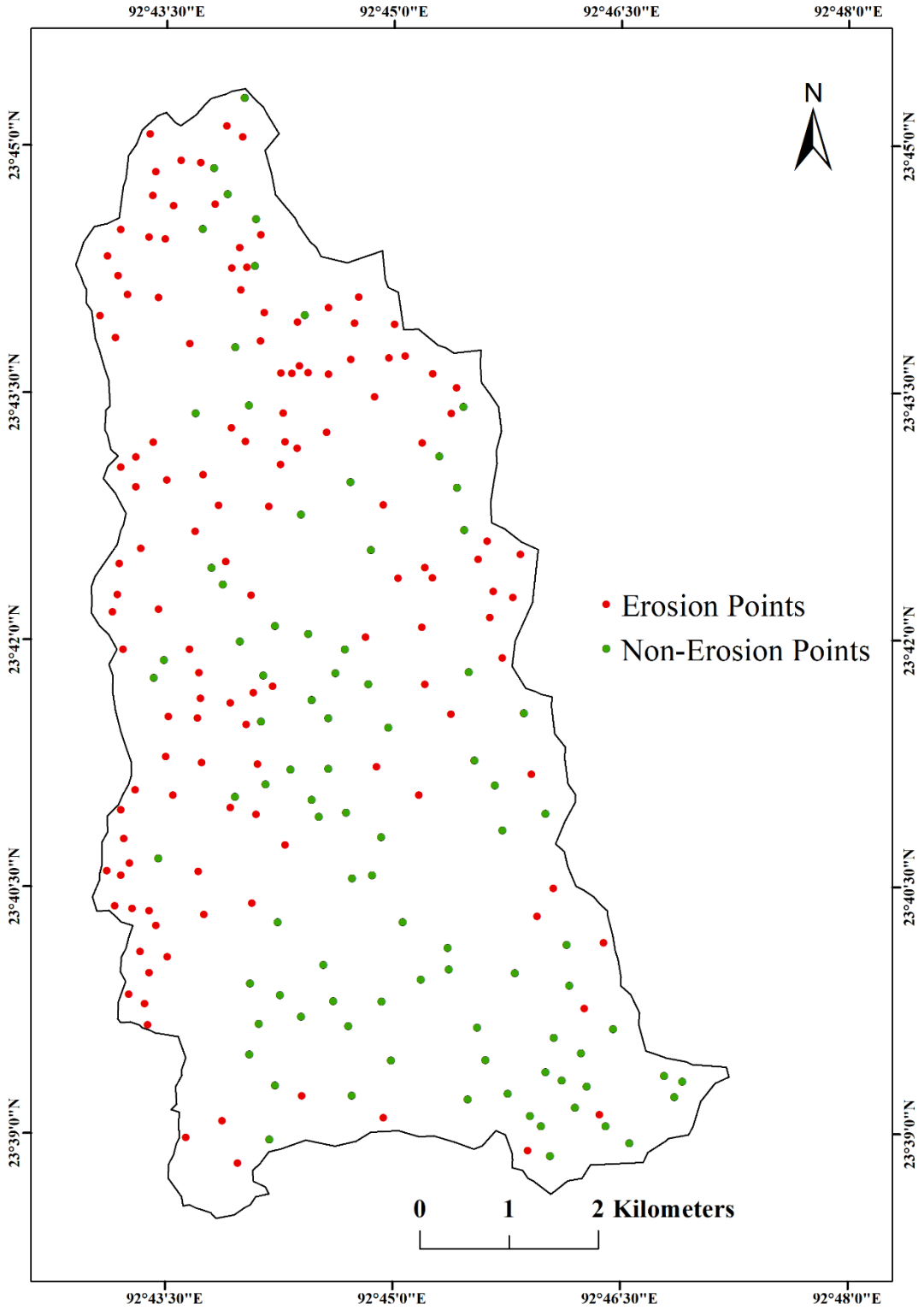

Fig 4.3: Erosion inventory map.

4.4.3 Preparation of erosion conditioning factors

As soil erosion is a dynamic phenomenon that involves a complex interaction of various causative factors, a comprehensive understanding of all these factors and their influence on erosion processes is necessary for erosion susceptibility mapping (Rahman et al., 2009). Based on a substantial literature review and through the knowledge gained from field observation, ten factors, viz. Elevation, slope, drainage density, distance from streams, rainfall intensity, normalized difference vegetation index (NDVI), land use/land cover (LULC), lithology, lineament density, and soil texture were believed to exert a substantial impact on the occurrences of soil erosion and were deliberately selected for the causative parameters. Thematic layers were then prepared for all these selected parameters and were projected under WGS1984 UTM Zone 46 in the ArcGIS platform to provide a comparable coordinate system. Furthermore, all the vector layers were also converted into raster layers under spatial analyst extension and a spatial resolution of 30 m was set for all the layers. All the necessary data required for preparing thematic layers were collected and organized from various authenticated sources, applying standard analytical procedures.

The preparation of thematic layers such as elevation, slope, and NDVI and the extraction of drainage networks, lineaments and lithological units are explained under the sub-heading 4.3, “Preparation of physical settings”.

Drainage density and distance from steams were prepared from the extracted drainage map from the SRTM DEM image. The line density tool was utilized for generating the drainage density layer. At the same time, distance from the steams layer was produced through the Euclidean Distance buffer in the ArcGIS platform. Lineament density was calculated as the length of structural linear features in km unit per km^2 of land area. The lineament density map was also prepared through line density tools based on the extracted lineament features.

Radiometrically corrected Sentinel-2 Imagery was used to develop the Land use/Land cover (LULC) map. The preparation of different LULC classes involved a Supervised - Maximum Likelihood Classification (MLC) method, which produced an overall accuracy and a kappa coefficient of 87% and 0.88, respectively.

In this study, rainfall intensity was established by employing the Modified Fournier Index adapted for the Indian context, which is given by the formula (Tiwari et al., 2015):

$$RI = \sum_{i=1}^{12} \frac{P_i^2}{P}$$

Where, P_i indicates the monthly average rainfall in mm for the i^{th} month.

P refers to the average annual rainfall in mm.

To generate the spatial pattern of rainfall intensity (RI), the calculated RI values for the three rain gauge stations were interpolated through the Inverse Distance Weighted (IDW) method.

The collected soil samples from 90 sampling sites (Fig 4.5) in and around the study area were analyzed through the Bouyoucos Hydrometer Method to determine particle size distribution using the following standard analytical procedures given by the Ministry of Agriculture (2011) and Motsara and Roy (2008). The soil textural class were then identified with the United States Department of Agriculture (USDA) Textural Triangle (Fig 4.4) based on the relative per cent of sand, silt and clay particles. Sub-classification was performed based on the revised and enlarged U.S. Department of Agriculture-Soil Survey Manual, Handbook No. 18 (USDA, 2017) to present a more distinct textural class. A soil texture map was prepared by interpolating all the obtained textural classes using the IDW method.

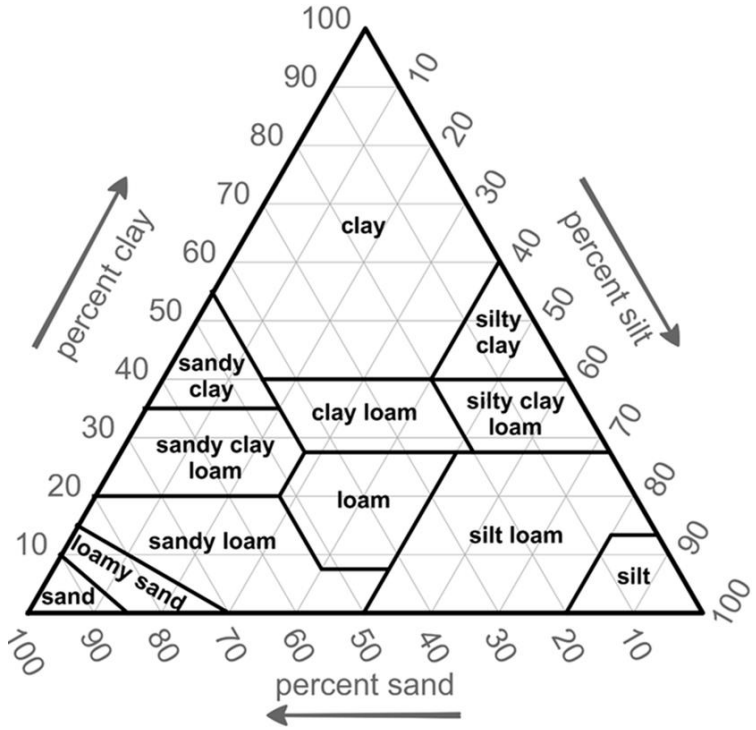

Fig 4.4: USDA Soil Textural Triangle.

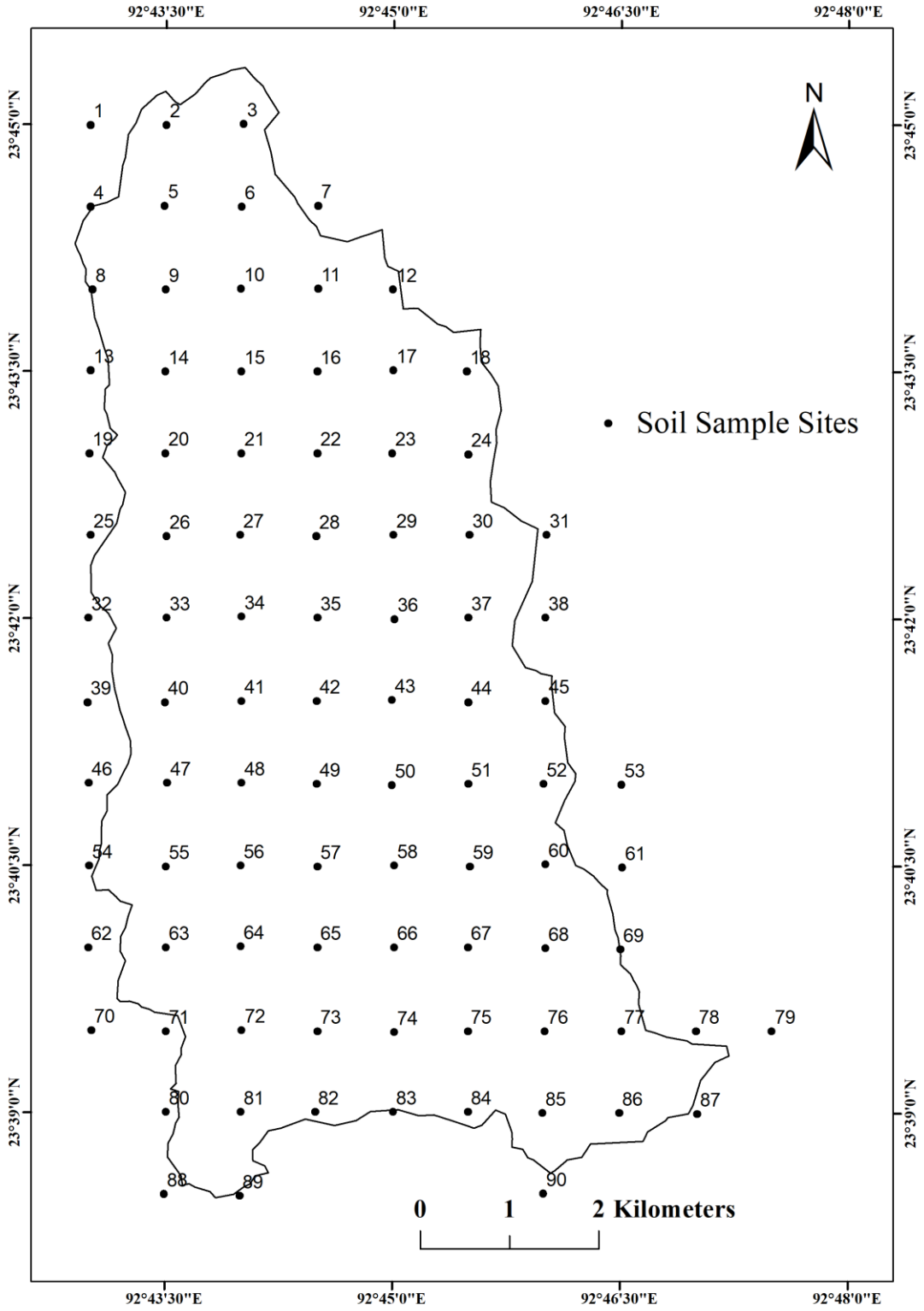

Fig 4.5: Soil sampling sites in Chite watershed.

4.4.4 Multicollinearity analysis

After completing the thematic layers preparation, multicollinearity analysis was conducted to check whether collinearity exists among independent variables. A pragmatic proof is crucial for multicollinearity in vulnerability analysis as the mathematical and machine learning algorithms may produce high correlation (Alqadhi et al., 2022). Hence, multicollinearity was examined by the Variance Inflation factor (VIF) and Tolerance (T) using IBM SPSS 25, which can be represented by the given expression (Myers et al., 2010):

$$T_i = 1 - R_i^2$$

$$VIF_i = \frac{1}{T_i}$$

Where, T_i = Tolerance of the i^{th} predictor variable.

VIF_i = Variance inflation factor of the i^{th} predictor variable.

R_i^2 = Coefficient of determination of the regression equation.

To assess multicollinearity issues, 700 random points were selected by the "Create Random Points" tool in ArcGIS software. The randomly chosen points for each thematic layer were then extracted by the "Extract Multi Values to Points" tool in Spatial Analyst Tools, and the multicollinearity test was conducted.

4.4.5 Assigning weights and ranks by the Analytical Hierarchy Process (AHP)

In this research, the AHP technique has been utilized to produce soil erosion susceptibility maps considering the relative influence of various thematic layers concerning different geo-environmental factors. This method can synthesize a complex subjective and objective factor that influences an intricate system through a pairwise comparison matrix, which involves the assignment of weights based on the relative significance of selected parameters using a dimensionless ratio scale ranging from 1 to 9 (Saaty, 2008; Forman and Gass, 2014) as shown in Table 4.1.

Table 4.1: Preference scale for criteria.

Preference scale	Level of preference
1	Equally important
3	Moderately important
5	Strongly important
7	Very strongly important
9	Extremely important
2,4,6,8	Intermediate values
Reciprocals	Inverse comparison

Source: Saaty (2008).

In this scale, it was suggested to assign a value of 1 to indicate "equal importance" between two comparative factors, whereas a value of 9 will be given to a situation where one factor is considered "extremely important" over the other factor in a comparison (Saaty, 1977; Saaty and Vargas, 1991). For an inverse comparison, the reciprocal values of relative preference level will be used, which range between 1/2 and 1/9 (Mondal and Maiti, 2013).

After formulating a pair-wise comparison matrix, the criteria weights were calculated from the matrix. The calculation first requires the addition of relative weight values of elements in each column, which were then used for dividing each cell's values in the corresponding columns. These computed values represent the normalized pair-wise comparison matrix, and the criteria weights (normalized weights or the principal eigenvalues) are obtained by determining the mean values for each row.

Subsequently, the eigenvector matrix calculated from the pairwise comparisons must be assessed to check the consistency of the judgement, as decision-makers may produce inconsistent judgement with unreliable results. To check consistency of the generated eigenvector matrix, the Consistency ratio (CR) must be calculated, which will determine the extent of approval or disapproval with the judgments using the given equation:

$$CR = \frac{CI}{RI}$$

In this context, RI refers to the random index, denoting the mean value for the observed consistency index, which depends upon the arrangement of the comparison matrix, as proposed by Saaty and Vargas (1991) (Table 4.2). The consistency index (CI) can be determined through the equation provided:

$$CI = \frac{\lambda_{max} - n}{n-1}$$

Where, λ_{max} = the principal eigenvalue in the comparison matrix

n = the number of criteria considered.

Table 4.2: Random Index (RI) for ten conditioning factors.

n	1	2	3	4	5	6	7	8	9	10
RI	0.00	0.00	0.58	0.90	1.12	1.24	1.32	1.41	1.45	1.49

Source: Saaty and Vargas (1991).

The calculated CR value is considered acceptable if it is ≤ 0.1; however, if the CR value is more than 0.1, the judgement made in the comparison matrix is regarded as unreliable; hence, a revision is necessary to derive a dependable outcome (Saaty, 1977).

4.4.6 Erosion susceptibility mapping.

Erosion susceptibility mapping has been performed by applying the ten erosion conditioning factors weight determined through the AHP techniques. The Soil Erosion Susceptibility Index (SESI) was calculated using the Weighted Sum method in ArcGIS software to produce the spatial model. The equation calculates this index:

$$SESI = \sum_{i=1}^{n} W_i^s \text{ x } S_i^s$$

Where, SESI = Soil Erosion Susceptibility Index

n = number of criteria considered

W_i^s = selected criteria's weight

S_i^s = criteria's sub-classes weight.

4.4.7 Model's validation

Validation of a model is necessary to assess its accuracy and reliability (Ali et al., 2019). To perform this operation, the erosion inventory map was compared with the generated soil erosion susceptibility map using the Receiver Operating Characteristics (ROC) curves. In this curve, the threshold values are illustrated in graphical coordinates where the true positive rate (sensitivity) is plotted on the ordinate (y-axis) and the complementary false positive rate (1-specificity) on the abscissa (x-axis) (Arabameri et al., 2019 (a)). Furthermore, the area under the ROC curve (AUC) was computed to express the model's accuracy in terms of numerical metrics, which should extend from 0.5 to 1, where a higher AUC value suggests a desirable prediction, while a lower value indicates the opposite (Myronidis et al., 2016; Saha et al., 2019). The ROC curve can be obtained by the given equation (Pourghasemi et al., 2013):

$$\text{False Positive Rate (x-axis)} = 1 - \left[\frac{TN}{TN+FP}\right]$$

$$\text{True Positive Rate (y-axis)} = 1 - \left[\frac{TN}{TN+FP}\right]$$

Where, TN indicates True negative, and FP represents False positives.

4.5 Estimation of Soil Loss and Sediment Yield

4.5.1 Introduction

Several erosion models have been developed and applied worldwide to quantify soil loss and sediment yield. Among these multiple models, the "Revised Universal Soil Loss Equation (RUSLE)" (Renard et al., 1997) and its antecedent, the "Universal Soil Loss Equation (USLE)" (Wischmeier and Smith, 1978) are the most frequently applied empirical models for estimating soil erosion rate or soil loss (Lu et al., 2004; Chen et al., 2011; Atoma et al., 2020; Ganasri and Ramesh 2015; Gupta and Kumar, 2017; Kumar and Kushwaha, 2013; Prasannakumar et al., 2011; Thomas et al., 2017; Uddin et al., 2016), and the acquired soil loss data are subsequently utilized

for determining the quantity of sediment yield or sedimentation rate in the watershed (Biswas and Pani, 2015; Kidane et al., 2019). The extensive applicability of the RUSLE model can be credited to several factors, which include its limited and feasible data requirements, simple and cost-effectiveness, its compatibility with the advanced techniques of Remote Sensing and GIS, and, more importantly, the adequate capacity of the model to represent the spatial patterns of erosion rates with accurate outcome. Although the model was initially designed to evaluate potential soil erosion rates in temperate regions, it has a proficient application with slight modification to ecologically sensitive areas like mountainous terrain, tropical and sub-tropical regions (Millward and Mersey, 1999; Angima et al., 2003; Prasannakumar et al., 2012; Negese et al., 2021; Petito et al., 2022). Moreover, it can even be employed for predicting soil loss within ungauged watersheds through simulation based on the watershed attributes and the prevailing environmental conditions (Garde and Kothyari, 1990; Ganasri and Ramesh, 2015). The overall methodology for soil loss and sediment yield modeling utilized in the present research is schematically shown in Fig. 4.6.

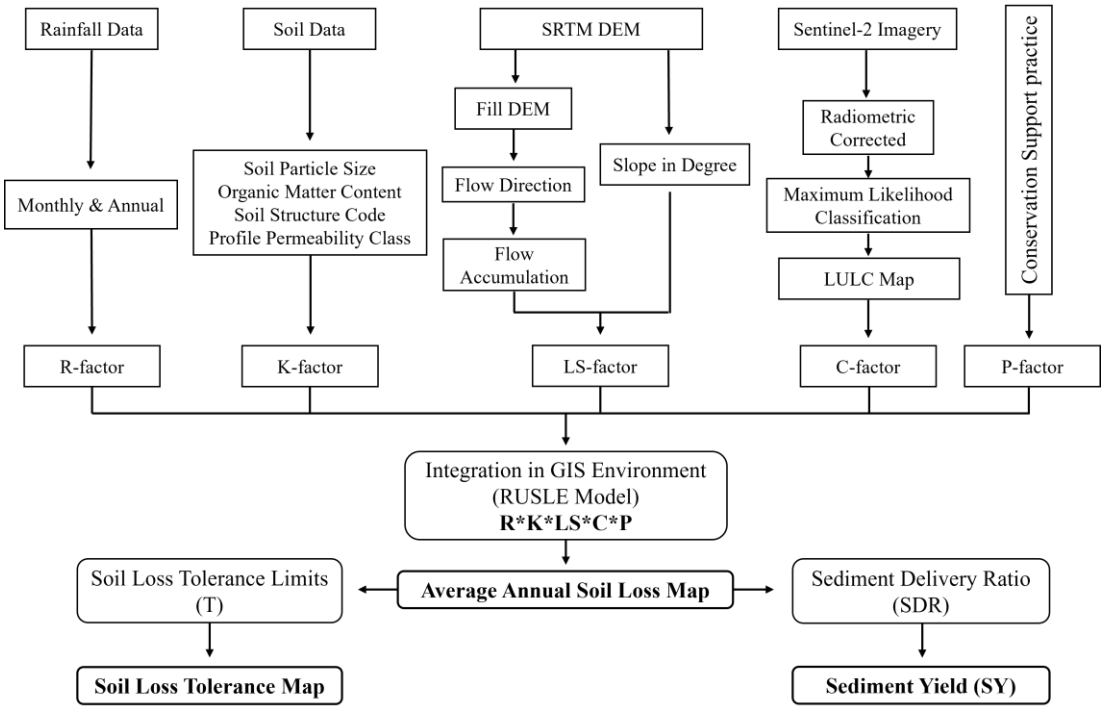

Fig 4.6: Methodological flowchart for soil loss and sediment yield estimation.

4.5.2 Soil loss estimation

This research estimates the amount of soil loss by the Revised Universal Soil Loss Equation (RUSLE). The RUSLE is an empirical model that estimates the long-term average soil loss in each unit of land area resulting from the combined interactions of five unique factors relating to rainfall, soil properties, topography, land use/land cover and vegetation or soil conservation support practice (Lee, 2004; Belayneh et al., 2019; Chatterjee et al., 2013; Gupta and Kumar, 2017). Modeling was undertaken by combining the RUSLE model with substantial remote sensing data under the ArcGIS environment. Hence, thematic layers were prepared for all the inherent parameters, which were arranged under a similar projection system, i.e., WGS1984 UTM Zone 46. To maintain accuracy, a uniform cell size of 30 x 30 m was set for all the raster layers. The amount of soil loss was then obtained through the product of all the RUSLE factor layers in a raster calculator following the formula given below (Renard et al. 1997):

$$A = R \times K \times LS \times C \times P$$

Where, A represents the potential soil loss (tons ha^{-1} $year^{-1}$)

R is the rainfall erosivity factor (MJ.mm/ha^{-1}.h^{-1}.$year^{-1}$)

K is the soil erodibility factor (tons.ha.h.ha^{-1}.MJ^{-1}.mm^{-1})

LS refers to the slope length and steepness factor (dimensionless)

C is the cover management factor (dimensionless)

P is the conservation management practice factor (dimensionless)

4.5.3 Preparation of the RUSLE factors

To successfully apply the RUSLE model in Indian conditions, a slight modification should be made while analyzing the factors (Parveen and Kumar, 2012). Therefore, a suitable methodology was selected and followed to determine some factors to derive adapted values that best represent the study area.

4.5.3.1 Rainfall erosivity (R-Factor)

The calculation of the R-Factor index in the RUSLE requires data on the kinetic energy of storm events and its maximum 30-minute intensity, which is not available

in many regions. With the limits to the availability of such high temporal resolution pluviographic records, monthly and annual rainfall data were commonly utilized to devise the R-factor in various parts of the world. In India, Ram Babu et al. (2004) developed a linear relationship for preparing an improved iso-erodent map of the country based on the annual and seasonal records from 623 stations covering the entire region. Hence, the R-Factor for the present study area was determined through this linear relationship, using the rainfall data collected from 3 stations covering 12 years. The equation is as given below:

$R = 81 + 0.38P$ For $340 \leq P \geq 3500$ mm (Annual Relationship)

$R = 71.9 + 0.361P$ For $293 \leq P \geq 3190$ mm (Seasonal Relationship)

Where, R represents rainfall erosivity in $MJ.mm.ha^{-1}.h^{-1}.yr^{-1}$.

P is the average annual rainfall in mm.

The R-factor layer was prepared by the IDW method using the calculated values.

4.5.3.2 Soil erodibility (K-Factor)

As soil erodibility is affected by a variety of soil properties and their interactions, numerous efforts have been carried out to establish a connection between the measured soil properties to derive K-factor values, among which the soil-erodibility nomograph (Wischmeier et al. 1971) is the most widely used (Renard et al. 1997). Thus, the K-factor values for the present study were computed using the given equation (Wischmeier and Smith 1978; Renard et al. 1997):

$$K = [2.1 \times 10^{-4} (12 - OM) M^{1.14} + 3.25 (a - 2) + 2.5 (b-3)] / 100$$

Where, K indicates the soil erodibility in $ton.ha.h.ha^{-1}.MJ^{-1}.mm^{-1}$

M is the particle size parameter (% Silt + % Very fine sand) (100 - % Clay)

OM is the amount of organic matter (in %)

‘a’ = soil structure code: 1 (very fine granular), 2 (fine granular), 3 (medium/coarse granular), 4 (blocky, platy, or massive), and ‘b’ = profile permeability class: 1 (rapid), 2 (moderate to rapid), 3 (moderate), 4 (slow to moderate), 5 (slow) and 6 (very slow).

The particle size distribution of soil was obtained from soil texture analysis, which is already explained in the “Methodology” section under the sub-heading “4.4.3 Preparation of erosion conditioning factors”. The obtained results for Organic Carbon (mentioned in the Methodology section under “4.2 Data acquisition”) were multiplied with a conversion factor of 2 for deriving the Organic Matter content, based on the recommendations made by Pribyl (2010).

The classification system for soil structure code ‘a’ and permeability class ‘b’ highlighted by Bagarello et al. (2009), as shown in Table 4.3, was followed in this research.

Table 4.3: Soil structural and permeability index.

Soil textural class	**‘a’**	**Soil textural class**	**‘b’**
Sandy, Loamy sand and Sandy loam soils	1	Sandy loam, Loamy sand and Sand	2
Sandy clay, Sandy clay loam, Loam, Silt loam and silt soils	2	Silt loam, Loam, Sandy clay loam	3
Clay loam and Silty clay loam soils.	3	Clay, Silty clay loam, Clay Loam, Sandy clay and silt	4
Clay and Silty clay soils	4	Silty clay	5

Source: Carsel and Parish, 1988; Giordano, 2004.

* ‘a’ = Structure index/ code, ‘b’ = Permeability index.

4.5.3.3 Slope length and steepness (LS-Factor)

The LS-factor was extracted from the SRTM DEM as it was reported to produce more accurate results (Parveen and Kumar, 2012; Ashiagbor et al., 2013; Chatterjee et al., 2013; Dissanayake et al., 2019). Since the LS-factor includes both the

length and steepness of the slope, the layers for flow accumulation and slope degree were first prepared through hydrology tools in Spatial Analyst extension and 3D Analyst tools, respectively (Belasri and Lakhouili, 2016; Bhat et al., 2017) (Fig. 4.7). Subsequently, the LS-factor was determined through the equation given by Moore and Burch (1986):

$$LS = \left(\frac{A_s}{22.13}\right)^{0.6} \left(\frac{\sin\theta}{0.0896}\right)^{1.3}$$

Where, A_s represents the upslope contributing area for a specific area in metres,

θ indicates the slope in degrees.

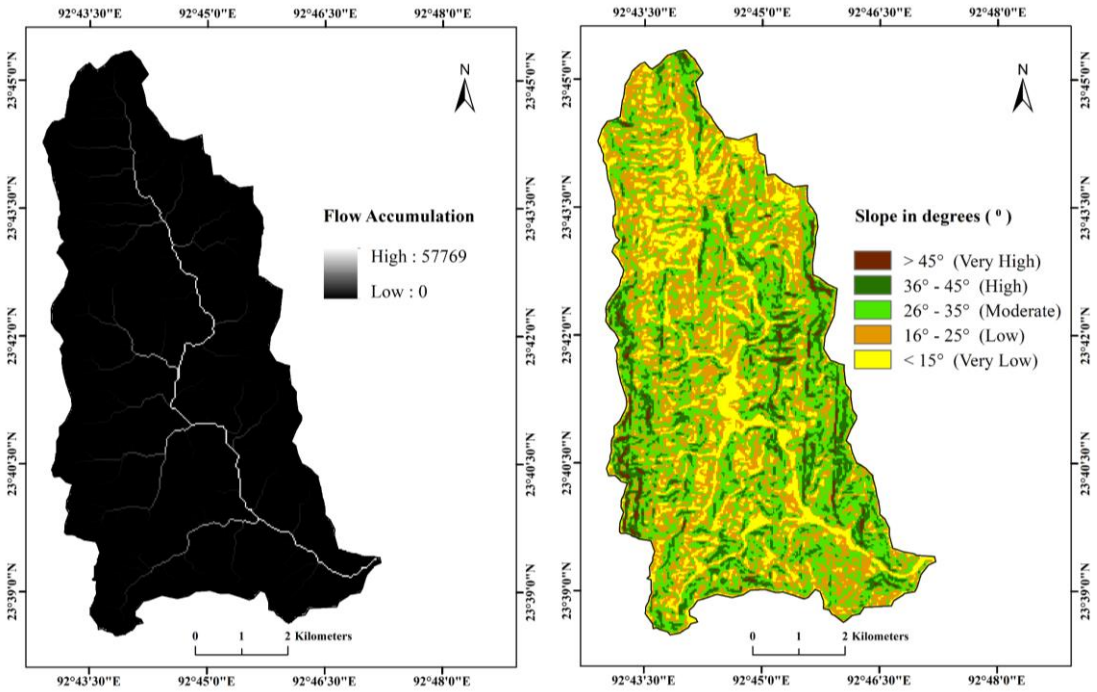

Fig. 4.7: Flow accumulation and slope layers.

The raster layer for LS-factor was then prepared by following the computation procedures developed by Mitasova et al. (1996) in Raster Calculator under the ArcGIS platform:

LS = Power ([Flow Accumulation] x Cell Size /22.13,0.6) x Power (Sin [Slope] x 0.01745 / 0.0896, 1.3)

Where, Pow is the map algebra expression for Power in the raster calculator,

Flow Accumulation is the extracted flow accumulation layer from DEM,

Cell resolution refers to the cell size of the DEM,

Sin slope is the slope layer in degrees,

0.01745 is a conversion factor for slope in degrees to convert into radians.

4.5.3.4 Cover management (C-Factor)

The cover management factor indicates the soil loss ratio at a specific land management and cover system to that loss on a reference unit plot. Hence, the C-factor values were acquired from the study area's land use/land cover (LULC) map. The factor values range between 0 and 1, in which the lower value, closer to 0, reveals a secure land surface, while values closer to 1 indicate higher ground vulnerability to soil loss (Ganasri & Ramesh, 2015; Biswas & Pani, 2015). For the present study, different LULC classes were assigned C-factor values based on the existing literature provided by Biswas and Pani (2015), Chatterjee et al. (2013) and Ganasri and Ramesh (2015).

4.5.3.5 Support practice (P-Factor)

The P-factor refers to the soil conservation support practices designed to reduce soil detachment rate by decreasing run-off capacity. The values of the P-factor are traditionally established between 0 and 1, in which higher values reveals the absence of conservation support practices for soil erosion, while the lower values are adopted for areas with better practices (Yue-Qing et al., 2008; Ganasri and Ramesh, 2015; Kayet et al., 2018). Thus, P-factor values are generally assigned based on the conservation support practices followed and the absence and presence of such activities. In several studies, it is suggested to assume 1.0 as the P-factor value in areas where conservation practices were not available (Morgan, 2005; Millward and Mersey, 1999; Pham et al., 2018; Pradhan et al., 2011; Chatterjee et al., 2013).

Subsequently, a P-factor value of 1 was multiplied with the calculated value of all the other factors.

4.5.4 Determining Soil Loss Tolerance Limits (T)

Soil loss tolerance limits (T) represents the highest permissible erosion level that can sustain a consistently high crop productivity cost-effectively and indefinitely (Wischmeier and Smith, 1978). Hence, the T-value for a particular region requires cautious assignment from soil scientists through a careful analysis of various soil properties under varying environmental conditions (Mandal et al., 2010). For land rehabilitation planning in India, a uniform T-value of 11.2 mg ha^{-1} is generally utilized as a conventional value, irrespective of the varying soil properties, climatic conditions, and vegetative growth (Lakaria et al., 2008). However, a site-specific T-value related to the local conditions is always crucial for identifying the apparent status of erosion risk in a particular region to prioritize critical areas that require immediate conservation and special treatment (Bhattacharya et al., 2008).

Considering the vulnerability of the eastern Himalayas owing to its prevailing delicate physical conditions coupled with reckless deforestation and unsystematic agricultural practices like that of Jhum, Mandal and Sharda, 2011(b) developed a distinct soil loss tolerance limit for the entire northeastern states. Hence, the specific T-value for the study area was also extracted from these pre-determined threshold values for tolerable soil loss. The established map of soil loss tolerance limits was first georeferenced under a similar reference system with the study area shapefile, and the T-value for the Chite watershed was extracted subsequently by clipping the layer with the watershed's shapefile using ArcGIS software.

4.5.5 Evaluation of Sediment Yield (SY)

The RUSLE model can predict only gross soil erosion within the watershed and is restricted to estimate sediment yield at the basin outlet. As a considerable amount of the gross soil erosion, i.e., the sediments removed from their original place, may get deposited elsewhere in the basin, the proportion of sediment transported to the basin's outlet concerning the overall soil erosion needs to be precisely determined (Swarnkar et al. 2018; Kothyari and Jain 1997). The sediment delivery ratio (SDR) is

the sediment transporting capacity of the watershed that represents the actual sediments delivered at the basin outlet in relation to the gross soil erosion within the upper catchment. It denotes the watershed potential for accumulating or transferring the detached soils (Gelagay, 2016). Hence, accurate sediment yield prediction at the basin outlet is commonly established with the product of gross soil erosion within the watershed and the estimated Sediment Delivery Ratio (SDR) (Walling, 1983; Magesh and Chandrashekhar, 2016).

4.5.6 Determination of Sediment Delivery Ratio (SDR)

Numerous methods were proposed to estimate the SDR values depending on different watershed attributes like size, land use, soil type, slope, drainage density, etc. Generally, the average slope progressively declines with an increase in the watershed's size, which reduces sediment transport and increases the chances of deposition within the watershed. Moreover, the slope generally extends longer towards the streams and there is a greater chance of trapping sediments. Hence, a larger area of the watershed will have lesser chances of sediment movement. Concerning this inverse relationship between the SDR and the basin size, the sediment delivery ratio is typically determined by considering the drainage basin area (USDA, 1972; Quyang et al., 1997; Thomas et al., 2018). In this study, the relationship developed by Vanoni (1975) to calculate the Sediment Delivery Ratio (SDR) was applied, which is given by the equation (Lim et al., 2005):

$$SDR = 0.4724 * A^{-0.125}$$

Where, SDR indicates the Sediment Delivery Ratio

A represents the drainage basin area in km^2.

4.5.7 Sediment Yield Estimation

In this research, the ensemble approach combining the estimated amount of soil erosion and the sediment delivery ratio (SDR), the 'RUSLE-SDR' model, was adopted to calculate the sediment yield, which is computed by the equation given below (Fistikoglu & Harmancioglu, 2002):

$$SY = GE * SDR$$

Where, SY indicates the Sediment Yield (tons $year^{-1}$),

GE is the Gross Erosion calculated by the RUSLE model,

SDR represents the Sediment Delivery Ratio (SDR)

Besides calculating sediment yield from estimated soil loss and the sediment delivery ratio (SDR) for the study area, the seasonal sediment yield was also predicted based on the calculated soil loss for different seasons. For calculating the seasonal soil loss, rainfall data for different months were divided into 4 seasonal groups, viz. "Winter (December-February), Pre-Monsoon (March-May), Monsoon (June-September), and Post-Monsoon (October and November)" based on the Indian Meteorological Department's (IMD) classification. The R-factor was then computed and generated with GIS software for each seasonal rainfall. Finally, the generated R-factor map was multiplied with the other factors using the raster calculator under the ArcGIS environment to derive the seasonal soil loss.

4.6 Watershed prioritization

4.6.1 Introduction

Prioritizing a watershed initially involves delineating the whole area into smaller conservation units, preferably sub-watersheds and assigning their respective ranks to implement essential soil erosion control measures for soil and water conservation.

4.6.2 Delineation of sub-watersheds

This research first delineates eight sub-watersheds (SW) from the Chite watershed to recognize conservation units in a smaller geographical segment. Among these eight geographical regions, SW-1, SW-2, SW-3, SW-5 and SW-7 were prepared from 3rd-order streams, while SW-4 and SW-6 were generated from 2nd-order streams. With the absence of such a relatively higher stream ordering in the southeastern corner of the watershed, SW-8 was extracted from a 1st-order stream to produce a comparable areal unit with that of higher-order sub-watersheds. Finally, all the other areas falling

outside the vicinity of these delineated spatial entities were merged with the adjacent sub-watersheds to represent the whole study area spatially.

4.6.3 Variables selection

In this research, the watershed prioritization was undertaken considering the various findings related to soil erosion and sedimentation assessment, including the predicted erosion susceptibility (ES), evaluated soil loss (A), derived soil loss tolerance limits (T), and the estimated sediment yield (SY), to represent the prevailing status of each sub-watershed.

For sub-watershed level erosion susceptibility zonation, the study area layer for erosion susceptibility was overlaid by the sub-watershed boundary shapefile with a similar reference system, i.e., WGS1984 UTM Zone 46. Then, the area under several classes of erosion susceptibility was extracted by clip functions in raster processing under data management tools, and the spatial distribution of high and very high erosion susceptibility classes were calculated for each geographical entity. At the same time, the rate of soil erosion and sediment yield for the eight sub-watersheds were obtained from the entire watershed's soil loss layer through zonal statistics as a table function in the ArcGIS platform. To derive the spatial distribution of soil loss tolerance limits (T), the raster layer of soil loss was grouped into two classes through symbology. The first class represents those areas with a T-value of 7.5 tons ha^{-1} $year^{-1}$ and below, while the other class shows areas lying above the T-value, and the overall extent of areas above the soil loss tolerance was calculated for each sub-watershed.

4.6.4 Determination of ranks and priority

The Compound value (C_V) method has been competently engaged to prioritize a watershed from multiple parameter's rank. As the Chite watershed comprised of eight sub-watersheds, each sub-watershed was allocated ranks, ranging from 1 to 8, considering the respective values of the selected parameters in each spatial unit. Lower values indicate a critical situation, while higher value implies the opposite, and hence, ranks are gradually assigned from 1 to 8 concerning the decreasing influence of each considered parameter. The Compound value (C_V) method is considered as one of the most effective methods to relate various processes occurring on the landforms in

comparable geographical units (Altaf et al., 2014). Hence, the C_V was calculated for each sub-watershed considering the areas under high and very high susceptibility class, average annual soil loss, areas above tolerable soil loss and the annual sediment yield quantity through the equation given below (Altaf et al., 2014):

$$C_V = \frac{1}{n} \sum_{i=1}^{n} R$$

Where, C_V represents a specific sub-watershed Compound value

R indicates the rank assigned to the parameters

N is the number of parameters considered

CHAPTER-5

SOIL EROSION SUSCEPTIBILITY

5.1 Introduction

Soil erosion susceptibility mapping involves a comprehensive understanding of soil erosion's spatial distribution and intensity, which enhances site-specific prioritization. Consequently, it plays a crucial role as an initial step in implementing effective soil and water conservation plans and suitable erosion control measures in any given region (Ghosh and Mukhopadhyay, 2021; Pandey et al., 2021). Therefore, stakeholders and decision-makers often prioritize erosion susceptibility mapping over the quantification of soil loss (Lu et al., 2004). Hence, soil erosion susceptibility mapping has been executed by applying an integrated approach combining the Analytical Hierarchy Process (AHP) method with remote sensing and GIS technology.

5.2 Structuring of thematic layers

To prepare an accurate erosion susceptible map, a crucial prerequisite is the deliberate evaluation of all the causative factors to determine their respective influence on soil erosion. The selected factors and their varying degree of potential impact on soil erosion processes are discussed below:

5.2.1 Elevation: Among the various topographical factors, elevation is widely recognized as a significant determinant of soil erosion susceptibility (Saha et al., 2019). Generally, higher elevation suggests greater run-off and less infiltration (Vijith and Dodge-Wan, 2019). As a result, there exists a direct relationship in which erosion increases with the rise in elevation (Aslam et al., 2021). The elevation of Chite watershed ranges between 172 to 1239 m (Fig. 5.1 (a)). To reveal its varying influence on soil erosion, elevation of the study area was categorized into five distinct classes: very low (<300 m), low (300-500 m), medium (500-700 m), high (700-900 m) and very high (>900 m), which covers about 2.36%, 19.49%, 31.98%, 31.56% and 14.61% of the watershed respectively (Table 5.6).

5.2.2 <u>Slope</u>: Slope is the most significant derivative of elevation, which measures the extent of elevation change at the surface, expressed in terms of degrees or percentage. In the present study, slope is measured in degree, which is the arc tangent of the ratio of rise over run (Chang, 2018). The increase in the steepness of the slope has a corresponding impact on the amount and velocity of run-off and infiltration rate, thus controlling the amount of soil loss, which might be doubled for every four times increase in the slope (Garde, 2006; Tideman, 1996). The slope of the study area was divided into five classes: very low (< 15º), low (15º - 25º), medium (25º - 35º), high (35º - 45º), and very high (> 45º), and higher ranks were allocated to slopes classes with greater degree of slope steepness (Table 5.6). The steepness of the slope generally increases from a very low class of less than 15º along the river valley, constituting 18.73% of the study area towards the hilltop where the maximum value of slope degree has even reached up to 59.61º occupying an area of about 1.86% (Fig. 5.1 (b)).

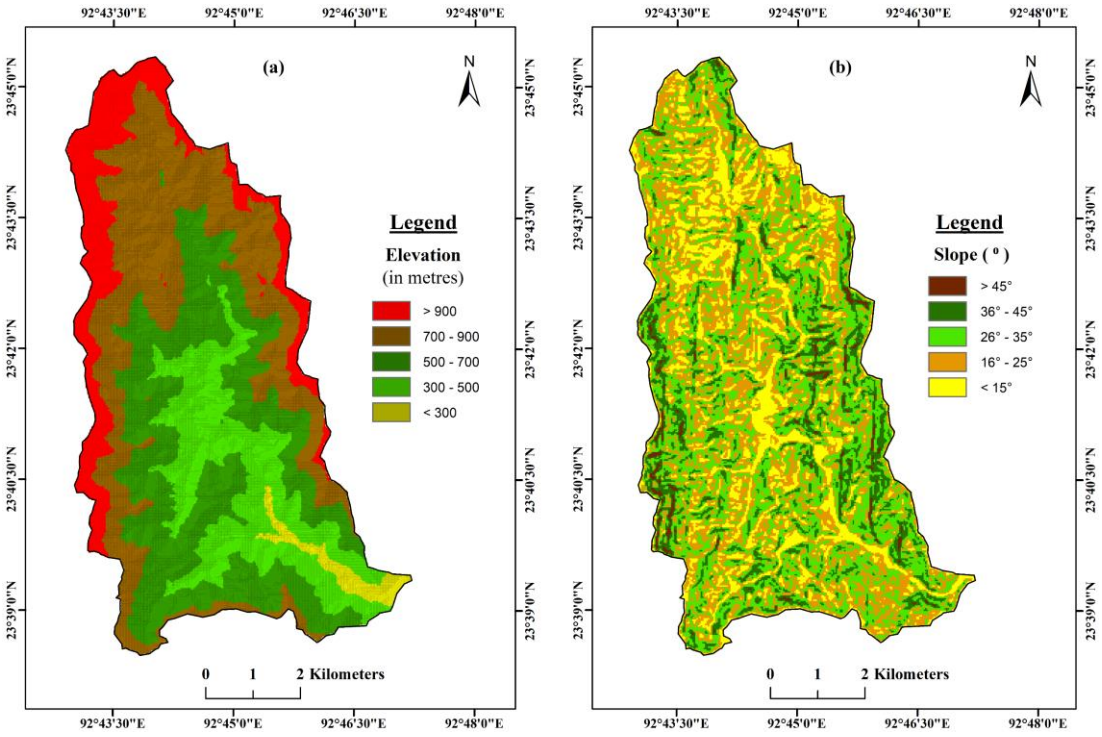

Fig. 5.1: Conditioning factors (a) Elevation and (b) Slope.

5.2.3 <u>Drainage density</u>: Higher density of watercourses within a watershed indicates more streams per unit area, which typically leads to increased surface run-off, resulting in a higher rate of erosion and sediment transport (Vojtek and Vojtekova, 2019; Das et al., 2020). Hence, a direct correlation can be observed between the density of drainage systems and the occurrence of soil erosion. Consequently, drainage density is a significant indicator for evaluating the risk of soil erosion, as it indicates the level of resistance within an area (Sajedi-Hosseini et al., 2018). Drainage density of Chite watershed ranges from 0.76 to 9.73 km/km^2 (Fig. 5.2 (a)). A reported high risk of soil erosion is linked to a particular threshold value of 0.09 km/km^2 or higher (Saini et al., 2015). Hence, the majority of the study area, i.e., 56.64% has higher chances of soil erosion occurrences under the influence of drainage density. Notwithstanding the watershed's significant drainage density, it has been categorized into five distinct groups: very low (0 – 0.76 km/km^2), low (0.77 – 2.1 km/km^2), medium (2.11 – 3.51 km/km^2), high (3.52 – 5.23 km/km^2) and very high (5.24 – 9.73 km/km^2) to reveal the varying degree of susceptibility (Table 5.6).

5.2.4 <u>Distance from streams</u>: Stream banks and the adjacent areas are naturally influenced by soil erosion due to the action of running water in the streams (Pimentel, 2006). Stream reduces the slope strength by gradually removing material that constitutes the slope bases. Consequently, regions closer to the watercourses are at an increased risk of experiencing greater susceptibility to soil erosion (Saha et al., 2002). Thus, the watershed has been divided into five classes with an interval of 100 metres depending upon their relative distance from the streams as: < 100 m (Very High), 100 – 200 m (High), 200 – 300 m (Medium), 300 – 400 m (Low) and > 400 m (Very Low) (Fig. 5.2 (b)) (Table 5.6).

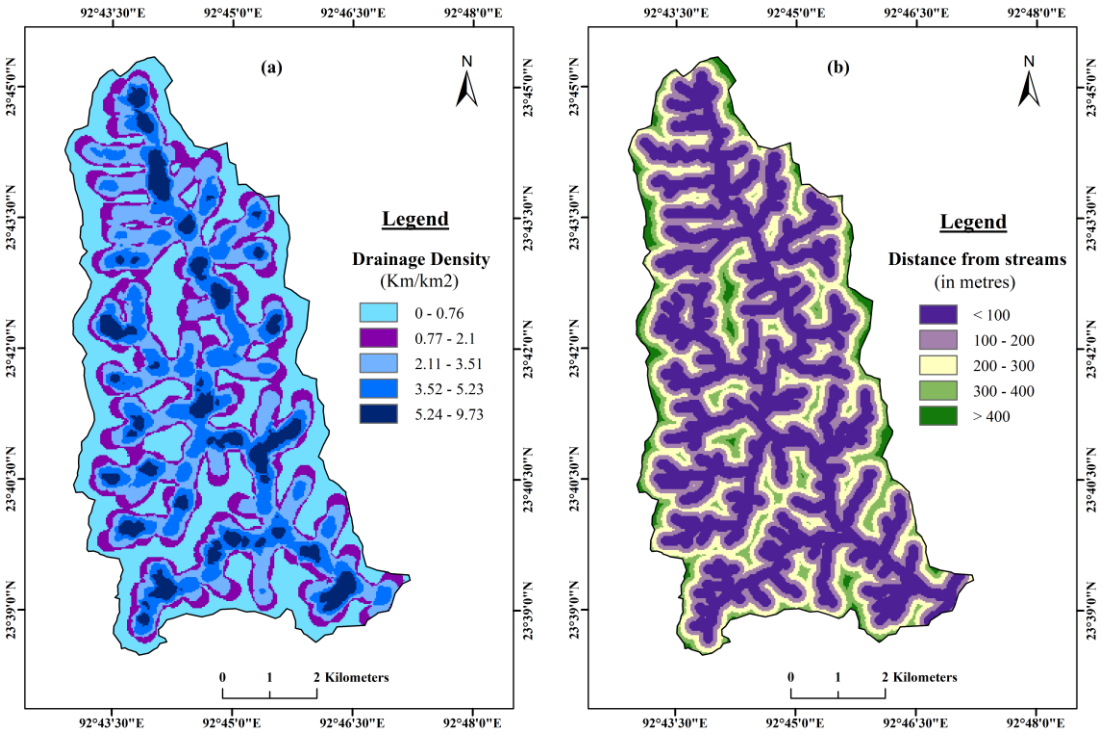

Fig. 5.2: Conditioning factors (a) Drainage density and (b) Distance from streams.

5.2.5 <u>Land use/land cover</u>: An area's land use and land cover (LULC) composition plays a crucial role in determining its susceptibility to erosion. This is due to the variations in factors such as run-off rates, infiltration, and evapotranspiration across different LULC types, which consequently leads to varying rates of soil erosion and sediment yield (Chen et al., 2001; Sharma and Singh, 2017). The LULC map of the study comprised of five different classes, viz., Built-up land, Dense Forest, Open Forest, Crop land and Bare land, covering an area of about 11.09%, 19.36%, 44%, 22.42%, and 3.13% respectively (Fig. 5.3 (a)) (Table 5.6). Due to the lack of soil and water conservation practices, the bare land and cropland in the research area are vulnerable to the direct influence of the prevailing environmental conditions like slope, rainfall, etc.; hence, they are more subjected to soil erosion. Generally, the built-up land has higher chances of run-off due to lesser infiltration. On the other hand, the areas with forest cover are relatively secure as they play a protective role against various factors that initiate erosion processes.

5.2.6 <u>Normalized Difference Vegetation Index</u>: Vegetation is paramount in shielding the surface from direct raindrop impacts, lowering run-off and enhancing infiltration rate, which reduces chances of soil erosion (Das and Saikia, 2013). On the contrary, a decrease in vegetation cover exposes the topsoil, thereby increasing an area's vulnerability to soil erosion (Issaka and Ashraf, 2017; Ebhouma et al., 2022). The quality and quantity of vegetation can be effectively manifested through the Normalized Difference Vegetation Index (NDVI). A high NDVI value of 0.6 to 0.8 indicates healthy vegetation like those of the rainforest, moderate values of 0.2 to 0.3 denote areas of shrubs and grasslands, while a value closer to 0 represents bare surface (Bhandari et al., 2012; Ghosh and Lepcha, 2019). Hence, higher NDVI indicates lesser chances of soil erosion and vice versa. The obtained NDVI values of the study area range between 0.09 and 0.62 and were classified into five categories as: very low (0.009 – 0.02), low (0.2 – 0.3), medium (0.3 – 0.4), high (0.4 – 0.5) and very high (0.51 – 0.62), using natural breaks (jenks) method (Fig. 5.3 (b)) (Table 5.6).

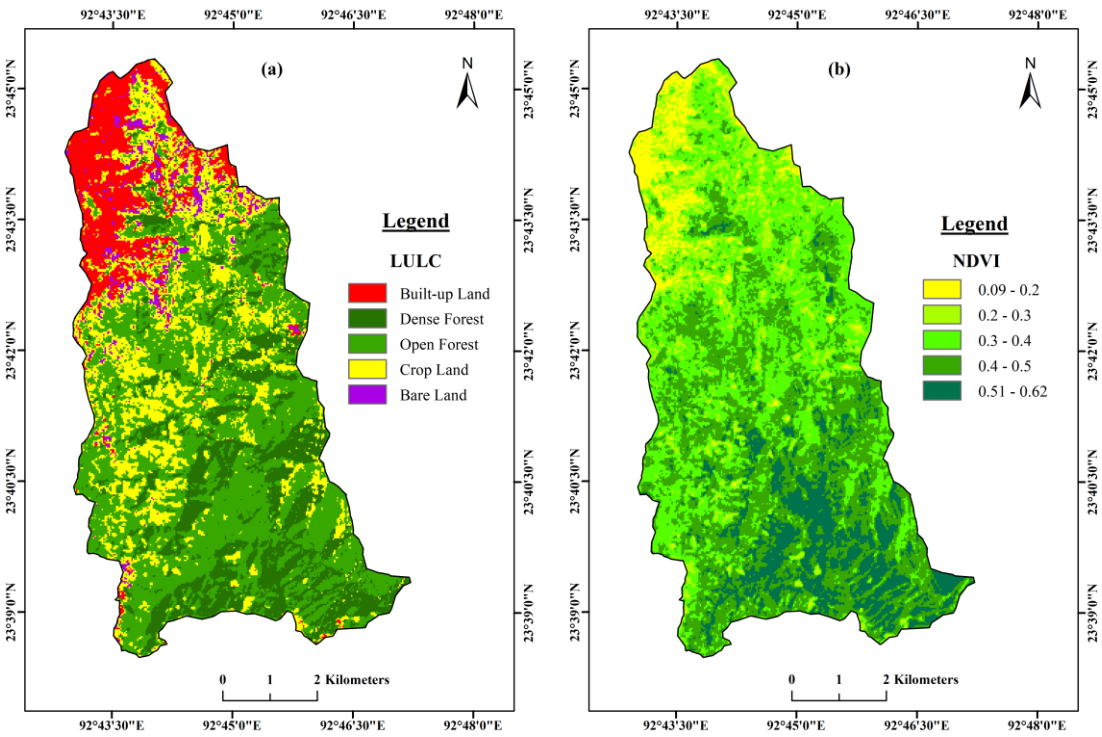

Fig. 5.3: Conditioning factors (a) LULC and (b) NDVI.

5.2.7 <u>Lithology</u>: Lithology typically refers to rocks' inherent physical characteristics, which significantly influence soil erosion processes (Aslam et al., 2021). Therefore, rocks of different lithological groups exhibit diverse levels of erodibility (Goudie, 2006). The study area comprise of two lithological units viz., sandstone with subordinate siltstone, mudstone and shale and grey sandy splintery shale, siltstone and mudstone, which are assigned codes as 1 and 2 respectively (Fig. 5.4 (a)). The lithological code 2 compared to code 1 is probably more conducive to soil erosion as it has a fine-grained particle size which has low permeability, and hence it supports high drainage density due to chances of significant run-off (Mat, 2021). Most of the area is characterized by lithological code 2 covering about 94.31% of the study area (Table 5.6).

5.2.8 <u>Lineament density</u>: Lineaments are linear landscape elements that depict the surface expression of geological features like faults and fractures. These linear arrangements mainly result from various morphological features like streams, mountain ridges, etc. (Lillesand et al., 2017). Lineaments render the ground more sensitive to denudational processes through different periods (Pradeep et al., 2014). Considering that a higher lineament density has more possibility of a degradational process, the lineament density layers of the watershed were divided into five classes to represent the varying influence as 0 – 0.48 km/km^2 (Very Low), 0.49 – 1.35 km/km^2 (Low), 1.36 – 2.11 km/km^2 (Medium), 2.12 – 3.09 km/km^2 (High) and 3.10 – 5.12 km/km^2 (Very High) (Fig. 5.4 (b)) (Table 5.6).

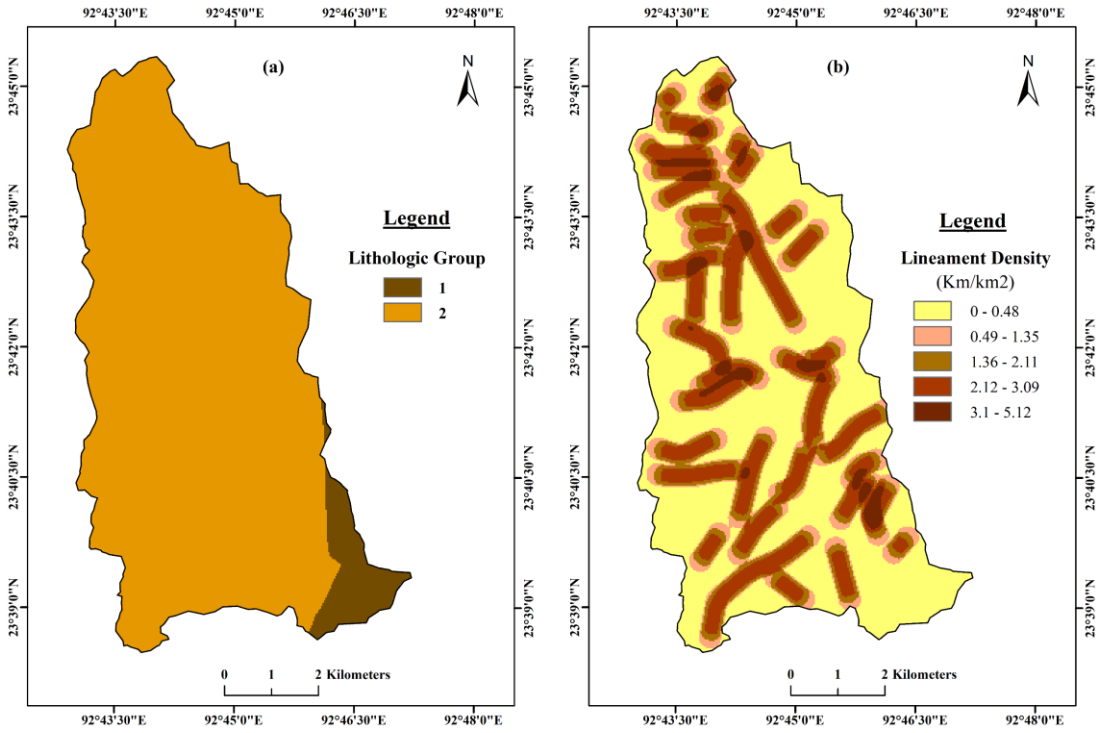

Fig. 5.4: Conditioning factors (a) Lithology (b) Lineament density.

5.2.9 Rainfall Intensity: Rainfall intensity, among various characteristics of rainfall, has been generally considered the most influential factor in soil erosion (Morgan, 2005). It plays a crucial role leading to significant soil loss because the direct impact of raindrops can quickly disintegrate soil aggregates, and the varying intensity may increase or decrease the rate and volume of run-off (Sharma and Singh, 2017; Tideman, 1996). The rainfall intensity of the study was represented using the Modified Fournier Index (MFI), as this index significantly reveals the aggressiveness of rainfall in inducing soil erosion (Costea, 2012). In the study area, the obtained rainfall intensity varies from 278.66 to 298.50 mm/year, and the erosive force of rainfall is found to be highest in the Northern parts of the watershed, which decreases slightly towards the south (Fig. 5.5 (a)).

5.2.10 Soil Texture: Soil texture is an inherent characteristic of soil that refers to the particle size distribution. It is considered the most critical attribute of soil that significantly influences erosion processes, as soil texture determines the infiltration rate, thereby controlling the rate of soil erosion (Tideman, 1996; Toy et al., 2002).

Generally, fine and medium-textured soils have lower infiltration rates and are more subjected to water-induced soil erosion due to high run-off (Pimentel, 2006). The obtained soil texture in the watershed were classified into sandy clay loam, fine sandy loam, sandy loam, coarse sandy loam, and loamy sand (**Table 5.1**). Sandy loam is found to have the most extensive areal coverage of about 64.67%, followed by coarse sandy loam, fine sandy loam, sandy clay loam and loamy sand, occupying 16.70%, 15.09%, 2.03% and 1.50% of the watershed respectively (Table 5.6). Subsequently, the study area has been classified into five categories which represents the observed textural class along with their respective control on soil erosion- sandy clay loam (Very high), fine sandy loam (High), sandy loam (Medium), coarse sandy loam (Low) and loamy sand (Very low) (Fig. 5.5 (b)).

Table 5.1: Particle size distribution for the obtained soil textural class.

Soil Textural Class	Descriptive Statistics	Sand (%)	Silt (%)	Clay (%)
Sandy clay loam	Min	54.47	15.58	21.16
	Max	61.38	23.86	23.69
	Mean	58.98	19.09	21.93
	SD	2.27	2.69	0.98
Fine sandy loam	Min	54.81	28.74	7.26
	Max	60.49	33.61	11.86
	Mean	57.94	31.94	10.12
	SD	1.78	1.41	1.41
Sandy loam	Min	60.34	18.86	6.22
	Max	64.82	31.92	18.76
	Mean	62.98	28.23	8.79
	SD	1.27	2.19	1.91
Coarse Sandy loam	Min	65.73	20.49	5.19
	Max	70.38	27.87	9.19
	Mean	68.40	24.26	7.33
	SD	1.57	2.28	1.15
Loamy sand	Min	75.69	14.36	5.53
	Max	80.11	17.83	6.48
	Mean	78.06	15.77	6.17
	SD	1.83	1.47	0.44

*Min=Minimum, Max=Maximum, SD=Standard Deviation.

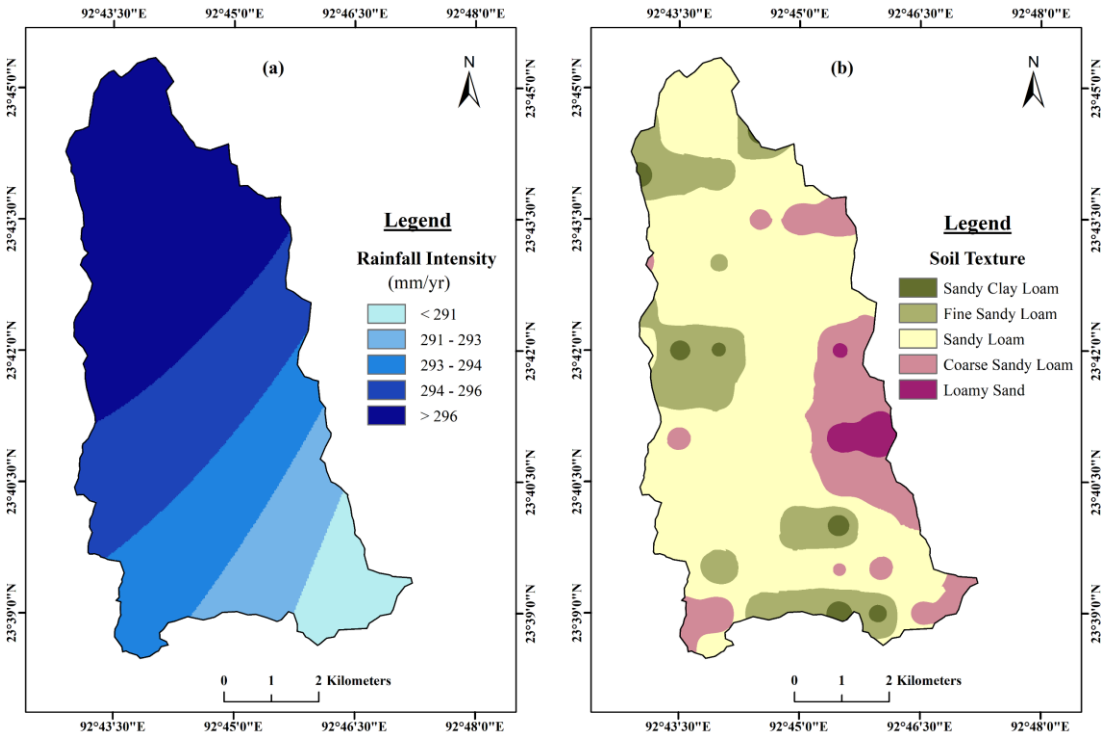

Fig. 5.5: Conditioning factors (a) Rainfall Intensity (b) Soil texture.

5.3 Multicollinearity results

Multicollinearity is a problem that occurs when there exists a high correlation among various predictors or independent variables. It can create problems in a regression model, altering significant variables to become statistically insignificant (Daoud, 2017). It is an interdependency condition that poses a considerable threat, affecting the effective specification and the accurate assessment of the complex relationships in a regression analysis (Ferrar and Glauber, 1967). Moreover, an independent variable must be independent, otherwise it can alleviate the model's precision.

Table 5.2 shows the results for multi-collinearity test for the 10 selected parameters in the study. According to Daoud, (2017), "VIF greater than 5 and Tolerance value lesser than 0.10 indicates collinearity". So, there is no collinearity or high correlation among our selected independent variables, and hence, all the 10 selected parameters were utilized for modelling erosion susceptibility.

Table 5.2: Collinearity statistics for Erosion Susceptibility Parameters.

SL.No	Parameters	Collinearity Statistics	
		Tolerance	VIF
1	Elevation	0.37	2.71
2	Lithology	0.56	1.77
3	Soil Texture	0.92	1.09
4	Land use / Land cover	0.91	1.09
5	Distance from streams	0.33	2.99
6	Drainage Density	0.34	2.96
7	Rainfall Intensity	0.36	2.80
8	Slope	0.89	1.12
9	Lineament Density	0.95	1.06
10	Normalized Difference Vegetation Index	0.52	1.93

5.4 Application of the Analytical Hierarchy Process (AHP)

The AHP based pairwise comparison matrix considering the relative importance of ten erosion conditioning factors are as given in Table 5.3. The rankings were assigned based on practical experience of the study area and experts' opinions through published literature (Alexakis et al., 2013; Pradeep et al., 2014; Arabameri et al., 2018; Sajedi-Hosseini et al., 2018; Arabameri et al., 2019(a); Avand et al., 2019; Saha et al., 2019; Das et al., 2020; Mosavi et al., 2020; Aslam et al., 2021).

Table 5.3: Pairwise comparison matrix for Erosion Susceptibility parameters.

Parameters	SLP	RI	NDVI	ELE	LULC	DFS	DD	ST	LD	LIT
SLP	**1**	3	4	4	5	6	6	7	9	9
RI	1/3	**1**	3	3	4	5	5	6	8	8
NDVI	1/4	1/3	**1**	1	3	4	4	5	7	7
ELE	1/4	1/3	1	**1**	3	4	4	5	7	7
LULC	1/5	1/4	1/3	1/1	**1**	3	3	4	6	6
DFS	1/6	1/5	1/4	1/4	1/3	**1**	1	2	4	4
DD	1/6	1/5	1/4	1/4	1/3	1	**1**	2	4	4
ST	1/7	1/6	1/5	1/5	1/4	1/2	1/2	**1**	3	3
LD	1/9	1/8	1/7	1/7	1/6	1/4	1/4	1/3	**1**	1
LIT	1/9	1/8	1/7	1/7	1/6	1/4	1/4	1/3	1	**1**

* SLP=Slope, RI=Rainfall Intensity, NDVI=Normalized Difference Vegetation Index, ELE=Elevation, LULC=Land use/ Land cover, DFS=Distance from streams, DD=Drainage density, ST=Soil Texture, LD=Lineament density, LIT=Lithology.

The obtained weights for all the ten conditioning factors make evident that the normalized eigenvector was highest for the slope (0.30), which indicates that slope has the highest influence on soil erosion, followed by rainfall intensity (0.20), NDVI (0.13) and Elevation (0.13) (Fig 5.6) (Table 5.4). Other factors with moderate impact on erosion process includes LULC (0.08), distance from streams (0.05), drainage density (0.05), while soil texture (0.03), lineament density (0.02) and lithology (0.02) are the lowest influencing factors.

Table 5.4: Normalized comparison matrix.

	SLP	**RI**	**NDVI**	**ELE**	**LULC**	**DFS**	**DD**	**ST**	**LD**	**LIT**	**Criteria Weights**
SLP	0.37	0.52	0.39	0.39	0.29	0.24	0.24	0.21	0.18	0.18	0.30
RI	0.12	0.17	0.29	0.29	0.23	0.20	0.20	0.18	0.16	0.16	0.20
NDVI	0.09	0.06	0.10	0.10	0.17	0.16	0.16	0.15	0.14	0.14	0.13
ELE	0.09	0.06	0.10	0.10	0.17	0.16	0.16	0.15	0.14	0.14	0.13
LULC	0.07	0.04	0.03	0.03	0.06	0.12	0.12	0.12	0.12	0.12	0.08
DFS	0.06	0.03	0.02	0.02	0.02	0.04	0.04	0.06	0.08	0.08	0.05
DD	0.06	0.03	0.02	0.02	0.02	0.04	0.04	0.06	0.08	0.08	0.05
ST	0.05	0.03	0.02	0.02	0.01	0.02	0.02	0.03	0.06	0.06	0.03
LD	0.04	0.02	0.01	0.01	0.01	0.01	0.01	0.01	0.02	0.02	0.02
LIT	0.04	0.02	0.01	0.01	0.01	0.01	0.01	0.01	0.02	0.02	0.02
Sum	1.00	1.00	1.00	1.00	1.00	1.00	1.00	1.00	1.00	1.00	1.00

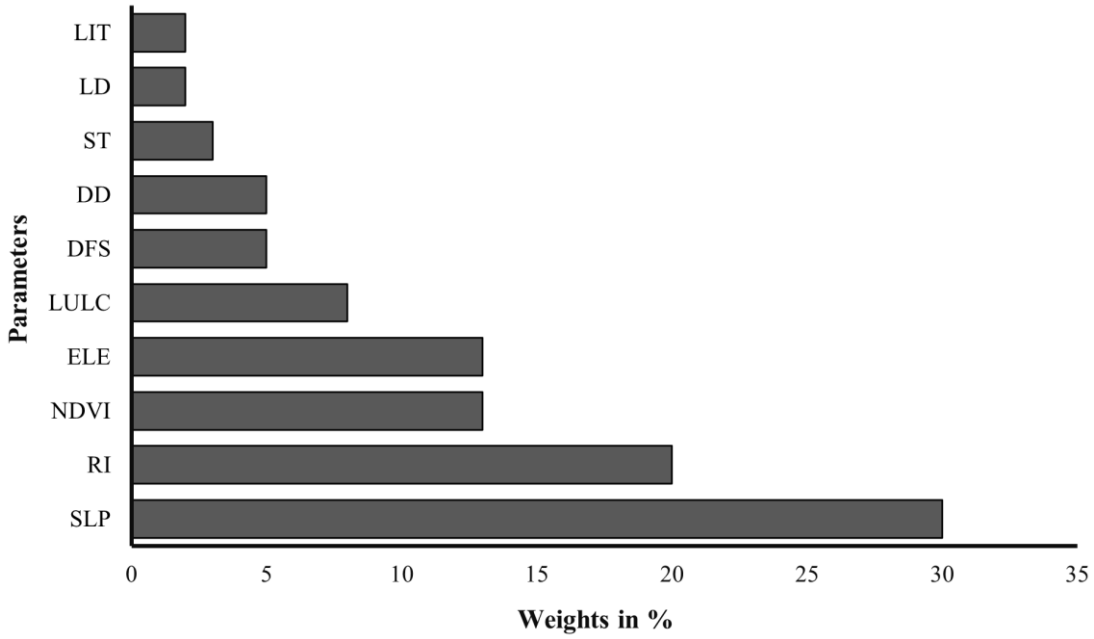

Fig. 5.6: Calculated AHP weights of the ten erosion conditioning factors.

Besides the varying influence among the selected variables on soil erosion, they all are found to have a suitable consistency, as the overall CR values (0.06) lies well within the consistency limit of ≤ 0.1 suggested by Saaty (1977) (Table 5.5). Hence, the selection of all parameters and the assigned weights are unbiased and reliable for susceptibility modelling. Besides the individual parameters and their respective AHP weights, all the sub-classes, areal extent and ratings are also calculated and presented in Table 5.6.

Table 5.5: Consistency ratio

Table: Consistency Ratio (CR)			
λmax	**N**	**CI**	**CR**
10.75	10	0.083	0.06

Table 5.6: Weights, erosion level, area, and ratings of parameters and their sub-classes.

Parameters	AHP Weight	Reclass Class	Sub-classes	Erosion Level	Area (km^2)	Area (%)	Rating
Elevation	0.127	1	< 300	Very Low	1.23	2.36	0.044
		2	300 – 500	Low	10.17	19.49	0.076
		3	500 – 700	Medium	16.68	31.98	0.144
		4	700 – 900	High	16.46	31.56	0.268
		5	> 900	Very High	7.62	14.61	0.468
Slope	0.301	1	< 15	Very Low	9.77	18.73	0.044
		2	15 – 25	Low	17.42	33.42	0.076
		3	25 – 35	Medium	17.37	33.30	0.144
		4	35 – 45	High	6.63	12.71	0.268
		5	> 45	Very High	0.97	1.86	0.468
Rainfall Intensity	0.201	1	< 291.37	Very Low	4.91	9.41	0.095
		2	291.38 - 293.23	Low	10.65	20.42	0.127
		3	293.24 - 294.69	Medium	12.07	23.14	0.182
		4	294.7 - 296.43	High	14.58	27.95	0.258
		5	> 296.44	Very High	9.95	19.08	0.337
Drainage Density	0.046	1	0 - 0.76	Very Low	17.92	34.35	0.055
		2	0.77 - 2.1	Low	10.07	19.31	0.090
		3	2.11 - 3.51	Medium	11.12	21.32	0.154
		4	3.52 - 5.23	High	9.05	17.35	0.265
		5	5.24 - 9.73	Very High	4.00	7.67	0.435
Distance from Streams	0.046	1	> 400	Very Low	1.32	2.53	0.062
		2	300 – 400	Low	4.34	8.32	0.099
		3	200 – 300	Medium	10.65	20.42	0.161
		4	100 – 200	High	14.51	27.82	0.262
		5	< 100	Very High	21.34	40.91	0.416
Soil Texture	0.033	1	Loamy Sand	Very Low	0.78	1.50	0.090
		2	Coarse sandy Loam	Low	8.72	16.72	0.126
		3	Sandy Loam	Medium	33.71	64.63	0.180
		4	Fine Sandy Loam	High	7.87	15.09	0.254
		5	Sandy Clay Loam	Very High	1.08	2.06	0.349
Lithology	0.017	1	Sandstone with subordinate	Low	2.95	5.66	0.164

			siltstone,mudstone, shale				
		2	Grey sandy splintery shale, siltstone and mudstone	High	49.21	94.34	0.252
Lineament Density	0.017	1	> 3.1	Very Low	27.22	52.19	0.044
		2	2.12 - 3.09	Low	5.64	10.81	0.076
		3	1.36 - 2.11	Medium	7.21	13.82	0.144
		4	0.49 - 1.35	High	10.32	19.79	0.268
		5	< 0.48	Very High	1.77	3.39	0.468
Land use / Land cover	0.084	1	Dense Forest	Very Low	10.07	19.30	0.053
		2	Open Forest	Low	22.97	44.05	0.089
		3	Biult-Up Land	Medium	5.76	11.04	0.153
		4	Cropland	High	11.71	22.45	0.262
		5	Bare Land	Very High	1.65	3.16	0.444
Normalized Difference Vegetation Index	0.127	1	> 0.5	Very High	6.89	13.21	0.044
		2	0.4 - 0.5	HIgh	19.12	36.66	0.076
		3	0.3 - 0.4	Medium	17.21	32.99	0.144
		4	0.2 - 0.3	Low	6.39	12.25	0.268
		5	< 0.2	Very Low	2.55	4.89	0.468

Based on the calculated AHP weights, the various conditioning factors were integrated to produce a soil erosion susceptibility index (SESI), calculated by weighted linear sum in ArcGIS software using the following equation:

$SESI_{AHP}$ = ((Slope x 0.30) + (Rainfall intensity x 0.20) + (NDVI x 0.13) + (Elevation x 0.13) + (LULC x 0.08) + (Distance from streams x 0.05) + (Drainage density x 0.05) + (Soil texture x 0.03) + (Lineament density x 0.02) + (Lithology x 0.02))

The SESI values calculated for the watershed vary between 0.070 and 0.362. Consequently, the index values were reclassified using the natural breaks (Jenks) method to produce a soil erosion susceptibility map for the Chite watershed (Pourghasemi et al., 2012), which represents various zones of erosion susceptibility as: Very low, Low, Moderate, High, and Very high, in the study area (Fig 5.7).

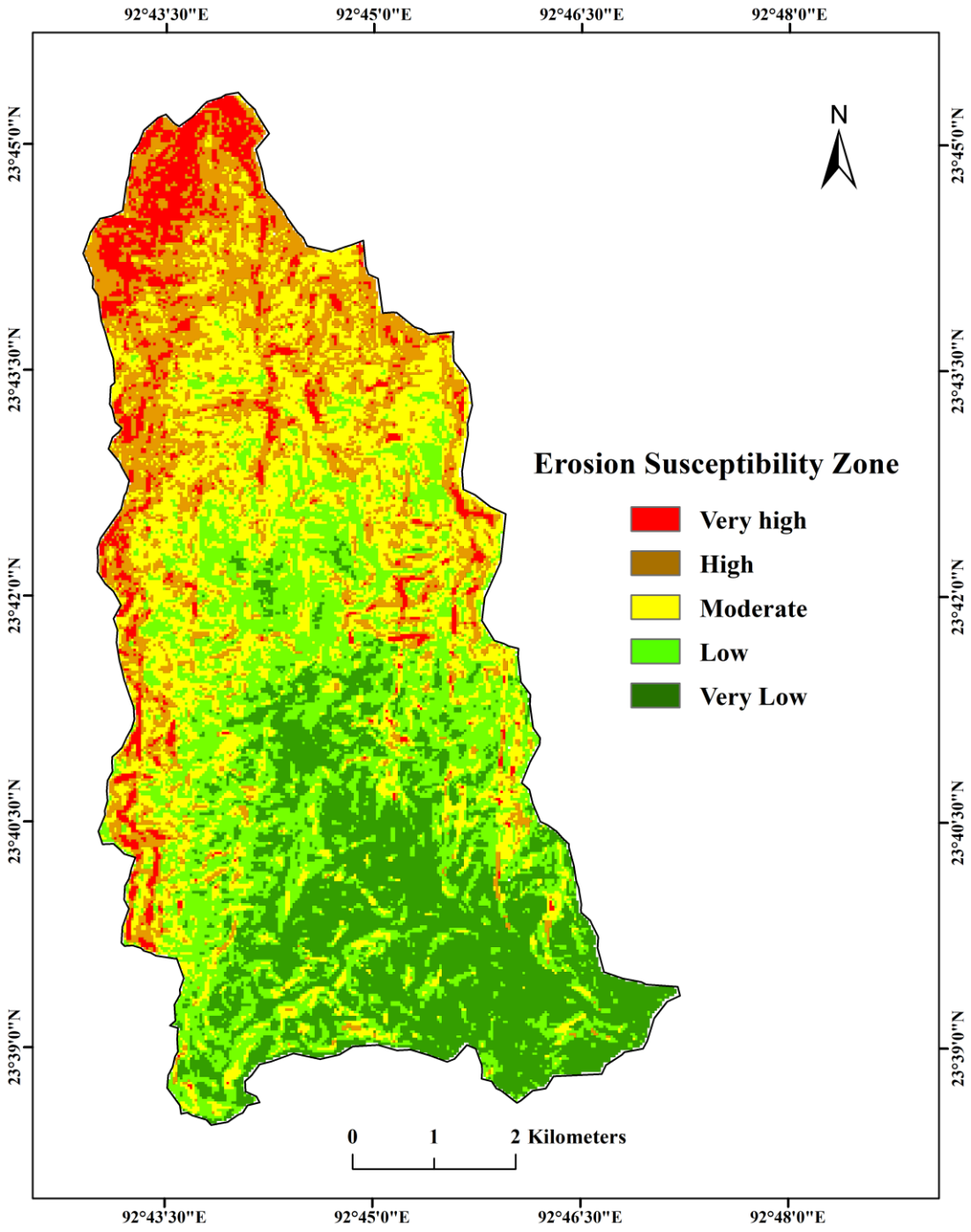

Fig 5.7: Soil erosion susceptibility map of Chite watershed.

Table 5.7 shows that the very high and high susceptibility zones cover an area of about 4.08 and 9.50 km^2, accounting for 7.83% and 18.21% of the study area, respectively (Fig 5.8). This signifies that about one-fourth, i.e., 26.04% of the total

geographical area, extending over 13.56 $km^{2,}$ have higher chances of soil erosion occurrences, which are mainly confined to the northern parts and along the eastern and western corners of the watershed (Fig 5.7). Generally, these zones have higher elevation, higher lineament density, higher rainfall intensity, steeper slopes, lesser vegetation, and lesser distance to steams and are primarily found in areas where anthropogenic activities like built-up land, cropland and bare land alter natural landscapes. About 13.25 km^2, representing 25.40% of the watershed, falls under the moderate susceptibility zone (Fig 5.8) (Table 5.7). This zone also falls mainly on areas where human-induced alteration occurs. However, a substantial decrease in erosion susceptibility may be attributed to the declining impact of intrinsic environmental factors like elevation, slope, etc., on the erosional processes. Besides, the presence of sparse vegetative cover in the area may be considered responsible for reducing the plausibility of erosion to a considerable extent. The low class of erosion susceptibility have the most extensive area coverage of about 26.21% (13.67 km^2), while the very low class occupies 22.35% (11.66 km^2) of the watershed (Fig 5.8) (Table 5.7). These zones are generally found in the watershed's central and southern parts, with lesser human interference, lower elevation, and higher vegetation cover (Fig 5.7). However, the lower susceptibility zones are also observed in those areas significantly dominated by various environmental factors. Apart from the existence of certain factors that may regulate soil erosion, the sole factor responsible for the area's lower susceptibility is vegetation, which has a remarkable capacity to reduce soil erosion (Issaka and Ashraf, 2017).

Table 5.7: Soil erosion susceptibility zone of the Chite watershed.

Susceptibility Zone	**Area**	
	(Km^2)	**(%)**
Very High	4.08	7.83
High	9.50	18.21
Moderate	13.25	25.40
Low	13.67	26.21
Very Low	11.66	22.35
Total:	**52.16**	**100.00**

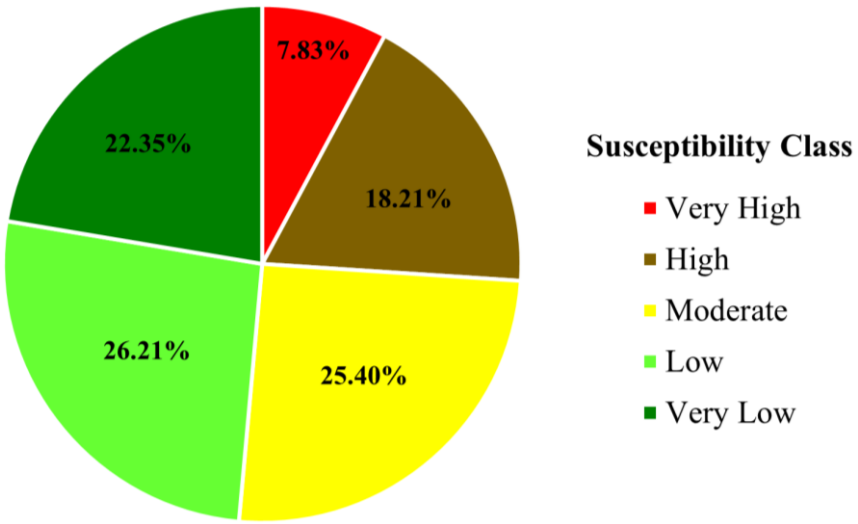

Fig 5.8: Spatial distribution of erosion susceptibility class in Chite watershed.

5.5 Validation of the model

The scientific significance of a predicted model must be proved through validation (Gayen and Saha, 2017). In this research, the accuracy of the AHP-generated erosion susceptibility map has been verified by Receiver Operating Characteristics (ROC) curves and the area under the ROC curve (AUC), using the ArcSDM tool in ArcGIS platform. The predicted model was tested against the erosion inventory map, separately for 133 erosion points and 90 non-erosion points in the study area. AUC values ranging from 0 to 1 can examine susceptibility maps' precision, in which an accurate and reliable model must have AUC above 0.5 (Chen et al., 2016; Achour et al., 2017). The ROC curve and the quantitative values of the AUC are presented in Fig 5.9 (a) and (b). The AUC results derived for erosion points compared with the predicted model is 0.812 (81%), while it is 0.922 (92%) for non-erosion points, which indicates “very good” and “excellent” results respectively (Pourghasemi et al., 2013). Therefore, it can be inferred that the utilization of the Analytical Hierarchy Process in this study exhibited a high level of precision in forecasting soil erosion susceptibility in the Chite watershed.

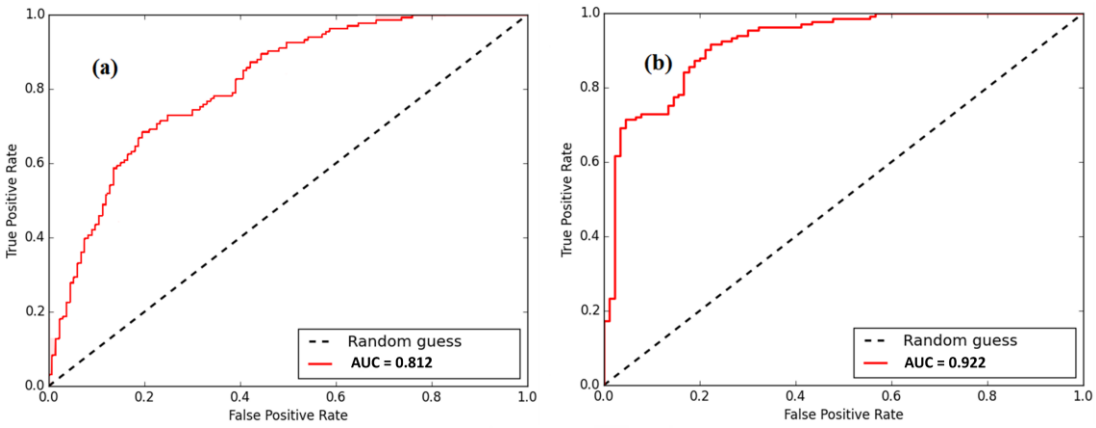

Fig 5.9: Success rate curves for erosion susceptibility model (a)Erosion and (b) Non-Erosion points.

CHAPTER-6

SOIL LOSS AND SEDIMENT YIELD

6.1 Introduction

The accelerated rate of soil erosion significantly impacts both the on-site and off-site, emphasizing the need for compelling management approaches to ameliorate land degradation, impaired water quality, and sedimentation (Devatha et al., 2015). Such an effective management strategy can be developed through the quantitative assessment constituting the rate or magnitude and spatial pattern of soil erosion (Prasannakumar et al., 2012; Ganasri and Ramesh, 2015; Markose and Jayappa, 2016; Singh and Panda, 2017; Belayneh et al., 2019). In such a situation, the application of geospatial technique-based modelling is very crucial and consistent for the quantitative analysis of soil erosion along with the sedimentation process in a river basin (Rajbanshi nad Bhattacharya 2020; Ganasri and Ramesh 2015; Biswas and Pani, 2015). Hence, the rate and amount of soil erosion and soil loss, as well as the rate of sedimentation, have been assessed with the Revised Universal Soil Loss Equation (RUSLE) model and the RUSLE-based Sediment Delivery Ratio (SDR) method: RUSLE-SDR approach respectively. The present study integrated these methods with Remote Sensing and Geographical Information System (GIS) technology.

6.2 RUSLE factors

6.2.1 Rainfall Erosivity (R- factor)

Rainfall erosivity (R-factor) is an index that represents the effects of both rainfall and run-off in soil erosion processes. It reflects the various rainfall characteristics like temporal interval, quantity, and intensity to generate soil detachment (Naqvi et al., 2012; Markose and Jayappa, 2016). The present study determined the R-factor from the average annual rainfall computed for the three rain gauge stations covering 12 years. The calculated R-factor are 841.08, 851.71, and 816.51 $MJ.mm/ha^{-1}.h^{-1}.year^{-1}$ for SMC, HQP and TBDO, respectively (Table 6.1).

Being derived from rainfall data, the R-factor has shown a close relationship with the average annual rainfall. The R-factor map shows that the erosivity factor ranges from 829.39 to 851.71 MJ.mm/ha^{-1}.h^{-1}.year^{-1}, with a mean and standard deviation value of 842.54 and 4.70, respectively. The R-factor map depicts the spatial pattern of rainfall erosivity in the study area, where the northern and the north-eastern parts have higher values, which indicates higher chances of rainfall energy to detached soil particles and induced soil loss (Fig. 6.1). Contrary to that, the erosivity rate is progressively declining towards the southern and south-eastern regions, leading to a reduced possibility of soil loss in those areas.

Table 6.1: Average annual rainfall & R-Factors.

YEARS	**Stations with average annual rainfall**		
	SMC	**HQP**	**TBDO**
2010	2650.8	2659.3	2226
2011	1909.4	1922.5	1578.8
2012	2543.1	2318.5	2236
2013	1920.8	1845	1285
2014	1790.6	1815	1637.8
2015	2412.3	2322.3	2326.5
2016	2161.1	2179.7	2172.5
2017	2686.7	2792.12	2827.4
2018	1749	1860.7	1940
2019	1709.8	1782	2052
2020	1741.5	1766.5	2109
2021	1917.6	2280.6	1989.5
Average Annual Rainfall	2099.39	2128.69	2031.71
R-Factor	841.08	851.71	816.51

* SMC = State Meteorological Centre, Directorate of Science & Technology, Govt. of Mizoram, HQP = HQ CE (P) Pushpak, Aizawl and TBDO = BDO Office, Thingsulthliah.

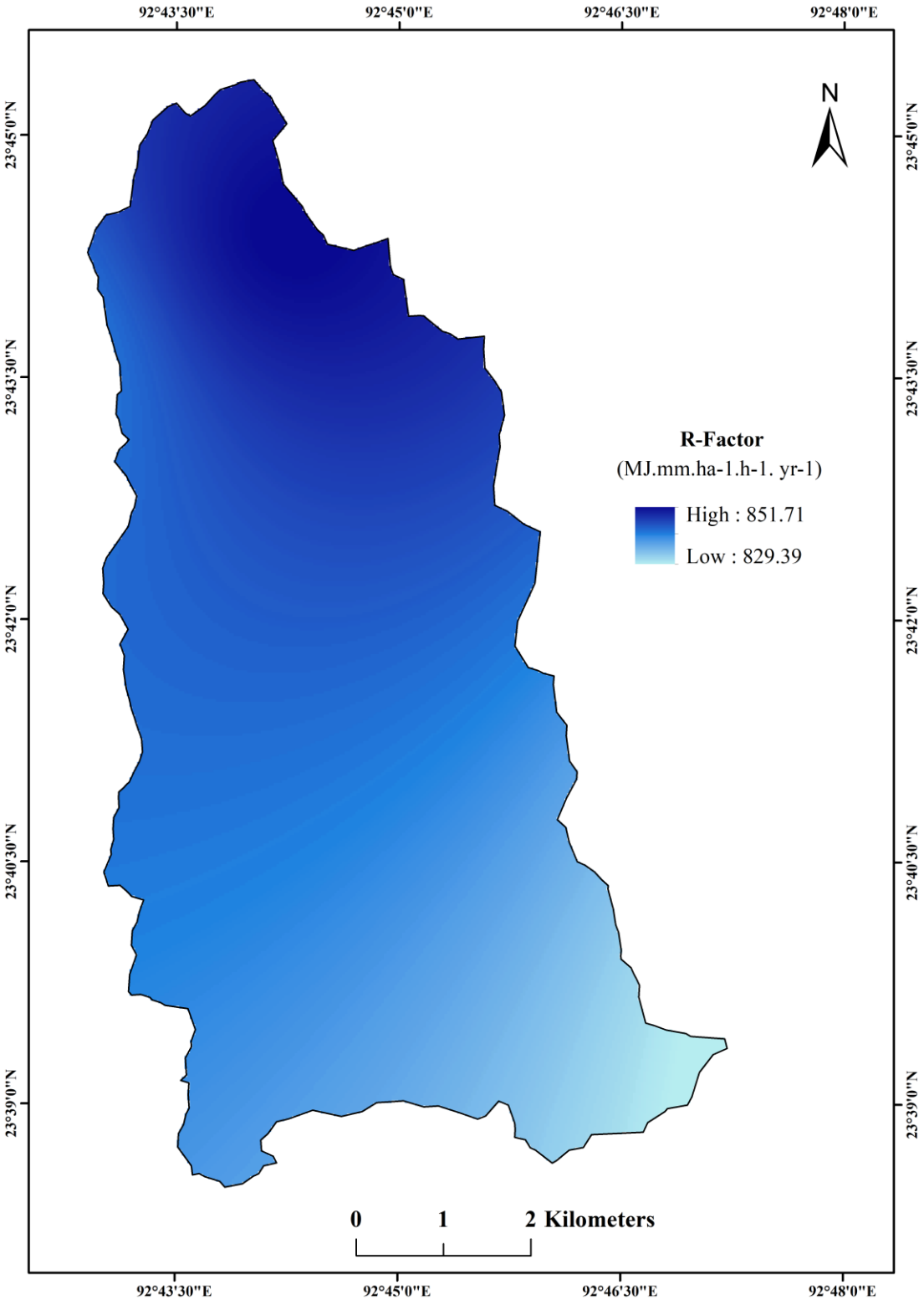

Fig. 6.1: R-factor map

6.2.2 Soil Erodibility (K- factor)

The soil erodibility factor (K) refers to the reaction of a specific soil property against the forces exerted by rainfall and the subsequent run-off. Likewise, it constituted the soil erosion rate relative to the rainfall erosivity index for that soil (Belasri and Lakhouili, 2016). Hence, the K-factor value indicates the natural predisposition of soil to erosion, which is determined based on the soil texture, organic matter content, structural composition, and permeability (Karaburun, 2010). Generally, fine and medium-textured soils have low infiltration rates and are more subjected to water-induced soil erosion due to high run-off (Pimentel, 2006). However, the calculated K-factor values for the study area show that the observed coarse-textured soils, like loamy sand, and the moderately coarse-textured soils, such as coarse sandy loam, sandy loam and fine sandy loam, have a higher erodibility compared to the relatively fine-textured soil, viz., sandy clay loam (Table 6.2). This may be attributed to the coarser-grained soils' lower content of clay and organic matter, as soils with relatively higher clay and organic matter content are more resistant to soil erosion (Bamutaze et al., 2021). Moreover, fine-textured soils generally have high clay content and thus reveal lower K values due to the strong cohesion of clay particles, making them less susceptible to detachment (Mhaske et al., 2021).

The calculated K-factor of the study area extends between 0.30 to 0.68 tons.ha.h.ha^{-1}.MJ^{-1}.mm^{-1}, with a mean value of 0.48 tons.ha.h.ha^{-1}.MJ^{-1}.mm^{-1}. The mean value was calculated for the five textural class, and the K-factor map was prepared to show the varying erodibility of soil in the watershed (Fig. 6.2). The map shows that the mid-eastern parts of the watershed characterized by loamy sand has high erodibility. The mean K-factor of this soil is 0.57 and occupies about 10.20% of the total geographical area. Soils with moderate erodibility, such as fine sandy loam, sandy loam and coarse sandy loam, with a mean K-factor value of 0.47, 0.48 and 0.49, are found in almost all parts of the watershed, covering an area of about 23.95%, 40.86% and 24.46% respectively. On the other hand, the least erodible soil, i.e., the sandy clay loam, occupies the modest segment of about 0.54% in the western corner of the study area, with a mean K-factor value of 0.40.

Table 6.2: Physical properties of soil and the calculated K-Factor.

Soil Textural Class	Descriptive Statistics	Sand (%)	Silt (%)	Clay (%)	OC (%)	OM (%)	'a'	'b'	Area (km^2)	Area (%)	Average 'M'	Average 'K-Factor'
Sandy clay loam	Min	54.47	15.58	21.16	0.83	1.66	2	3	0.28	0.54	6095.19	0.40
	Max	61.38	23.86	23.69	2.31	4.62	2	3				
	Mean	58.98	19.09	21.93	1.59	3.21	2	3				
	SD	2.27	2.69	0.98	0.51	1.02	2	3				
Fine sandy loam	Min	54.81	28.74	7.26	0.68	1.36	1	2	12.49	23.95	8080.66	0.47
	Max	60.49	33.61	11.86	2.08	4.16	1	2				
	Mean	57.94	31.94	10.12	1.56	3.12	1	2				
	SD	1.78	1.41	1.41	0.39	0.78	1	2				
Sandy loam	Min	60.34	18.86	6.22	0.52	1.04	1	2	21.31	40.86	8323.59	0.48
	Max	64.82	31.92	18.76	2.35	4.70	1	2				
	Mean	62.98	28.23	8.79	1.64	3.28	1	2				
	SD	1.27	2.19	1.91	0.40	0.79	1	2				
Coarse Sandy loam	Min	65.73	20.49	5.19	0.56	1.12	1	2	12.76	24.46	8588.16	0.49
	Max	70.38	27.87	9.19	2.21	4.42	1	2				
	Mean	68.40	24.26	7.33	1.71	3.43	1	2				
	SD	1.57	2.28	1.15	0.39	0.78	1	2				
Loamy sand	Min	75.69	14.36	5.53	0.67	1.34	1	2	5.32	10.20	8804.22	0.57
	Max	80.11	17.83	6.48	1.43	2.86	1	2				
	Mean	78.06	15.77	6.17	1.21	2.43	1	2				
	SD	1.83	1.47	0.44	0.36	0.73	1	2				

* OC = Organic Carbon, OM = Organic Matter Content, 'a' = Soil structural code, 'b' = Soil permeability class, 'M' = particle size parameter.

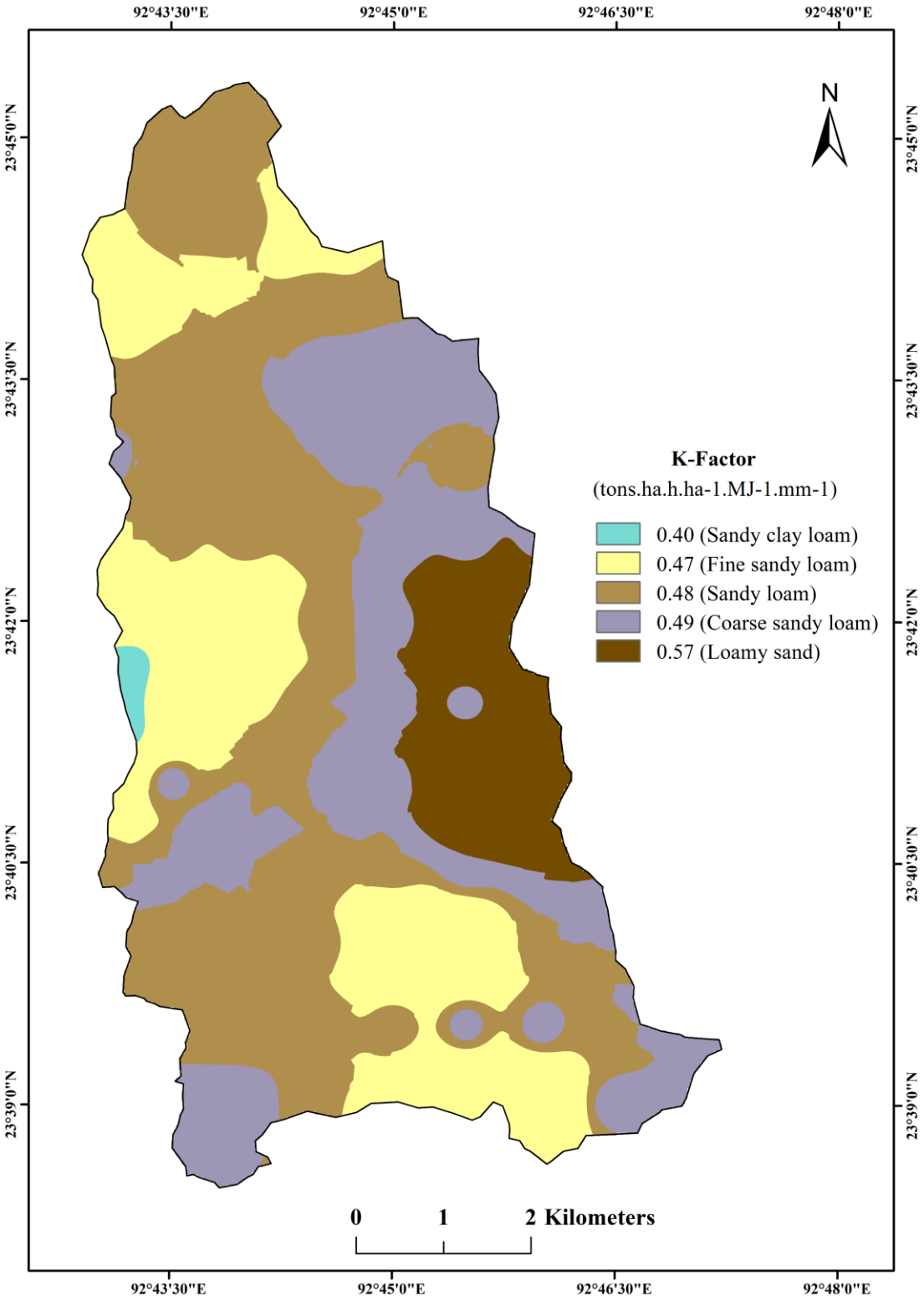

Fig 6.2: K-Factor map

6.2.3 Slope length and steepness (LS- factor)

In the RUSLE model, topographical impact towards soil erosion is determined through the LS-factor, which incorporates the influence of both the length (L) and steepness (S) of the slope (Prasannakumar et al., 2011; Alexakis et al., 2013). As the erosive force of water is influenced by slope characteristics, an increase in these factors results in a higher rate of soil erosion but will simultaneously diminish when they decrease (Koirala et al., 2019; Dutta et al., 2015). The LS factor indicates the proportion of soil loss on a specific topography compared to a standard unit plot, with a slope dimension of 72.6 ft in length and a 9% gradient (Renard et al., 1997).

As the study area is a hilly watershed with undulating terrain, the slopes are generally steep, and about 31% of the area has a slope exceeding 30º of inclination. The computed LS-factor for the study area ranges between 0 and 41.34, having a mean value of 0.21 and a standard deviation of 0.98 (Fig 6.3). It has been observed that about 95% of the watershed has an LS-factor less than 0.25, which is mainly associated with the steep but short length of the slope (Pham et al., 2018). These lower values are primarily found in the upper catchment. On the other hand, the higher LS-factor values are mainly concentrated along the main river course, Chite Lui. This may be attributed to the more continuous slope along the river channel and the steep inclination of the adjoining hillside slopes (Farhan and Nawaiseh, 2015).

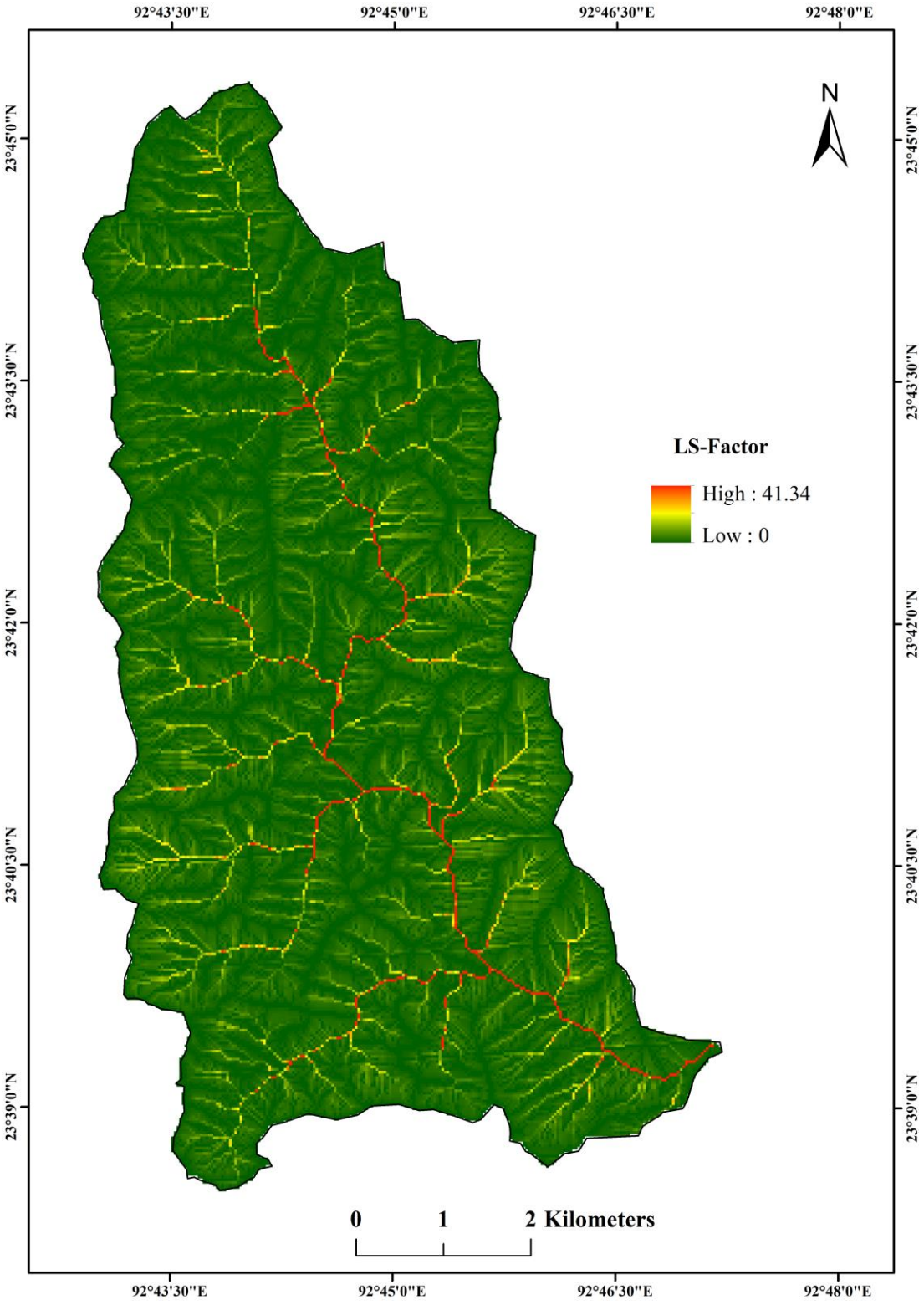

Fig. 6.3: LS-Factor map.

6.2.4 Cover management factor (C)

The soil loss ratio may significantly fluctuate depending on land management and cover conditions (Renard and Ferreira, 1993). Modification in the land use/land cover (LULC) has the most dominant control over the soil erosion rate at a particular site with various cover and management systems (Kabede et al., 2021). Hence, the C-factor are generally represented by land use/land cover of a given area and the C-factor values are assigned based on their corresponding LULC classes (Karaburun, 2010; Ashiagbor et al., 2013; Biswas and Pani, 2015; Ganasri and Ramesh, 2016; Singh and Panda, 2017; Rajbanshi and Bhattacharya, 2020).

The derived C-factor layer from the LULC map reveals that C-factor values of the watershed range from 0.003 in the forested area to 1 in unprotected bare land, with a mean value of 0.11 and a standard deviation of 0.18 (Fig 6.4) (Table 6.3). Vegetation cover, in the case of forest and open forest, has a remarkably lower chance of soil loss exhibiting a meagre C-factor value of 0.003 and 0.006 respectively. This is due to the significant role played by vegetation in protecting the soil from direct rainfall impact and reducing runoff velocity, improving the infiltration rate, and sustaining the physico-chemical and biological properties of soil (Atoma et al., 2020). On the other hand, the bare land comprising of several earth spoils dumping areas, cleared land for shifting cultivation, constructional sites, etc., has the highest C-factor because these unprotected surfaces consisting of loose soil materials are exposed to the direct influence of rainfall. Due to the absence of remarkable soil and water conservation practise and the prevailing shifting cultivation, the cropland covering 22.42% of the total geographical area is at risk of soil loss and thus has a moderately higher C-factor value of 0.28. Built-up land has a somewhat lower C-factor value of 0.09, which can be attributed to the hard surface coverage of soil by residential areas, public buildings and commercial areas, roads, recreational centres, etc. However, the low infiltration capacity of these impervious surfaces may produce massive run-off, thereby producing soil loss at the adjoining uncovered surfaces.

Table 6.3: Land use / land cover classes with C-factor values.

LULC Class	C-Factor Value
Built-up land	0.09
Dense Forest	0.003
Open Forest	0.006
Cropland	0.28
Bare land	1

Source: Biswas and Pani (2015), Chatterjee et al. (2013) and Ganasri and Ramesh (2015)

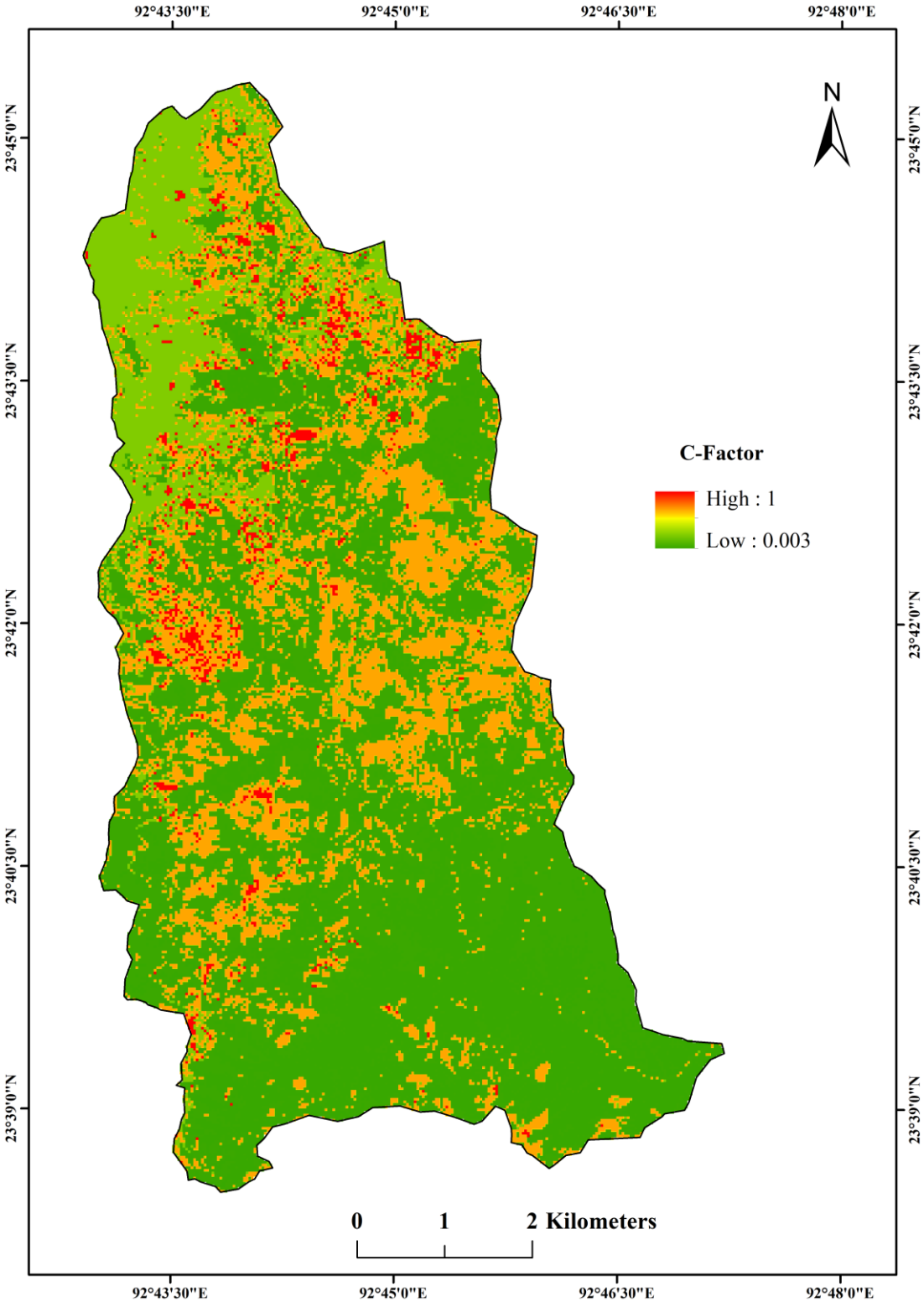

Fig. 6.4: C-Factor map.

6.2.5 Conservation management practise factor (P)

P-Factor has been defined as "the ratio of soil loss with a specific support practice to the corresponding loss with upslope and downslope tillage". The soil conservation support practices were designed and intended to reduce soil detachment rate by decreasing run-off capacity. In an agricultural field with sloping land, contour and terrace farming, strip-cropping, and underground drainage pathways are the most significant supporting practices factor (Wischmeier and Smith, 1965; Wischmeier and Smith, 1978; Renard et al., 1997). In the study area, the various conservation strategies were considered negligible as some of the observed sporadic terraces and contour farming extend for only a few meters or more, and that too in a very limited plot of agricultural land. Therefore, a P-factor value of 1 is used in the absence of such remarkable conservation support practices based on the suggestions obtained from various referenced literature.

6.3 Estimated Soil loss of Chite Watershed

The soil loss from the Chite watershed was calculated by using an empirically based model, i.e., the Revised Universal Soil Loss Equation (RUSLE), considering the combined influence of the five pre-evaluated factors, viz. rainfall erosivity (R), soil erodibility (K), slope length and steepness factor (LS), cover management factor (C), and conservation management practise factor (P). The detailed assessment of each parameter revealed the possible occurrences of considerable soil loss in the current study (Fig.6.5). Based on the estimates, Chite watershed has an average annual soil erosion rate of 6.10 tons ha^{-1} $year^{-1}$, which ranges from a minimum and maximum rate of 0 and 4928.90 tons ha^{-1} $year^{-1}$, respectively. The evaluated amount of the total soil loss within the watershed is about 357580.90 tons $year^{-1}$. The obtained soil erosion rate was categorized into five erosion severity classes following the classification systems of Chatterjee et al. (2013), and Sharda et al. (2013) as Very low (Below 5 tons ha^{-1} $year^{-1}$), Low (5 - 10 tons ha^{-1} $year^{-1}$), Moderate (10 – 20 tons ha^{-1} $year^{-1}$), Severe (20 – 40 tons ha^{-1} $year^{-1}$) and Very Severe (Above 40 tons ha^{-1} $year^{-1}$) . The classified soil

erosion severity class, erosion rate, area coverage, and detailed soil loss data are presented in Table 6.4 and Fig. 6.5.

Table 6.4: Severity class and distribution of soil loss in Chite watershed.

Erosion Class	CER (tons ha^{-1} $year^{-1}$)	Area		MASL (tons ha^{-1} $year^{-1}$)	Gross soil erosion	
		(km^2)	(%)		(tons $year^{-1}$)	(%)
Very Low	< 5	41.99	80.51	0.51	23981.12	6.71
Low	5 - 10	3.80	7.29	7.23	30487.26	8.53
Moderate	10 - 20	3.35	6.41	14.09	52343.83	14.64
Severe	20 - 40	1.66	3.18	27.45	50621.74	14.16
Very Severe	> 40	1.36	2.61	149.59	200146.95	55.97
TOTAL:		**52.16**	**100.00**		**357580.90**	**100**

* CER = Classified soil erosion rate, MASL = Mean annual soil loss

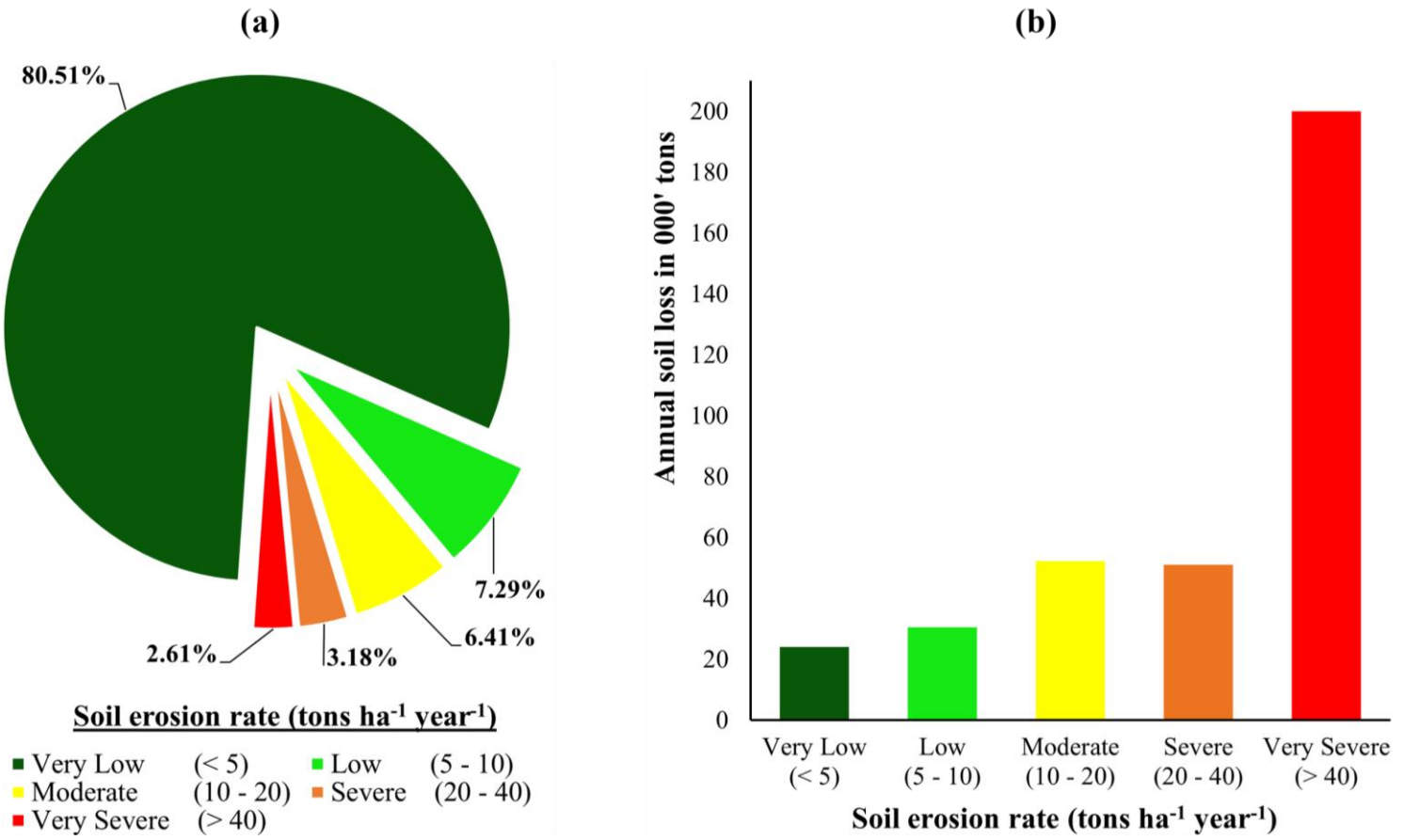

Fig. 6.5: (a) Spatial extent, and (b) annual soil loss of various erosion severity classes.

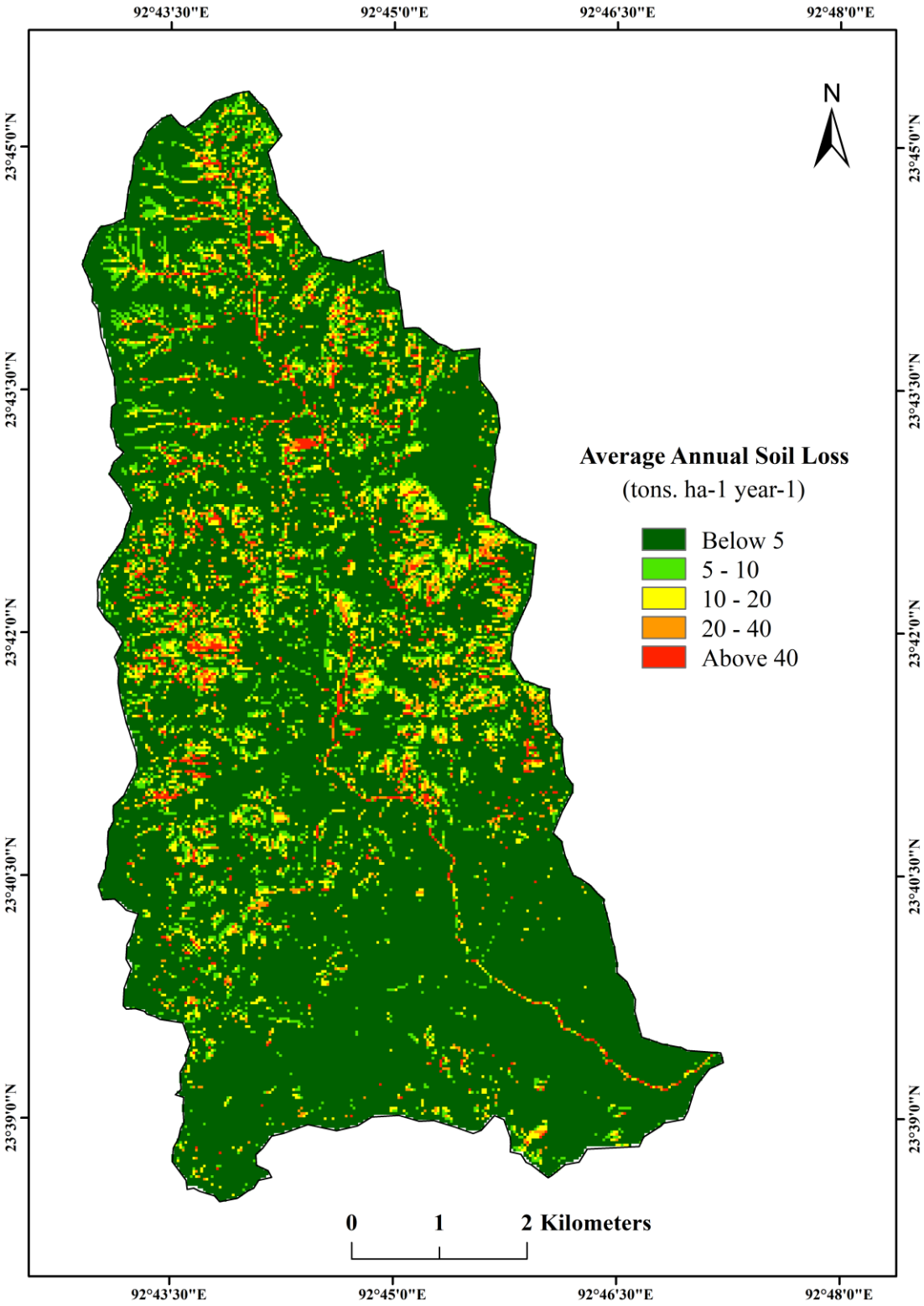

Fig. 6.6: Soil loss map of Chite watershed.

Fig. 6.6 illustrates the spatial pattern of the average annual rate of soil erosion and their respective class in the Chite watershed. About 80.51% and 7.29% of the study area covering 41.99 and 3.80 km^2 has a very low (below 5 tons ha^{-1} $year^{-1}$) and low (5 – 10 tons ha^{-1} $year^{-1}$) rate of soil erosion, respectively. The zone falling under the moderate class (10 – 20 tons ha^{-1} $year^{-1}$) of soil erosion extends to about 3.35 km^2 (6.41%) in the watershed. Those regions experiencing severe (20 – 40 tons ha^{-1} $year^{-1}$) and very severe (above 40 tons ha^{-1} $year^{-1}$) soil loss occupy approximately 1.66 and 1.36 km^2, accounting for only 3.18 and 2.16 % of the total geographical area, respectively. Besides the limited areal extent of both the severe and very severe soil erosion classes, they have contributed to about 250,768.31 tons of soil loss every year, 70.13% of the total soil loss from the watershed. This indicates that most soil detachment occurs at relatively small areas within the study area.

Although rainfall erosivity is the single most effective independent variable that controls the quantity of soil loss in the present research, its influence is not significantly evident in spatial variability, primarily due to the small size of the watershed. However, the spatial pattern of soil erosion rate can be remarkably related to the land use/land cover (LULC) classes, as it is the ultimate manifestation of various anthropogenic activities in the study area. The comparatively secure units of land are found extensively throughout the watershed and are generally confined to those areas with substantial vegetative covers. Moreover, definite locations of the built-up areas are also found well protected against soil detachment, which may be attributed to the protective response of impervious surfaces from the direct impact of rainfall. On the contrary, the croplands have shown a high possibility of soil loss, as shifting cultivation predominates the agricultural system in the study area besides a few plots utilized for subsistence plantations. No such significant conservation activities are worth mentioning throughout the area, resulting in soil loss of very severe intensity.

Moreover, the bare land representing earth spoil dumping sites, constructional sites, and unsurfaced agriculture link roads are also prominent sources of unconsolidated sediments. Apart from all the previously mentioned locations, soil loss of severe to very severe intensity is also observed in the hillside slopes of built-up areas adjoining the tributary streams and along the entire course of the main river. This

may be attributed to the high erosive power of streams due to steep and narrow channels and high run-off produced from the impermeable built-up areas. Most of the severe and very severe zones of soil loss are also observed in the vicinity of the terrain affected by landslides in the study area.

6.4 Erosion risk assessment based on soil loss tolerance limits

The soil loss tolerance limits or tolerable soil loss limits (T-value) refers to the most severe erosion rate a particular soil can endure while maintaining optimal crop production for an extended period (McCormack et al., 1982). This tolerable value is a significant indicator for ascertaining the possible risk of soil erosion in a watershed as it distinctly represents the possible on-site and off-site impact like that of soil fertility reduction and sedimentation, respectively, which is imperative for developing effective measures to conserve the long-term economic and ecological sustainability of soil (Mandal and Sharda, 2011 (a); Li et al., 2009). Therefore, a reliable site-specific T-value is necessary for maintaining a sustained coexistence between erosion rates and tolerable soil loss in a specific region. If the soil erosion rates surpass the T-value, it will consequently result in a negative impact, reducing soil productivity and may further enhance the sediment transportation downstream. Due to this possible adverse effect on productivity and off-site consequences, the erosion rate should be reduced within a specific permissible limit to maintain the long-term viability of a production system and ecological sustainability. Hence, the soil loss tolerance limits may be a significant tool for prioritizing critical areas that require effective soil erosion control measures (Bhattacharya et al., 2008; Lakaria et al., 2008; Lenka et al., 2014).

The extracted soil loss tolerance limit (T) from the base map prepared by Mandal and Sharda, (2011 (b)) for the Chite watershed is 7.5 tons ha^{-1} $year^{-1}$. Based on this threshold value, it was found that about 44.23 km^2, i.e., 84% of the study area, has a tolerable soil loss, but the remaining 7.93 km^2 (15.20%) has exceeded the maximum limit of soil erosion rate, indicating a higher risk of soil erosion (Table 6.5). Almost all the areas with soil loss above the soil loss tolerance limit are observed from the cropland and comprise the low, moderate, severe and very severe categories of soil

erosion rate in the watershed. Moreover, these critically sensitive zones with a higher risk of soil erosion are mainly concentrated in the central parts of the watershed, where the land use is primarily confined to agriculture and is also distributed throughout the study area in a varying rate and extent (Fig. 6.7). Besides agricultural land use, there has been excessive deforestation in the upper catchment, which is a highly urbanized land area. However, built-up areas were not considered, as soil loss tolerance is exclusively recommended based on agriculture (Morgan, 2005). The results clearly reflected the absence of significant soil conservation measures and management in the study area. Hence, systematic prioritization of these relatively smaller areas is crucial to formulate necessary conservation measures for reducing the characteristics of the high rate of soil loss within a desirable degree to ensure higher productivity of soil along with maintaining its ecological sustainability.

Table 6.5: Status of Chite watershed with respect to soil loss tolerance.

Soil loss tolerance limit (T)	**Soil loss rate**	**Area**		**Total Soil Loss**	
(tons ha^{-1} $year^{-1}$)	**(tons ha^{-1} $year^{-1}$)**	**(km^2)**	**(%)**	**(tons $year^{-1}$)**	**(%)**
7.5	≤ 7.5	44.23	84.80	39293.30	10.99
	> 7.5	7.93	15.20	318287.60	89.01
Total:		52.16	100.00	357580.90	100

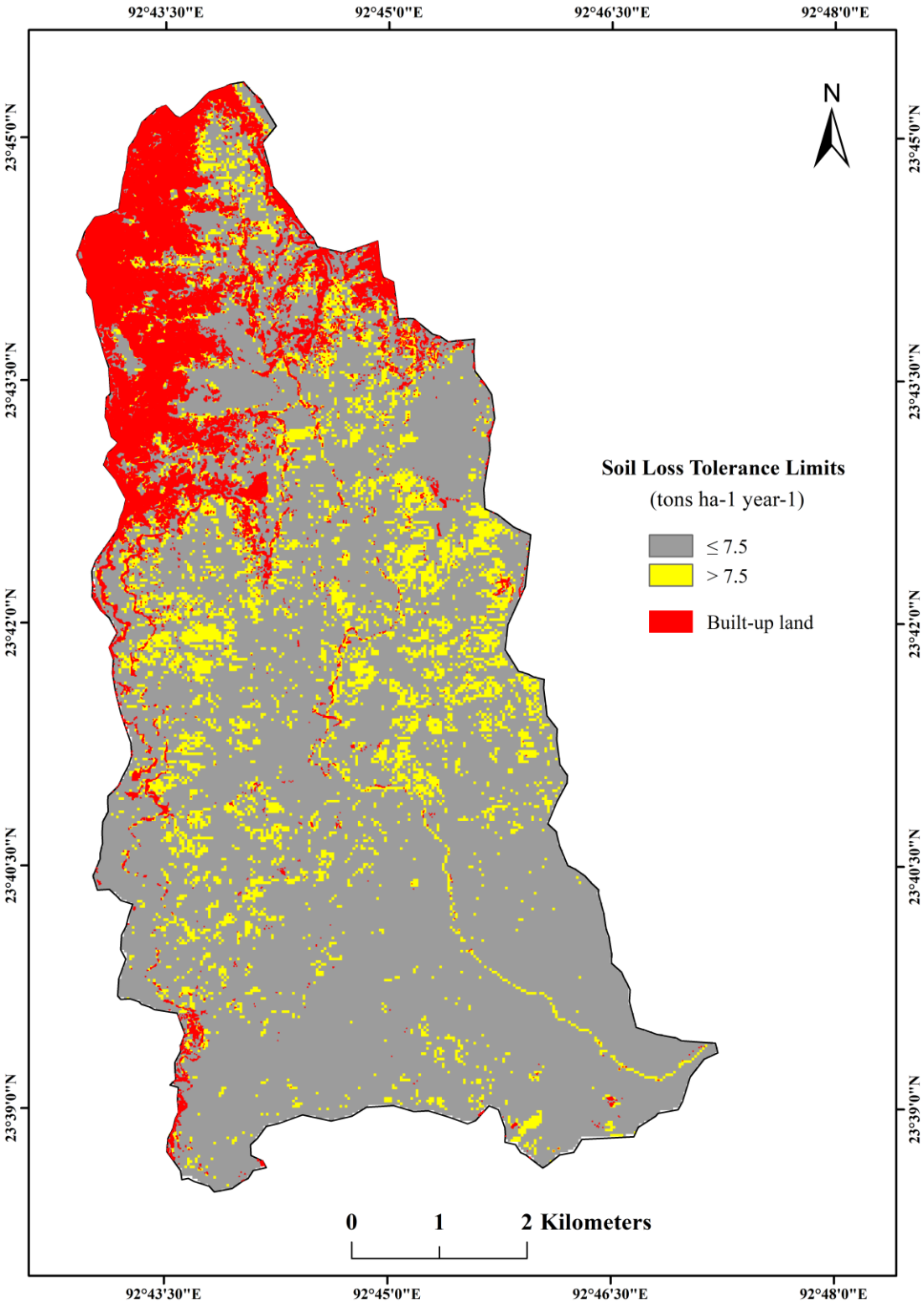

Fig 6.7: Spatial distribution of area below and above the tolerable soil loss limit.

6.5 Evaluated Sediment Yield of Chite Watershed.

The quantity of sediment yield at the river mouth represents the sedimentation rate from the watershed (Tamene et al., 2006; Kidane et al. 2019). In the case of an ungauged watershed, applying a geospatial model is crucial to quantitatively analyze soil erosion along with the sedimentation process (Rajbanshi and Bhattacharya 2020). Hence, the sedimentation rate in the Chite watershed has been determined from the total soil loss calculated by integrating the RUSLE model with the sediment delivery ratio (SDR). The study area has a calculated sediment delivery ratio (SDR) of 0.288, and the estimated sediment yield (SY) is about 102983.29 tons year^{-1}, which accounts to 28.80% of the gross soil erosion in the watershed (Table 6.6). This indicates that approximately 71.20% of the soil detached from different parts of the watershed was deposited elsewhere within the watershed, while the remaining 28.80% has been transported through the basin outlet. As the watershed's size and the sediment delivery ratio (SDR) have shown an inverse relationship, a relatively larger area generally produces a lesser SDR value and vice versa, indicating the watershed potential for accumulating or transferring the detached soil particles (Gelagay, 2016). Hence, the present study has recorded high sediment yield, as more sediments are generally transported from smaller-sized watersheds with relatively shorter and steeper slopes (de Vente et al. 2007). However, most of the sediments generated by soil erosion were re-deposited in different watershed locations.

Table 6.6: Annual & seasonal soil loss and sediment yield.

	Mean annual soil loss		**Total soil loss**		**Sediment Delivery Ratio**		**Sediment Yield (SY)**	
	(tons ha^{-1} year^{-1})		**(tons year^{-1})**		**(SDR)**		**(tons year^{-1})**	
Al	6.1		357580.9		0.288		102983.30	
Sl	**Winter**		**Pre-Monsoon**		**Monsoon**		**Post-Monsoon**	
	A	**SY**	**A**	**SY**	**A**	**SY**	**A**	**SY**
	37943.58	10927.75	109828.48	31630.60	264358.33	76135.19	66717.73	19214.49

* Al = Annual, Sl = Seasonal, A = Total soil loss (tons year^{-1}), SY = Sediment Yield (tons year^{-1}).

The seasonal pattern of soil loss and sediment yield is significantly similar to that of the annual soil loss and sediment yield in the watershed (Fig. 6.8). However, the sediment yield during the monsoon season was significantly higher than in other seasons. Therefore, the highest predicted sediment yield of about 76135.19 tons year^{-1} was observed in the monsoon season, contributing to 55.21% of the total sediment yield in the watershed computed for the whole year. On the other hand, the dry months of the winter season have recorded the lowest sediment yield. During the winter season, the least amount of sediment yield, which accounts for about 10927.75 tons year^{-1} is observed, contributing to only 7.92% of the total annual sediment yield.

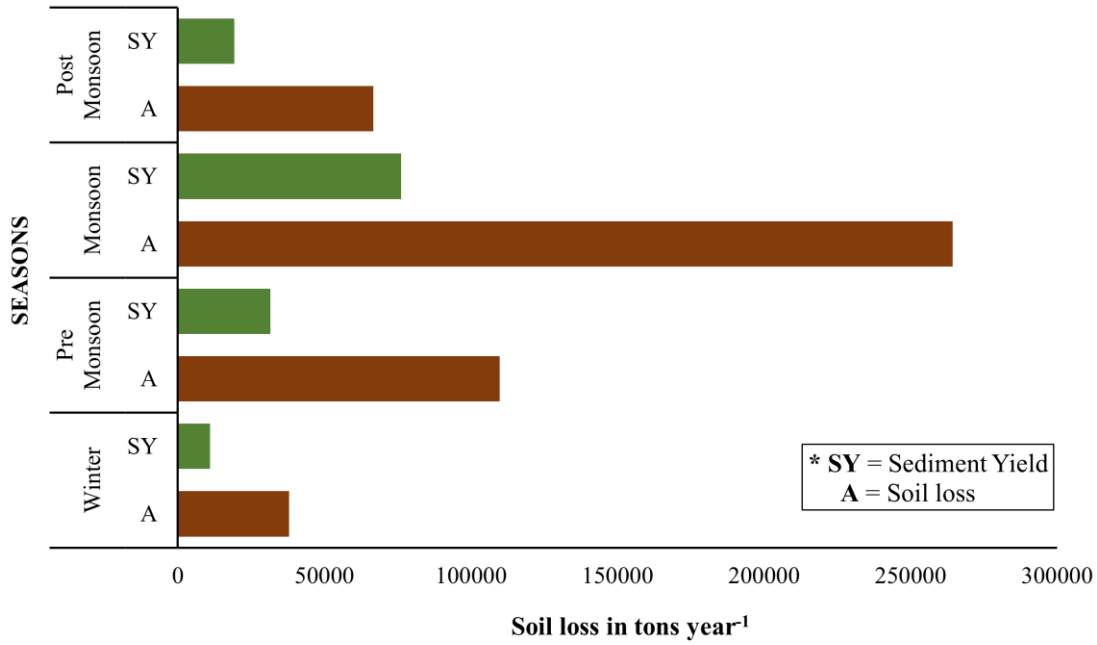

Fig. 6.8: Seasonal soil loss (A) and sediment yield (SY) in the Chite watershed.

The rapid rate of soil loss and sedimentation in the Chite watershed has resulted from various geo-environmental and anthropogenic activities occurring in the study area. The high rainfall erosivity, steep slopes, human activities' alteration of the natural environment, and faulty agricultural practices without proper conservation management have led to accelerated soil erosion and sedimentation rates. The high-intensity rainfall with an extended period during the monsoon season has a remarkable

impact on soil loss and sediment yield through run-off as the study area falls under the direct influence of the southwest monsoon. Besides, the various land use/land cover classes have exerted a varying response towards the sediment yield depending upon the soil loss severity in such areas. The slope has also shown a prominent influence on the accumulation and transportation of sediments because there is a greater chance of sediment deposition in a relatively larger watershed as the slope generally extends longer towards the streams. In contrast, more sediments are generally transported from smaller watersheds with relatively shorter and steeper slopes (de Vente et al., 2007). Nevertheless, the actual amount of sediment yield is directly related to the quantity of the potential soil loss, as the sediment yield represents only a fraction of the gross soil erosion in a watershed (Wu et al., 2017). Hence, the more potential of soil loss may result in higher sediment yield and vice versa.

CHAPTER-7

WATERSHED PRIORITIZATION

7.1 Introduction

Watershed prioritization is a systematic approach involving identifying more critical areas in the watershed that require immediate attention in terms of various environmental issues. Executing effective erosion control and resource conservation measures considering the entire watershed is often impractical. Such a challenging task is generally associated with several capital, time, and labour limitations, as soil erosion is a universal phenomenon. It is, therefore, necessary to identify those significant zones in the watershed that require immediate treatment and attention (Gajbhiye et al., 2013; Mhaske et al., 2021). As it focuses more on the significant units considering the prevailing geo-environmental and socio-economic conditions, it has a significant role to successfully implement erosion control measures and conservation of natural resources. Hence, prioritising a watershed can facilitate sustainable watershed management by enhancing ecological and social benefits to a considerable extent. Therefore, watershed prioritization has been undertaken in the present research to identify the most imperative zones that urgently require appropriate responses for safeguarding the Chite watershed regarding soil erosion and sedimentation.

7.2 Prioritization of Chite Watershed

Globally, different modeling approaches, viz., morphometric analysis, Universal Soil Loss Equation or Revised Universal Soil Loss Equation (USLE/RUSLE), Sediment Delivery Ratio (SDR), Multi Criteria Decision Making (MCDM), Soil and Water Assessment Tool (SWAT), Sediment Yield Index (SYI), Soil loss tolerance limits (T), etc. were successfully employed individually or as an integration using GIS techniques for watershed prioritization (Thakkar and Dhiman, 2007; Chatterjee et al., 2013; Chowdary et al., 2013; Sudhrishi et al., 2014; Farhan and Anaba, 2016; Markose and Jayappa, 2016; Bhattacharya et al., 2020; Mhaske et al.,

2021; Sinshaw et al., 2021). However, the predicted result of each model is unique; therefore, determining priority based on a single model or a particular model combined with its derived models may be somehow extremely focused only on the inherent variables, leading to partial knowledge of the existing watershed conditions (Ayele et al., 2020). Therefore, an effort has been undertaken to integrate extensive information from various evaluations to create a strong and thorough comprehension of the watershed.

The study area, Chite watershed, was delineated into eight sub-watersheds to determine those geographical units which necessitate urgent intervention and greater attention (Fig. 7.1). For prioritization, four different assessments used in this research including areas under higher erosion susceptibility class (Fig. 7.2), average annual soil loss (Fig 7.3), areas above tolerable soil loss (Fig. 7.4) and the annual sediment yield (Fig. 7.5) were determined simultaneously in each geographical segments, i.e., the eight sub-watersheds (Table 7.1). In the case of erosion susceptibility zones, only the areas falling under high and very high susceptibility categories were considered to address their higher requirement for urgent intervention. Ranks were then assigned for such higher erosion susceptibility zones with respect to their relative percentage of spatial extent in each sub-watershed. Similarly, the proportion of area above soil loss tolerance limits (T) was based on allotting rank, where more considerable area coverage of 'T' in relation to a particular sub-watershed was assigned higher rank and the other way round for those with smaller area. For soil loss and sediment yield, ranks were assigned based on the average annual rate of soil erosion (in tons ha^{-1} $year^{-1}$) and the annual sediment yield (in tons $year^{-1}$) for each sub-watershed.

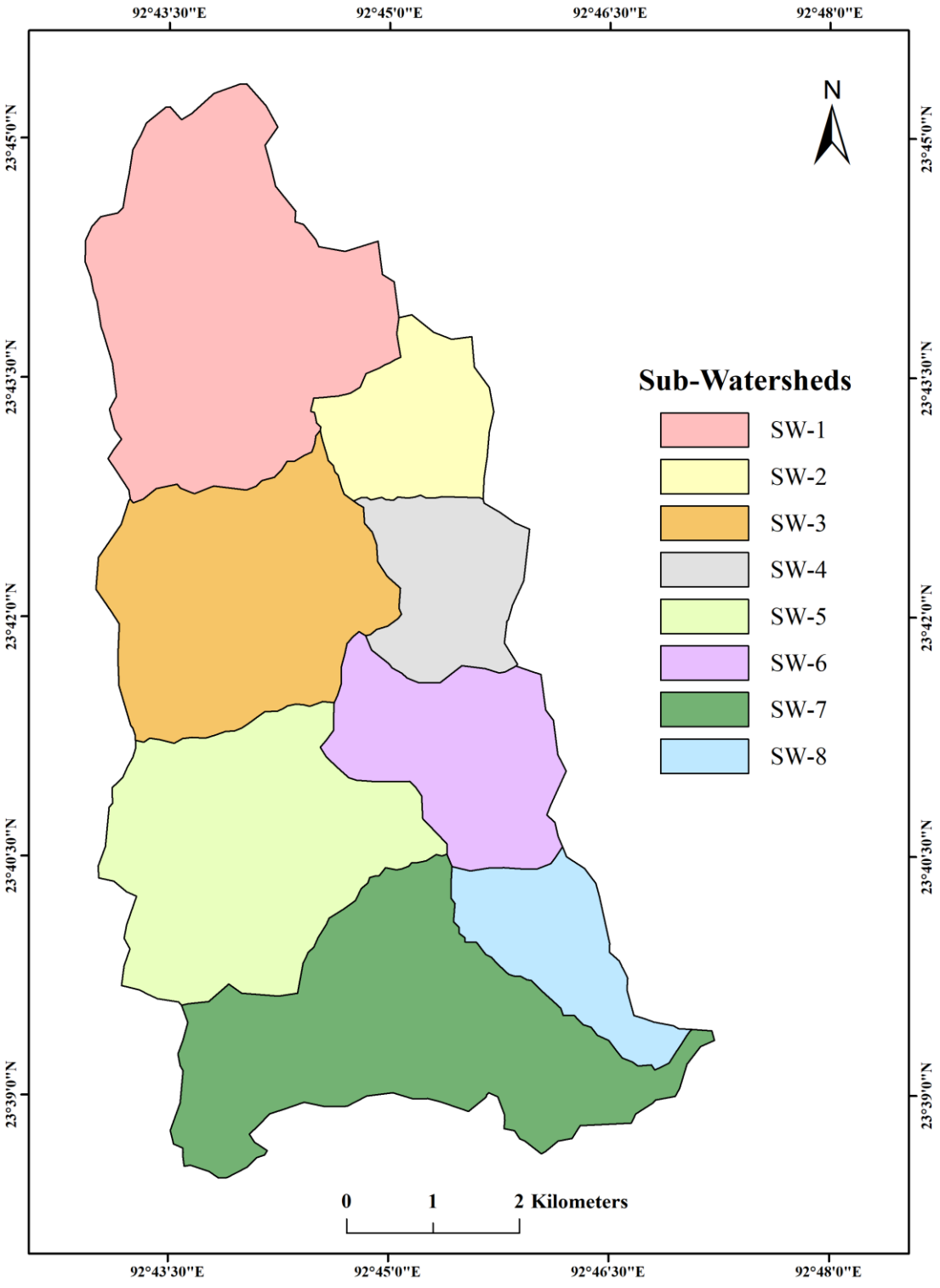

Fig. 7.1: Delineated sub-watersheds of the study area.

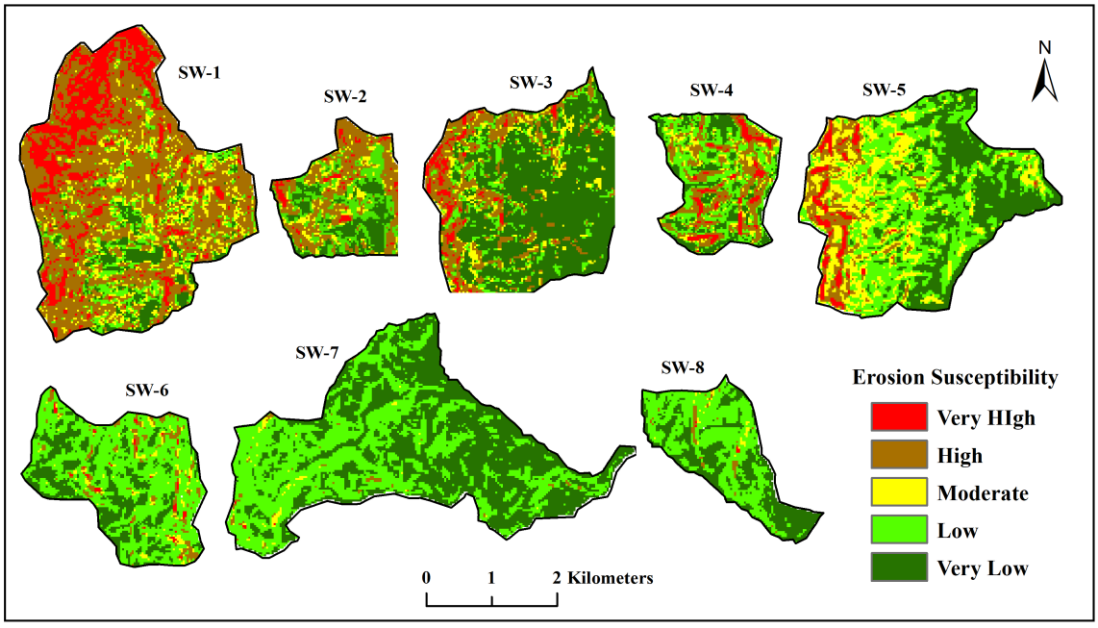

Fig. 7.2: Soil erosion susceptibility map of the sub-watersheds.

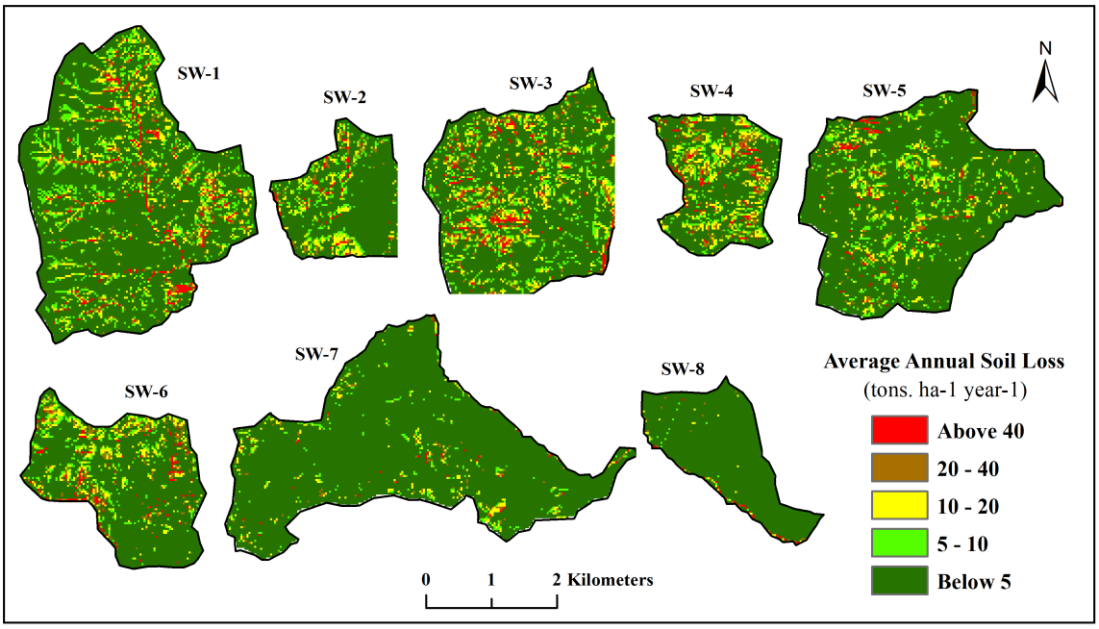

Fig. 7.3: Soil loss map of the sub-watersheds.

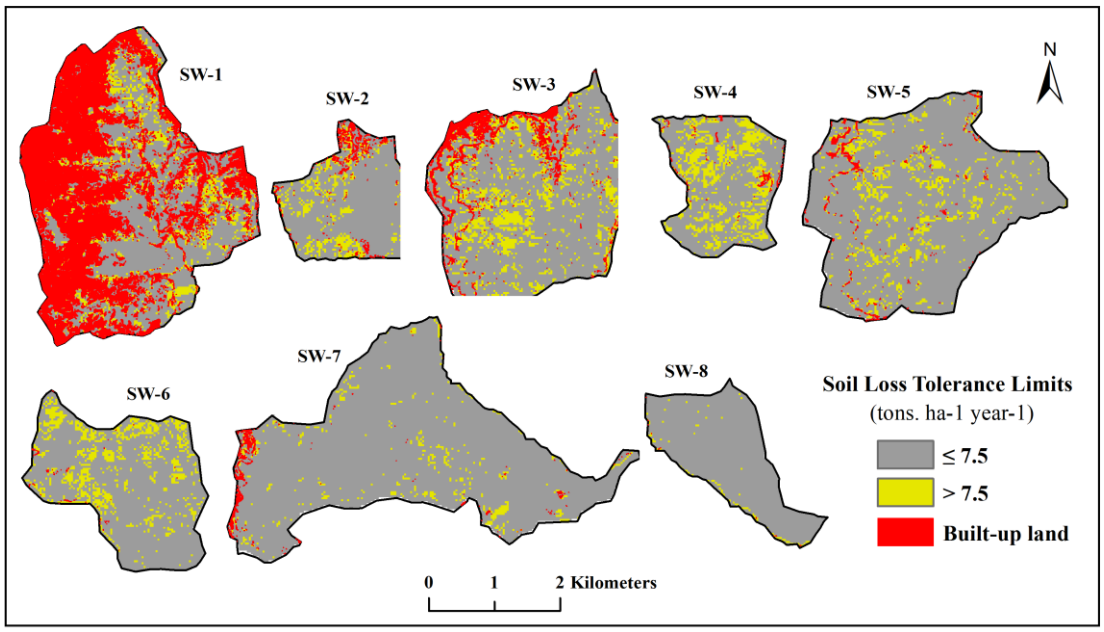

Fig. 7.4: Spatial distribution of area below and above the tolerable soil loss limit.

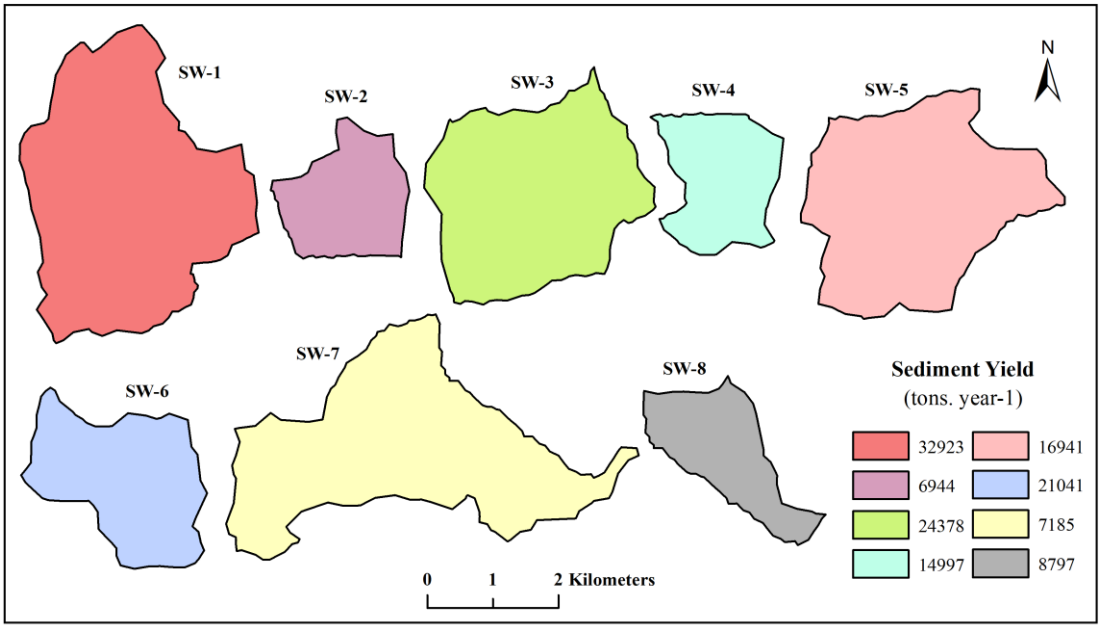

Fig. 7.5: Sediment Yield of the sub-watersheds.

Table 7.1: Obtained results from selected parameters.

Sub-Watershed	Area (km^2)	ES	A	T	SY
		(%)	(tons ha^{-1} $year^{-1}$)	(tons ha^{-1} $year^{-1}$)	(tons $year^{-1}$)
SW-1	11.1	68.32	7.61	17.97	32923.26
SW-2	3.06	37.86	4.29	17.10	6943.56
SW-3	8.12	23.74	7.25	21.35	24378.35
SW-4	3.15	39.25	10.47	30.43	14997.40
SW-5	8.75	12.97	4.43	12.46	16940.80
SW-6	4.76	7.33	9.27	19.76	21040.55
SW-7	10.27	0.78	1.31	4.65	7185.41
SW-8	2.95	2.59	4.18	2.87	8796.79

* ES = % of areas under high and very high class of erosion susceptibility, A = Mean annual soil loss rate, T = % of areas above soil loss tolerance limits, SY = Annual sediment yield.

As all the selected parameters directly relate to soil erosion conditions in the watershed, an increase in their value represents more extensive erosion-sensitive areas, higher amount of soil loss, more areas above soil loss tolerance limits, and sedimentation rate and vice versa. Since the study area comprised 8 sub-watersheds, ranks were allocated from 1 to 8. The highest value of the classified results in each analysis has been assigned rank 1, representing maximum contribution, while the lowest value was ranked 8 to indicate its minimum contribution. Subsequently, the combined results of all four parameters were incorporated through the compound value (C_V) method, which is the calculated average of all the ranks assigned to these parameters. After determining the relative C_V for each geographical unit, the sub-watersheds were categorized into three priority classes: Low (> 5.67 C_V), Medium (3.50 – 5.50 C_V) and High (< 3.5 C_V) respectively (Fig. 7.6) (Table 7.2). The lower the C_V value, the higher the priority class, reflecting the ranking system where 1 was assigned to represents the maximum contribution and 8 for those having most insufficient involvement.

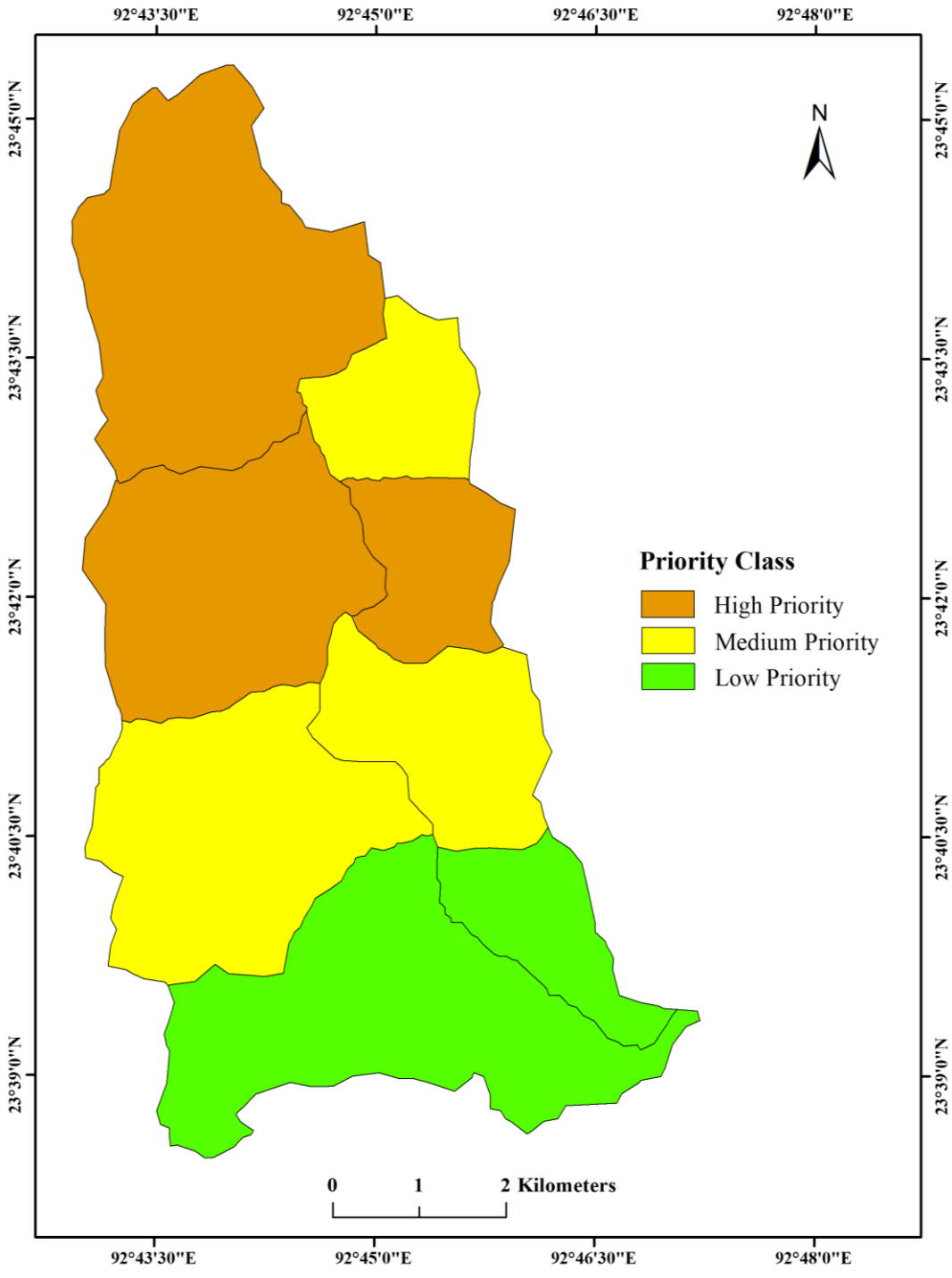

Fig. 7.6: Prioritized map of Chite Watershed.

Table 7.2: Ranks of parameters, calculated compound value and priority class.

Sub-Watershed	Parameters				C_V	Priority Class
	ES	A	T	SY		
SW-1	1	3	4	1	2.25	**High**
SW-2	3	6	5	8	5.50	**Medium**
SW-3	4	4	2	2	3.00	**High**
SW-4	2	1	1	5	2.25	**High**
SW-5	5	5	6	4	5.00	**Medium**
SW-6	6	2	3	3	3.50	**Medium**
SW-7	8	8	7	7	7.50	**Low**
SW-8	7	7	8	6	7.00	**Low**

* ES = % of areas under high and very high class of erosion susceptibility, A = Mean annual soil loss rate, T = % of areas above soil loss tolerance limits, SY = Annual sediment yield, C_V = Compound value.

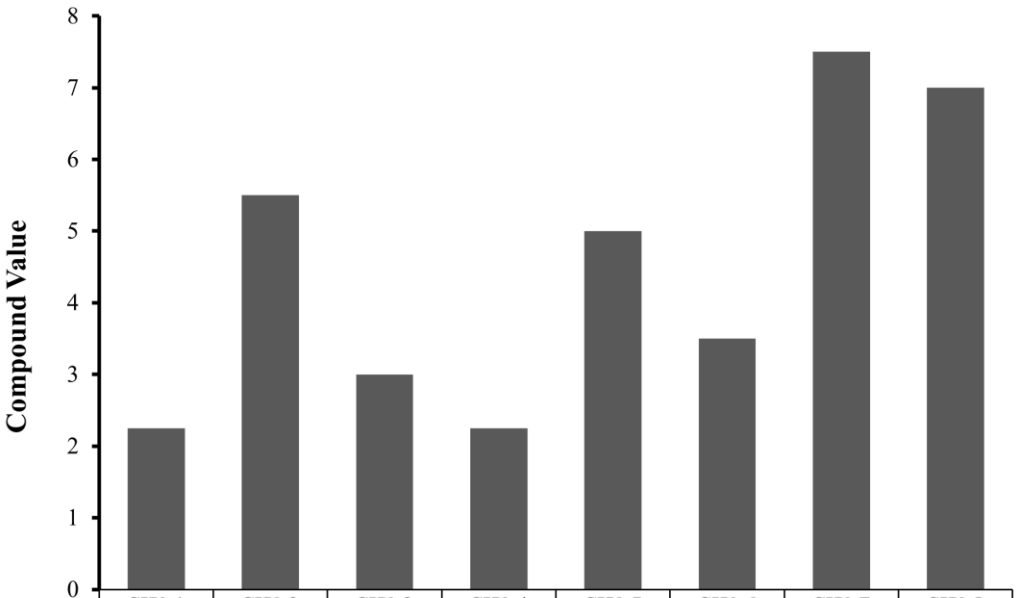

	SW-1	SW-2	SW-3	SW-4	SW-5	SW-6	SW-7	SW-8
Final Priority	HIGH	MEDIUM	HIGH	HIGH	MEDIUM	MEDIUM	LOW	LOW
Cv	2.25	5.5	3	2.25	5	3.5	7.5	7

Fig. 7.7: Compound value and Priority class of the sub-watersheds.

From Table 7.2 and Fig 7.7, the low-priority class includes SW-7 and SW-8. Considering the size of the sub-watershed, SW-7 and SW-8 are the 2nd largest and the smallest, respectively. However, the evaluated results of all the parameters are found to be low for both units, which may be attributed to the relatively lower level of natural resource depletion. Only a few anthropogenic activities are observed in these areas, and as a result, they have good natural vegetation cover, comprising both open and dense forests. Hence, the two sub-watersheds covering about 25.35% of the study area can be considered secure and well-protected. The medium priority class extending to approximately 31.78% of the watershed's area includes SW-2, SW-5 and SW-6. These geographical segments have experienced a relatively higher influence of soil erosion compared to the low-priority class, as the sub-watersheds embraced certain forms of human interventions like peripheral settlement sites, sporadic agricultural land, unsurfaced agricultural link roads and deforested areas overgrown with grasses, bamboos and scattered bushes. Besides moderate results of soil erosion impact, these three sub-watersheds necessitate implementing specific measures on soil erosion control and natural resource conservation due to the ever-increasing land

encroachment, which gradually depletes the natural environment. The high-priority classes, including SW-1, SW-3 and SW-4, are the most critical areas, occupying about 42.89% of the study area. These sub-watersheds are primarily encompassed by highly urbanized Aizawl municipal areas and agricultural land dominated mainly by shifting cultivation. Rapid urbanization is observed in SW-1 and some parts of SW-3, located in the upper catchment where numerous development activities and extensive deforestation are found. This urban settlement largely produces enormous urban waste and on-site unmanaged construction debris.

Moreover, several large and small earth spoils dumping sites are also found along the roadside slope just adjacent to the settlement areas, which have enormous unconsolidated sediments. Generally, these massive accumulated loose sediments are directly discharged into the watercourses, significantly impacting the streams and causing severe environmental deterioration. Some of the many consequences include severe water pollution and excessive sedimentation within and beyond the watershed downstream. Just beyond the urban land use, in most parts of SW-3 and SW-4, there is a profound modification of the natural landscape in terms of agricultural practice, which mainly comprises the traditional shifting cultivation from just adjacent to the settlement areas and extending to a few kilometres away. The complete clearance of natural vegetation and the reduced fallow periods in this cultivation system have led to a significant increase in run-off rate on the area's hilly terrain. In the absence of proper soil conservation practices during cultivation, numerous signs of erosion, including sheets, rills, and inter-rills, clearly indicate the ongoing erosion processes in these regions. Hence, taking immediate measures in these crucial sub-watersheds is essential to interrupt the ongoing exacerbation of erosion and sedimentation within the Chite watershed.

CHAPTER-8

CONCLUSIONS AND RECOMMENDATIONS

8.1 Conclusions

The study aimed to develop a structured framework for valuable insight into soil erosion and sedimentation in the Chite watershed. It encompasses four principal objectives: identification of the spatial distribution of soil erosion susceptibility, assessment of soil erosion rate, determination of the spatial pattern of soil loss tolerance, estimation of sediment yield and the prioritization of watershed concerning soil erosion and sedimentation in the study area. To achieve the objectives, this thesis represents a comprehensive investigation based on various erosion modeling approaches leveraging the advanced technology of Remote Sensing (RS) and Geographic Information Systems (GIS). This study mainly focused on the comprehensive understanding of the dynamic processes of erosion and sedimentation within the context of sustainable land management and environmental conservation.

In the present study, the prepared erosion susceptibility map produced high prediction accuracy for the study area. The generated map reveals that more than one-fourth of the watershed, occupying the northern parts and the eastern and western margins, are highly sensitive to the potential impact of soil erosion. Quantitative soil erosion modeling in the watershed has shown that about 70.13% of the total soil loss is produced exclusively from the severe and very severe zone of erosion rate, which covers only 5.34% of the watershed. This indicated that most of the estimated soil loss were generated from very few pockets of excessively disturbed land areas. The spatial distribution and magnitude of soil erosion tend to increase in the relatively fragile landforms where cultural activities are more dominant. Based on the estimated erosion rates, a comparison was made with the pre-determined soil loss tolerable limits. The result implies that most agricultural land use is at risk of soil erosion, and it is attributed mainly to the unsustainable agricultural system besides the absence of remarkable soil conservation measures and management systems in the watershed. Moreover, the evaluated sediment yield significantly manifests the prevailing erosion rate at the

watershed. Hence, a higher proportion of potential soil loss produced more sediment yield, enhancing the possible offsite consequences on the downstream ecosystem. Finally, watershed prioritization has been carried out to identify those critical areas of erosion and sedimentation at the sub-watershed level, considering the combined influence of the abovementioned analysis.

The findings of this research have a couple of implications relating to erosion control, sustainable management of natural resources and environmental conservation. Considering the integration of multiple methodologies, Watershed prioritisation improved a comprehensive understanding of the area of interest. It helps identify areas with a relatively higher erosion susceptibility and augmented erosion rates with the potential offsite consequences of sediment yield and the propensity of exceeding soil loss permissible limits. Subsequently, the prioritized critical areas of soil erosion and sedimentation processes will facilitate the foundation of executing site-specific developmental programmes for resource allocation and targeted conservation measures in the watershed. At the same time, employing remote sensing and Geographic Information System (GIS) technologies in this research has enabled a rapid and precise visual representation of the watershed status for implementing a successful conservation measure.

To conclude, the present research has substantially contributed to addressing the watershed dynamics, showcasing the need for continuous research and active engagement towards environmental protection. An integrated approach combining the Analytical Hierarchy Process (AHP), Revised Universal Soil Loss Equation (RUSLE), Soil Loss Tolerance Limits (T), Sediment Delivery Ratio (SDR) and Combined Value (C_V) method with remote sensing and GIS technologies offered a robust methodology in the comprehensive assessment of soil erosion and sedimentation in the study area. These research findings may be valuable to stakeholders, policymakers and researchers for implementing several measures of soil erosion and sedimentation control and sustainable resource management plans. Ultimately, this research is expected to significantly contribute to the sphere of knowledge pertaining to sustainable watershed management and encourage further research studies and conservation initiatives in the future.

8.2 Recommendations

The problems of soil erosion and sedimentation have been observed to significantly influence the economic and environmental sustainability of the Chite watershed. This challenging situation can be primarily attributed to the rapidly increasing anthropogenic activities in this fragile landscape without any remarkable environment conservation and management approaches. Based on the research findings and their implications, as well as the obtained knowledge through field observations, the following recommendations are made for the sustainable management of the Chite watershed: -

- The critical areas of the watershed comprising the medium and high-priority classes such as SW-1, SW-2, SW-3, SW-4, SW-5, and SW-6 must be treated with appropriate erosion control and resource conservation measures which embrace agronomic, vegetative and mechanical practices. As soil erosion is predominantly suffered in agricultural land, agronomic measures, including contour farming, mulching, strip cropping, crop rotation, conservation tillage, organic manure application, etc., are primarily preferred, contemplating its capability, feasibility and cost-effective manner.
- Shifting cultivation, the predominant form of agricultural practice in the watershed, is characterized by widespread clearing and complete burning of natural vegetation, exposing the surface to the direct impacts of raindrops and runoff. The complete abolition of this traditional system will exhibit an impactful solution in terms of prosperous soil and water conservation. However, considering the marginal farmers' social and economic capacity, it is impracticable in the present situation. Hence, it is necessary to adopt specific regulations for improving the system. Restrictions on site selection for jhum land to relatively steep slopes is regarded as the most effective strategy to reduce topsoil removal and nutrient loss from the agricultural land.
- Besides the agricultural land, the high and medium class of prioritized areas comprise non-agricultural land use, including settlement sites, construction sites, quarrying sites, road networks and earth spoils dumping sites. The transformation of vast natural landscape to impervious built-up surface in case

of settlement and road networks disrupt water infiltration and produces excessive run-off. At the same time, the removal and disposal of enormous quantities of earth materials along construction sites and roadways, quarrying sites, and earth spoils dumping sites generates a significant quantity of loose soil. Hence, vegetative measures such as afforestation, grass strips, vegetative filter strips, etc. should be implemented in and around these areas as they are considered to be the most practically suitable and accessible methods for controlling rapid run-off and reducing the enormous supply of sediment.

- Urban development has significantly increased the run-off rate in channels through stormwater drainage system, resulting in soil loss of high intensity along the streams. Establishing a riparian buffer zone to protect stream banks by planting vegetative buffer strips like trees or grasses with higher resistance to erosive water flow is necessary. In the more severe cases of bank erosion, channels should be lined with rock rip rap or rock-filled gabions, utilizing the readily available pebbles, cobbles and boulders in the river course.
- Protected areas should be established in ecologically sensitive zones, mainly on steep slopes. In addition to the preservation of natural vegetation, appropriate reforestation or afforestation programs should be carried out in these areas. Furthermore, no developmental activities should be allowed in these protected areas to promote the stability of this ecologically susceptible landscape, supporting effective erosion control within the watershed.
- The region receives abundant rainfall through the southwest monsoon. Therefore, harvesting rainwater directly or indirectly on the ground will support erosion control and soil and water conservation. Different types of rainwater harvesting systems like check dams, infiltration basins, retention ponds, detention basins, rainwater recharge well, etc., in agricultural and non-settlement areas and rooftop harvesting in settlement areas should be cautiously implemented throughout the study area. This will significantly decrease the amount of run-off and overland flow, reducing soil detachment and subsequent sediment transport and deposition downstream. At the same time, the water stored at the surface or sub-surface can provide a reliable source

of water for agricultural land, degraded forest areas and households to a desirable extent.

- A watershed management body or committee that comprises farmers, conservationists, NGOs, local authorities and state governments should be established to develop and enforce policies and regulations related to unwarranted deforestation and illicit land encroachment in the region, which will competently facilitate measures for soil erosion control and resource conservation.
- Government intervention is urgently required to investigate and address the issue of earth spoils dumping sites found in several locations along the roadways. These sites generate a massive quantity of unconsolidated sediments directly discharged into the watercourses, causing significant detrimental impacts on the streams and severe environmental deterioration. Some of the many consequences include severe water pollution and excessive sedimentation within and beyond the watershed downstream.
- The government should also provide financial assistance or take initiatives towards constructing and maintaining various erosion control structures such as terracing, check dams, silt fences, retaining walls, gabions, etc., to protect soil erosion and sediment discharge in the study area.
- Awareness campaigns about the importance and benefits of controlling soil erosion and conservation of soil and water resources should be organized through educational outreach programs like workshops and training. As implementing various erosion control and conservation efforts involves community participation, public awareness initiatives may produce a meaningful response. The engagement of local communities is expected to nurture a sense of belongingness and responsibility towards watershed sustainability.

Uninterrupted soil erosion and sedimentation appraisal is necessary to evaluate the watershed conditions at varying time intervals and the long-term efficacy of conservation measures adopted. Regular monitoring can be successfully executed by utilising various geospatial modeling techniques. In addition to this, conventional

methods like determination of soil nutrient levels, direct measurement of run-off and sediment yield through stream gauging, and regular feedback from local farmers and stakeholders should be carried out to provide comprehensive surveillance for successful erosion control as well as soil and water conservation in Chite watershed.

PLATE NO. 1

Photo A

Photo B

Photo A: Erosional features like sheet, rill, inter-rill and gully observed during field surveys.

Photo B: Stream bank erosion observed along the Chite river.

PLATE NO. 2

Photo A

Photo B

Photo A: Constructional activities in the upper catchment.

Photo B: Earth spoils dumping sites.

PLATE NO. 3

Photo A

Photo B

Photo A: Sediment saturated streams.

Photo B: Muddy embankments.

PLATE NO. 4

Photo: Soil sample collection.

References:

Achour, Y., Boumezbeur, A., Hadji, R., Chouabbi, A., Cavaleiro, V. and Bendaoud, E. A. (2017). Landslide susceptibility mapping using analytic hierarchy process and information value methods along a highway road section in Constantine, Algeria. *Arabian Journal of Geosciences*, 10, pp. 1-16.

Ahmed, F. and Srinivasa, R. K. (2015). Geomorphometric analysis for estimation of sediment production rate and run-off in Tuirini watershed, Mizoram, India. *International Journal of Remote Sensing Applications*, 5, pp. 67-77.

Alexakis, D. D., Hadjimitsis, D. G. and Agapiou, A. (2013). Integrated use of remote sensing, GIS and precipitation data for the assessment of soil erosion rate in the catchment area of "Yialias" in Cyprus. *Atmospheric Research*, 131, pp. 108-124.

Ali, S. A., Khatun, R., Ahmad, A. and Ahmad, S. N. (2019). Application of GIS-based analytic hierarchy process and frequency ratio model to flood vulnerable mapping and risk area estimation at Sundarban region, India. *Modeling Earth Systems and Environment*, 5, pp. 1083-1102.

Alqadhi, S., Mallick, J., Talukdar, S., Bindajam, A. A., Saha, T. K., Ahmed, M., and Khan, R. A. (2022). Combining logistic regression-based hybrid optimized machine learning algorithms with sensitivity analysis to achieve robust landslide susceptibility mapping. *Geocarto International*, 37(25), pp. 9518-9543.

Altaf, S., Meraj, G. and Romshoo, S. A. (2014). Morphometry and land cover based multi-criteria analysis for assessing the soil erosion susceptibility of the western Himalayan watershed. *Environmental monitoring and assessment*, 186, pp. 8391-8412.

Anbazhagan, S., Subramanian, S. K. and Yang, X. (Eds.). (2011). *Geoinformatics in applied geomorphology*. Boca Raton: CRC Press.

Angima, S. D., Stott, D. E., O'neill, M. K., Ong, C. K. and Weesies, G. A. (2003). Soil erosion prediction using RUSLE for central Kenyan highland conditions. *Agriculture, ecosystems & environment*, 97(1-3), pp. 295-308.

Arabameri, A., Rezaei, K., Pourghasemi, H. R., Lee, S. and Yamani, M. (2018). GIS-based gully erosion susceptibility mapping: a comparison among three data-driven models and AHP knowledge-based technique. *Environmental earth sciences*, 77, pp. 1-22.

Arabameri, A., Pradhan, B., Rezaei, K. and Conoscenti, C. (2019). Gully erosion susceptibility mapping using GIS-based multi-criteria decision analysis techniques. *Catena*, 180, pp. 282-297.

Ashiagbor, G., Forkuo, E. K., Laari, P. and Aabeyir, R. (2013). Modeling soil erosion using RUSLE and GIS tools. *International Journal of Remote Sensing and Geosciences*, 2(4), pp. 1-17.

Aslam, B., Maqsoom, A., Alaloul, W. S., Musarat, M. A., Jabbar, T. and Zafar, A. (2021). Soil erosion susceptibility mapping using a GIS-based multi-criteria decision approach: Case of district Chitral, Pakistan. *Ain Shams Engineering Journal*, 12(2), pp. 1637-1649.

Atoma, H., Suryabhagavan, K. V. and Balakrishnan, M. (2020). Soil erosion assessment using RUSLE model and GIS in Huluka watershed, Central Ethiopia. *Sustainable Water Resources Management*, 6, pp. 1-17.

Avand, M., Janizadeh, S., Naghibi, S. A., Pourghasemi, H. R., Bozchaloei, S.K. and Blaschke, T. (2019). A comparative assessment of random forest and k-nearest neighbor classifiers for gully erosion susceptibility mapping. *Water*, 11(10), 2076.

Ayele, N. A., Naqvi, H. R. and Alemayehu, D. (2020). Rainfall induced soil erosion assessment, prioritization and conservation treatment using RUSLE and SYI models in highland watershed of Ethiopia. *Geocarto International*, 37(9), pp. 2524-2540.

Babu, R., Dhyani, B. L. and Kumar, N. (2004). Assessment of erodibility status and refined Iso-Erodent Map of India. *Indian Journal of Soil Conservation*, 32(2), pp. 171-177.

Bagarello, V., Stefano, C.D., Ferro, V., Giuseppe, G. and Iovino, M. (2009). A pedotransfer function for estimating the soil erodibility factor in Sicily. *Journal of Agricultural Engineering*, 40(3), pp. 7-13.

Belasri, A. and Lakhouili, A. (2016). Estimation of soil erosion risk using the universal soil loss equation (USLE) and geo-information technology in Oued El Makhazine Watershed, Morocco. *Journal of Geographic Information System*, 8(01), pp. 98-107.

Belayneh, M., Yirgu, T. and Tsegaye, D. (2019). Potential soil erosion estimation and area prioritization for better conservation planning in Gumara watershed using RUSLE and GIS techniques'. *Environmental Systems Research*, 8, pp. 1-17.

Bhandari, A. K., Kumar, A. and Singh, G. K. (2012). Feature extraction using Normalized Difference Vegetation Index (NDVI): A case study of Jabalpur city. *Procedia technology*, 6, pp. 612-621.

Bhat, S. A., Hamid, I., Dar, M. U. D., Rasool, D., Pandit, B. A. and Khan, S. (2017). Soil erosion modeling using RUSLE & GIS on micro watershed of J&K. *Journal of Pharmacognosy and Phytochemistry*, 6(5), pp. 838-842.

Bhattacharyya, P., Bhatt, V. K. and Mandal, D. (2008). Soil loss tolerance limits for planning of soil conservation measures in Shivalik–Himalayan region of India. *Catena*, 73(1), pp. 117-124.

Bhattacharya, R. K., Chatterjee, N. D. and Das, K. (2020). Sub-basin prioritization for assessment of soil erosion susceptibility in Kangsabati, a plateau basin: a comparison between MCDM and SWAT models. *Science of the Total Environment*, 734, 139474.

Bhattacharyya, R., Ghosh, B.N., Mishra, P.K., Mandal, B., Rao, C.S., Sarkar, D., Das, K., Anil, K.S., Lalitha, M., Hati, K.M. and Franzluebbers, A.J., (2015).

Soil degradation in India: challenges and potential solutions. *Sustainability*, 7(4), pp. 3528–3570.

Biswas, S.S. and Pani, P. (2015). Estimation of soil erosion using RUSLE and GIS techniques: a case study of Barakar River basin, Jharkhand, India. *Modeling Earth Systems and Environment*, 1(4), pp. 1-13.

Bloom, A.L. (1979). *Geomorphology: A Systematic analysis of Late Cenozoic landforms*. Prentice Hall of India, New Delhi, p. 3.

Carsel, R. F. and Parrish, R. S. (1988). Developing joint probability distributions of soil water retention characteristics. *Water resources research*, 24(5), pp. 755-769.

Chakrabortty, R., Pal, S. C., Sahana, M., Mondal, A., Dou, J., Pham, B. T. and Yunus, A. P. (2020). Soil erosion potential hotspot zone identification using machine learning and statistical approaches in eastern India. *Natural Hazards*, 104, pp. 1259-1294.

Chang, K.T. (2018). *Introduction to Geographic Information Systems*. 9th edition, McGraw Hill Education (India) Pvt Ltd., Chennai, India, p. 287.

Chatterjee, S., Krishna, A. P. and Sharma, A. P. (2013). Geospatial assessment of soil erosion vulnerability at watershed level in some sections of the Upper Subarnarekha river basin, Jharkhand, India. *Environmental earth sciences*, 71, pp. 357-374.

Chen, L., Wang, J., Fu, B. and Qiu, Y. (2001). Land use change in a small catchment of northern Loess Plateau, China. *Agriculture, Ecosystems & Environment*, 86, pp. 163–172

Chen, T., Niu, R. Q., Li, P. X., Zhang, L. P. and Du, B. (2011). Regional soil erosion risk mapping using RUSLE, GIS, and remote sensing: a case study in Miyun Watershed, North China. *Environmental Earth Sciences*, 63, pp. 533-541.

Chen, W., Li, W., Chai, H., Hou, E., Li, X. and Ding, X. (2016). GIS-based landslide susceptibility mapping using analytical hierarchy process (AHP) and certainty factor (CF) models for the Baozhong region of Baoji City, China. *Environmental Earth Sciences*, 75, pp. 1-14.

Choudhury, B. U., Nengzouzam, G., Ansari, M. A. and Islam, A. (2022). Causes and consequences of soil erosion in northeastern Himalaya, India. *Current Science* (00113891), 122(7), pp. 772 – 789.

Chowdary, V. M., Chakraborthy, D., Jeyaram, A., Murthy, Y. K., Sharma, J. R. and Dadhwal, V. K. (2013). Multi-criteria decision making approach for watershed prioritization using analytic hierarchy process technique and GIS. *Water resources management*, 27, pp. 3555-3571.

Costea, M. (2012). Using the Fournier Indexes in estimating rainfall erosivity. Case Study-The Secasul Mare. *Air & Water Components of the Environment / Aerul si Apa Componente ale Mediului*. pp. 313-320.

Daoud, J. I. (2017). Multicollinearity and regression analysis. In Journal of Physics: Conference Series (Vol. 949, No. 1, p. 012009). IOP Publishing. DOI 10.1088/1742-6596/949/1/012009

Das, B., Bordoloi, R., Thungon, L. T., Paul, A., Pandey, P. K., Mishra, M. and Tripathi, O. P. (2020). An integrated approach of GIS, RUSLE and AHP to model soil erosion in West Kameng watershed, Arunachal Pradesh. *Journal of Earth System Science*, 129, pp. 1-18.

Das, M.M. and Saikia, M.D. (2013). *Watershed Management*. PHI Learning Private Limited, New Delhi. pp. 1 – 303.

Dewangan, C. L. and Ahmad, I. (2020). Assessment of reservoir sedimentation and identification of critical soil erosion zone in Kodar Reservoir Watershed of Chhattisgarh State, India. In Applications of Geomatics in Civil Engineering: Select Proceedings of ICGCE 2018, Springer Singapore, pp. 203-214.

Dissanayake, D. M. S. L. B., Morimoto, T. and Ranagalage, M. (2019). Accessing the soil erosion rate based on RUSLE model for sustainable land use management: A case study of the Kotmale watershed, Sri Lanka. *Modeling Earth Systems and Environment*, 5, pp. 291-306.

Ebhuoma, O., Gebreslasie, M., Ngetar, N. S., Phinzi, K. and Bhattacharjee, S. (2022). Soil erosion vulnerability mapping in selected rural communities of uThukela Catchment, South Africa, using the analytic hierarchy process, *Earth Systems and Environment*, 6(4), pp. 851-864.

Farhan, Y. and Anaba, O. (2016). A remote sensing and GIS approach for prioritization of Wadi Shueib Mini-Watersheds (Central Jordan) based on morphometric and Soil erosion susceptibility analysis. *Journal of Geographic Information System*, 8(1), pp. 1-19.

Farrar, D. E. and Glauber, R. R. (1967). *Multicollinearity in regression analysis: the problem revisited. The Review of Economic and Statistics*, Sloan School of Management, Massachusetts Institute of Technology, Cambridge 39, Massachusetts. p. 5.

Fistikoglu, O. and Harmancioglu, N. B. (2002). Integration of GIS with USLE in assessment of soil erosion. *Water Resources Management*, 16, pp. 447-467.

Forman, E. H. and Gass, S. I. (2014). The analytic hierarchy process—an exposition, *Operations research*, 49(4), pp. 469-486.

Gajbhiye, S., Mishra, S. K. and Pandey, A. (2013). Prioritizing erosion-prone area through morphometric analysis: an RS and GIS perspective. *Applied Water Science*, 4, pp. 51-61.

Ganasri, B. P. and Ramesh, H. (2015). Assessment of soil erosion by RUSLE model using remote sensing and GIS-A case study of Nethravathi Basin. *Geoscience Frontiers*, 7(6), pp. 953-961.

Gandhi, G.M., Parthiban, B. S., Thummalu, N. and Christy, A. (2015). Ndvi: Vegetation change detection using remote sensing and gis–A case study of Vellore District. *Procedia computer science*, 57, pp. 1199-1210.

Ganju, J. L. (1975). *Geology of Mizoram*. Bulletin Geology, Mineralogical, Metallurgical Society of India, 48, pp. 17-26.

Garde, R. J. and Kothyari, U. C. (1990). Flood estimation in Indian catchments. *Journal of Hydrology*, 113(1-4), pp. 135-146.

Garde, R.J. (2006). *River Morphology*. New Age International Publishers, New Delhi.

Gayen, A. and Saha, S. (2017). Application of weights-of-evidence (WoE) and evidential belief function (EBF) models for the delineation of soil erosion vulnerable zones: a study on Pathro river basin, Jharkhand, India. *Modeling Earth Systems and Environment*, 3(3), pp. 1123-1139.

Gelagay, H. S. and Minale, A. S. (2016). Soil loss estimation using GIS and remote sensing techniques: A case of Koga watershed, Northwestern Ethiopia. *International Soil and Water Conservation Research*, 4(2), pp. 126-136.

Gelagay, H.S. (2016). RUSLE and SDR Model Based Sediment Yield Assessment in a GIS and Remote Sensing Environment; A Case Study of Koga Watershed, Upper Blue Nile Basin, Ethiopia, *Hydrology Current research*, 7(2), pp. 1-10.

Ghosh, B. and Mukhopadhyay, S. (2021). Erosion susceptibility mapping of sub-watersheds for management prioritization using MCDM-based ensemble approach. *Arabian Journal of Geosciences*, 14, pp. 1-18.

Ghosh, P. and Lepcha, K. (2019). Weighted linear combination method versus grid based overlay operation method–A study for potential soil erosion susceptibility analysis of Malda district (West Bengal) in India. *The Egyptian Journal of Remote Sensing and Space Science*, 22(1). pp. 95-115.

Giordano, G., Ferro, V., Bagarello, V., Stefano, C.D., Iovino, M. and Minacapilli, M. (2004). Application studies for the realization of the map of the potential

erosion of the Sicilian territory and of the related territorial information system, *Edizioni Anteprima s.r.l., Palermo*, 2004, pp. 1-71.

Goudie, A. S. (2006). *Encyclopedia of Geomorphology*. Taylor & Francis e-Library. https://courses.ess.washington.edu/ess306/links/Goudie_Encyclopedia_of_Geomorphology.pdf.

Grogan, P., Lalnunmawia, F. and Tripathi, S. K. (2012). Shifting cultivation in steeply sloped regions: a review of management options and research priorities for Mizoram state, Northeast India. *Agroforestry Systems*, 84, pp. 163-177.

Gupta, S. and Kumar, S. (2017). Simulating climate change impact on soil erosion using RUSLE model− A case study in a watershed of mid-Himalayan landscape. *Journal of Earth System Science*, 126, pp. 1-20.

Haidara, I., Tahri, M., Maanan, M. and Hakdaoui, M. (2019). Efficiency of Fuzzy Analytic Hierarchy Process to detect soil erosion vulnerability. *Geoderma*, 354, 113853.

Halefom, A. and Teshome, A. (2019). Modelling and mapping of erosion potentiality watersheds using AHP and GIS technique: a case study of Alamata Watershed, South Tigray, Ethiopia. *Modelling Earth Systems and Environment*, 5(3), pp. 819-831.

Harker, P. T. and Vargas, L. G. (1987). The theory of ratio scale estimation: Saaty's analytic hierarchy process. *Management science*, 33(11), pp. 1383-1403.

IRDAS (1994). *Soil Erosion and Land Degradation Problems in Mizoram*, Institute of Resource Development and Social Management, Hyderabad, pp. 1 - 110.

Issaka, S. and Ashraf, M.A. (2017). Impact of soil erosion and degradation on water quality: a review, *Geology, Ecology, and Landscapes*, 1:1, pp. 1-11.

Kachouri, S., Achour, H., Abida, H. and Bouaziz, S. (2015). Soil erosion hazard mapping using Analytic Hierarchy Process and logistic regression: a case

study of Haffouz watershed, central Tunisia. *Arabian Journal of Geosciences*, 8, pp. 4257-4268.

Kalambukattu, J. and Kumar, S. (2017). Modelling soil erosion risk in a mountainous watershed of Mid-Himalaya by integrating RUSLE model with GIS. *Eurasian Journal of Soil Science*, 6(2), pp. 92-105.

Kayet, N., Pathak, K., Chakrabarty, A. and Sahoo, S. (2018). Evaluation of soil loss estimation using the RUSLE model and SCS-CN method in hillslope mining areas. *International Soil and Water Conservation Research*, 6(1), pp. 31-42.

Khaira, A. and Dwivedi, R. K. (2018). A state of the art review of analytical hierarchy process. Materials Today: Proceedings. 5(2), Pp. 4029-4035.

Kidane, M., Bezie, A., Kesete, N. and Tolessa, T. (2019). The impact of land use and land cover (LULC) dynamics on soil erosion and sediment yield in Ethiopia. *Heliyon*, 5(12), e02981.

Kothyari, U. C. and Jain, S. K. (1997). Sediment yield estimation using GIS. *Hydrological sciences journal*, 42(6), pp. 833-843.

Kothyari, U. C. (1996). Erosion and sedimentation problems in India. In: Proc. of the Exeter Symposium on Erosion and Sediment Yield: Global and Regional Perspectives, IAHS Publ. No. 236, pp. 531-540.

Kucuker, D. M. and Giraldo, D. C. (2022). Assessment of soil erosion risk using an integrated approach of GIS and Analytic Hierarchy Process (AHP) in Erzurum, Turkiye. *Ecological Informatics*, 71, 101788.

Kumar, S. and Kushwaha, S. P. S. (2013). Modelling soil erosion risk based on RUSLE-3D using GIS in a Shivalik sub-watershed. *Journal of Earth System Science*, 122, pp. 389-398.

Lakaria, B. L., Biswas, H. and Mandal, D. (2008). Soil loss tolerance values for different physiographic regions of Central India. *Soil use and management*, 24(2), pp. 192-198.

Lal, R. (2001). Soil degradation by erosion. *Land degradation & development*, 12(6), pp. 519-539.

Langbein, W.B. (1947). Topographic characteristics of drainage basins. USGS Water-Supply paper 968-C, pp. 125 – 158.

Lee, S. (2004). Soil erosion assessment and its verification using the universal soil loss equation and geographic information system: a case study at Boun, Korea. *Environmental Geology*, 45, pp. 457-465.

Lillesand, T., Kiefer, R. W. and Chipman, J. (2017). *Remote Sensing and Image Interpretation, 6th Edition*. John Wiley & Sons.

Lim, K.J., Sagong, M., Engel, B.A., Tang, Z., Choi, J. and Kim, K.S. (2005). GIS-based sediment assessment tool. *Catena*, 64(1), 61-80.

Lu, D., Li, G., Valladares, G. S. and Batistella, M. (2004). Mapping soil erosion risk in Rondonia, Brazilian Amazonia: using RUSLE, remote sensing and GIS. *Land degradation & development*, 15(5), pp. 499-512.

Magesh, N. S. and Chandrasekar, N. (2016). Assessment of soil erosion and sediment yield in the Tamiraparani sub-basin, South India, using an automated RUSLE-SY model. *Environmental Earth Sciences*, 75, pp. 1-17.

Makaya, N., Dube, T., Seutloali, K., Shoko, C., Mutanga, O. and Masocha, M. (2019). Geospatial assessment of soil erosion vulnerability in the upper uMgeni catchment in KwaZulu Natal, South Africa. *Physics and Chemistry of the Earth*, Parts A/B/C, 112, pp. 50-57.

Mandal, D. and Sharda, V. N. (2011) (a). Assessment of permissible soil loss in India employing a quantitative bio-physical model. *Current Science*, pp. 383-390.

Mandal, D. and Sharda, V. N. (2011) (b). Appraisal of soil erosion risk in the Eastern Himalayan region of India for soil conservation planning. *Land Degradation & Development*, 24(5), pp. 430-437.

Mandal, D., Sharda, V. N. and Tripathi, K. (2010). Relative efficacy of two biophysical approaches to assess soil loss tolerance for Doon Valley soils of India. *Journal of soil and water conservation*, 65(1), pp. 42-49.

Markose, V. J. and Jayappa, K. S. (2016). Soil loss estimation and prioritization of sub-watersheds of Kali River basin, Karnataka, India, using RUSLE and GIS. *Environmental monitoring and assessment*, 188, pp. 1-16.

Mat, M. (2021). *Geologyscience*. Accessed from https://geologyscience.com/rocks-2/ on 24th November 2021.

Mhaske, S. N., Pathak, K., Dash, S. S. and Nayak, D. B. (2021). Assessment and management of soil erosion in the hilltop mining dominated catchment using GIS integrated RUSLE model. *Journal of Environmental Management*, 294, 112987.

Millward, A. A. and Mersey, J. E. (1999). Adapting the RUSLE to model soil erosion potential in a mountainous tropical watershed. *Catena*, 38(2), pp. 109-129.

Ministry of Agriculture. (2011). *Methods manual-Soil Testing in India*, Department of Agriculture & Cooperation, Government of India, New Delhi.

Mitasova, H., Hofierka, J., Zlocha, M. and Iverson, L. R. (1996). Modelling topographic potential for erosion and deposition using GIS. *International journal of geographical information systems*, 10(5), pp. 629-641.

Mondal, S. and Maiti, R. (2013). Integrating the analytical hierarchy process (AHP) and the frequency ratio (FR) model in landslide susceptibility mapping of Shiv-khola watershed, Darjeeling Himalaya. *International Journal of Disaster Risk Science*, 4, pp. 200-212.

Moore, I. D. and Burch, G. J. (1986). Physical basis of the length-slope factor in the universal soil loss equation. *Soil Science Society of America Journal*, 50(5), pp. 1294-1298.

Morgan, R.P.C. (2005). *Soil Erosion and Conservation*, 3rd Edition, John Wiley & Son, Inc., 111 River Street, Hoboken, New Jersey, USA.

Mosavi, A., Sajedi-Hosseini, F., Choubin, B., Taromideh, F., Rahi, G. and Dineva, A. A. (2020). Susceptibility mapping of soil water erosion using machine learning models. *Water*, 12(7), 1995.

Motsara, M.R. and Roy, R.N. (2008) *Guide to laboratory establishment for plant nutrient analysis*. FAO fertilizer and plant nutrition bulletin 19. FAO, Rome, Italy.

Mushtaq, F., Farooq, M., Tirkey, A. S. and Sheikh, B. A. (2023). Analytic Hierarchy Process (AHP) Based Soil Erosion Susceptibility Mapping in Northwestern Himalayas: A Case Study of Central Kashmir Province, *Conservation*, 3(1), pp. 32-52.

Myers, J.L., Well, A.D. and Lorch Jr, R.F. (2010). Introduction to multiple regression. In: Myers, J.L. - Well, A.D. - Lorch Jr, R.F. (Eds) (2010): Research Design and Statistical Analysis. Routledge. New York. 528-547. https://doi.org/10.4324/9780203726631

Myronidis, D., Papageorgiou, C. and Theophanous, S. (2016). Landslide susceptibility mapping based on landslide history and analytic hierarchy process (AHP), *Natural Hazards*, 81, pp. 245-263.

Narayana, D. V. and Babu, R. (1983). Estimation of soil erosion in India. *Journal of Irrigation and Drainage Engineering*, 109(4), pp. 419-434.

Negese, A., Fekadu, E. and Getnet, H. (2021). Potential soil loss estimation and erosion-prone area prioritization using RUSLE, GIS, and remote sensing in Chereti Watershed, Northeastern Ethiopia. *Air, Soil and Water Research*, 14, pp. 1-17.

Neji, N., Ayed, R. B. and Abida, H. (2021). Water erosion hazard mapping using analytic hierarchy process (AHP) and fuzzy logic modeling: a case study of the Chaffar Watershed (Southeastern Tunisia), *Arabian Journal of Geosciences*, 14, pp. 1-15.

Ouyang, D. and Bartholic, J. (1997). Predicting sediment delivery ratio in Saginaw Bay watershed. In: Proceedings of the 22nd National Association of

Environmental Professionals Conference, 19–23 May 1997, Orlando, Florida, pp. 659–671.

Pachuau, R. (2009). *Mizoram – A Study in Comprehensive Geography*, Northern Book Centre, New Delhi, pp. 41 - 42.

Pandey, S., Kumar, P., Zlatić, M., Nautiyal, R. and Panwar, V. P. (2021). Recent advances in the assessment of soil erosion vulnerability in watersheds. *Glasnik Sumarskog fakulteta*, (123), pp. 9-32.

Parveen, R. and Kumar, U. (2012). Integrated approach of universal soil loss equation (USLE) and geographical information system (GIS) for soil loss risk assessment in Upper South Koel Basin, Jharkhand. *Journal of Geographic Information System*, 2012, 4, pp. 588-596

Petito, M., Cantalamessa, S., Pagnani, G., Degiorgio, F., Parisse, B. and Pisante, M. (2022). Impact of Conservation Agriculture on Soil Erosion in the Annual Cropland of the Apulia Region (Southern Italy) Based on the RUSLE-GIS-GEE Framework. *Agronomy*, 12(2), 281.

Pham, T. G., Degener, J. and Kappas, M. (2018). Integrated universal soil loss equation (USLE) and Geographical Information System (GIS) for soil erosion estimation in A Sap basin: Central Vietnam. *International Soil and Water Conservation Research*, 6(2), pp. 99-110.

Pike, R. J. and Wilson, S. E. (1971). Elevation-relief ratio, hypsometric integral, and geomorphic area-altitude analysis. *Geological Society of America Bulletin*, 82(4), pp. 1079-1084.

Pimentel, D. (2006). Soil erosion: a food and environmental threat. *Environment, development and sustainability*, 8, pp. 119-137.

Pourghasemi, H. R., Moradi, H. R. and Fatemi Aghda, S. M. (2013). Landslide susceptibility mapping by binary logistic regression, analytical hierarchy process, and statistical index models and assessment of their performances. *Natural hazards*, 69, pp. 749-779.

Pourghasemi, H. R., Pradhan, B. and Gokceoglu, C. (2012). Application of fuzzy logic and analytical hierarchy process (AHP) to landslide susceptibility mapping at Haraz watershed, Iran. *Natural hazards*, 63, pp. 965-996.

Pradeep, G. S., Krishnan, M. V. N. and Vijith, H. (2014). Identification of critical soil erosion prone areas and annual average soil loss in an upland agricultural watershed of Western Ghats, using analytical hierarchy process (AHP) and RUSLE techniques. *Arabian Journal of Geosciences*, 8(6), pp. 3697–3711.

Pradhan, B., Chaudhari, A., Adinarayana, J. and Buchroithner, M. F. (2011). Soil erosion assessment and its correlation with landslide events using remote sensing data and GIS: a case study at Penang Island, Malaysia. *Environmental monitoring and assessment*, 184, pp. 715-727.

Prasannakumar, V., Shiny, R., Geetha, N. and Vijith, H. (2011). Spatial prediction of soil erosion risk by remote sensing, GIS and RUSLE approach: a case study of Siruvani river watershed in Attapady valley, Kerala, India. *Environmental Earth Sciences*, 64, pp. 965-972.

Prasannakumar, V., Vijith, H., Abinod, S. and Geetha, N. J. G. F. (2012). Estimation of soil erosion risk within a small mountainous sub-watershed in Kerala, India, using Revised Universal Soil Loss Equation (RUSLE) and geo-information technology. *Geoscience frontiers*, 3(2), pp. 209-215.

Pribyl, D. W. (2010). A critical review of the conventional SOC to SOM conversion factor. *Geoderma*, 156(3-4), pp. 75-83.

Rahman, M. R., Shi, Z. H. and Chongfa, C. (2009). Soil erosion hazard evaluation—an integrated use of remote sensing, GIS and statistical approaches with biophysical parameters towards management strategies. *Ecological Modelling*, 220(13-14), pp. 1724-1734.

Rajbanshi, J. and Bhattacharya, S. (2020). Assessment of soil erosion, sediment yield and basin specific controlling factors using RUSLE-SDR and PLSR approach in Konar River basin, India, *Journal of Hydrology*, 587:124935.

Ranganath, B.K., Roy, P.S., Dutt, C.B.S. and Divakar, P.G. (2000). *Use of Modern Technologies and Information Systems for Sustainable Forest Managements: Status Report*, ISRO, Department of Space.

Rashid, B., Iqbal, J. and Su, L. J. (2020). Landslide susceptibility analysis of Karakoram highway using analytical hierarchy process and scoops 3D. *Journal of Mountain Science*, 17(7), pp. 1596-1612.

Renard, K.G., Foster. G.R., Weesies, G.A., McCool, D.K. and Yoder, D.C. (1997). *Predicting Soil Erosion by Water: A Guide to Conservation Planning With the Revised Universal Soil Loss Equation (RUSLE)*. U.S. Department of Agriculture, Agriculture Handbook No. 703.

Ritter, D.F., Kochel, R.C. and Miller, J.R. (2002). *Process Geomorphology*. McGrow Hill, Boston.

Rouse, J.W., Haas, R.H., Schell, J.A. and Deering, D.W. (1974). Monitoring Vegetation Systems in the Great Plains with ERTS, Proceedings of 3rd Earth Resources Technology Satellite-1 Symposium, Greenbelt: NASA Special Publication, 351(1), pp. 3010 – 3017.

Saaty, T.L. and Vargas, L.G. (1991). *Prediction, projection, and forecasting: Applications of the analytic hierarchy process in economics, finance, politics, games and sports*, Kluwer Academic Publishers, Boston. 251.

Saaty, T. L. (1977). A scaling method for priorities in hierarchical structures, *Journal of mathematical psychology*, 15(3), pp. 234-281.

Saaty, T.L. (1980). *The analytic hierarchy process*. McGraw Hill, New York.

Saaty, T. L. (2008). Decision making with the analytic hierarchy process, *International journal of services sciences*, 1(1), pp. 83-98.

SAC (2021). *Desertification and Land degradation Atlas of India (Assessment and analysis of changes over 15 years based on remote sensing)*, Space Application Centre, ISRO, Ahmedabad.

Saha, A.K., Gupta, R.P. and Arora, M.K. (2002). GIS-based landslide hazard zonation in the Bhagirathi (Ganga) valley, Himalayas. *International Journal of Remote Sensing*, 23(2), pp. 357 – 369.

Saha, R., Chaudhary, R. S. and Somasundaram, J. (2012). Soil health management under hill agroecosystem of North-East India. *Applied and Environmental Soil Science*, 2012, pp. 1 – 9.

Saha, S., Gayen, A., Pourghasemi, H. R. and Tiefenbacher, J. P. (2019). Identification of soil erosion-susceptible areas using fuzzy logic and analytical hierarchy process modeling in an agricultural watershed of Burdwan district, India. *Environmental Earth Sciences*, 78, pp. 1-18.

Sahoo, U. K., Singh, S. L., Gogoi, A., Kenye, A. and Sahoo, S. S. (2019). Active and passive soil organic carbon pools as affected by different land use types in Mizoram, Northeast India. *PloS one*, 14(7), e0219969. https://doi.org/10.1371/journal.pone.0219969.

Saini, S. S., Jangra, R. and Kaushik, S. P. (2015). Vulnerability assessment of soil erosion using geospatial techniques-A pilot study of upper catchment of Markanda river. *International journal of advancement in remote sensing, gis and geography*, 3(1). pp. 9-21.

Sajedi-Hosseini, F., Choubin, B., Solaimani, K., Cerdà, A. and Kavian, A. (2018). Spatial prediction of soil erosion susceptibility using a fuzzy analytical network process: Application of the fuzzy decision-making trial and evaluation laboratory approach. *Land degradation & development*, 29(9), pp. 3092-3103.

Sandeep, P., Reddy, G. O., Jegankumar, R. and Arun Kumar, K. C. (2020). Modeling and assessment of land degradation vulnerability in semi-arid ecosystem of Southern India using temporal satellite data, AHP and GIS. *Environmental Modeling & Assessment*, 26, pp. 143-154.

Semlali, I., Ouadif, L. and Bahi, L. (2019). Landslide susceptibility mapping using the analytical hierarchy process and GIS. *Current Science*, 116(5), pp. 773-779.

Sharma, T. and Singh, O. (2017). Soil erosion susceptibility assessment through geo-statistical multivariate approach in Panchkula district of Haryana, India. *Modeling Earth Systems and Environment*, 3, pp. 733-753.

Sinshaw, B. G., Belete, A. M., Tefera, A. K., Dessie, A. B., Bizuneh, B. B., Alem, H. T., Atanaw, S.B., Eshete, D.G., Wubetu, T.G., Atinkut, H.B. and Moges, M. A. (2021). Prioritization of potential soil erosion susceptibility region using fuzzy logic and analytical hierarchy process, upper Blue Nile Basin, Ethiopia. *Water-Energy Nexus*, 4, pp. 10-24.

Strahler, A. N. (1952). Hypsometric (area-altitude) analysis of erosional topography. *Geological society of America bulletin*, 63(11), pp. 1117-1142.

Strahler, A.N. (1957). Quantitative analysis of watershed geomorphology, *Transactions of the American Geophysical Union*, Vol. 38, No. 6, pp. 913–920.

Strahler, A. N. (1964). *Quantitative geomorphology of drainage basin and channel networks*. In: VT Chow (ed.), Handbook of applied hydrology. McGraw Hill, New York, pp. 4.39 – 4.76.

Sudhishri, S., Kumar, A., Singh, J. K., Dass, A. and Nain, A. S. (2014). Erosion tolerance index under different land use units for sustainable resource conservation in a Himalayan watershed using remote sensing and geographic information system (GIS). *African Journal of Agricultural Research*, 9(41), pp. 3098-3110.

Sujatha, E. R. and Sridhar, V. (2018). Spatial Prediction of Erosion Risk of a small mountainous watershed using RUSLE: A case-study of the Palar sub-watershed in Kodaikanal, South India. *Water*, 10(11), 1608.

Swarnkar, S., Malini, A., Tripathi, S. and Sinha, R. (2018). Assessment of uncertainties in soil erosion and sediment yield estimates at ungauged

basins: an application to the Garra River basin, India. *Hydrology and Earth System Sciences*, 22(4), pp. 2471-2485.

Thakkar, A. K. and Dhiman, S. D. (2007). Morphometric analysis and prioritization of miniwatersheds in Mohr watershed, Gujarat using remote sensing and GIS techniques. *Journal of the Indian society of Remote Sensing*, 35, pp. 313-321.

Thapa, G. B. and Weber, K. E. (1991). Soil erosion in developing countries: a politicoeconomic explanation. *Environmental Management*, 15(4), pp. 461-473.

Thomas, J., Joseph, S. and Thrivikramji, K. P. (2017). Assessment of soil erosion in a tropical mountain river basin of the southern Western Ghats, India using RUSLE and GIS. *Geoscience Frontiers*, 9(3), pp. 893-906.

Thomas, J., Joseph, S. and Thrivikramji, K. P. (2018). Assessment of soil erosion in a monsoon-dominated mountain river basin in India using RUSLE-SDR and AHP. *Hydrological sciences journal*, 63(4), pp. 542-560.

Tideman, E.M. (1996). *Watershed Management: Guidelines for Indian conditions*. Omega Scientific Publishers, New Delhi.

Tiwari, H., Rai, S. P., Kumar, D. and Sharma, N. (2015). Rainfall erosivity factor for India using modified Fourier index. *Journal of Applied Water Engineering and Research*, 4(2): pp. 83-91.

Tiwari, R.P. and L.K. Jha (1997). *Morphometric Analysis of the Watersheds of Mizoram for Estimation of Run-off and Soil Loss*, in L.K. Jha (Ed.), Natural Resource Management in Mizoram, Ashish Publishing House, New Delhi.

Toy, T.J., Foster, G.R. and Renard, K.G. (2002). *Soil Erosion: Processes, Prediction, Measurement and Control*, John Wiley & Sons Inc., New York.

Tripathi, R.P. and Singh, H.P. (1993). *Soil Erosion and Conservation*, New Age International Publishers, p. 242.

Uddin, K., Murthy, M. S. R., Wahid, S. M. and Matin, M. A. (2016). Estimation of soil erosion dynamics in the Koshi basin using GIS and remote sensing to assess priority areas for conservation. *PloS one*, 11(3), e0150494.

USDA. (1972). *Sediment sources, yields, and delivery ratios*, National Engineering Handbook, Section 3 Sedimentation, pp. 3-4.

USDA. (2017). *Soil Survey Manual: by Soil Science Division Staff*. Revised and enlarged, U.S. Department of Agriculture Handbook No. 18. https://www.nrcs.usda.gov/resources/guides-and-instructions/soil-survey-manual

Vaidya, O. S. and Kumar, S. (2006). Analytic hierarchy process: An overview of applications, *European Journal of operational research*, 169(1), pp. 1-29.

Vanoni, V.A. (1975). *Sedimentation engineering. Manuals and reports on engineering practice*—No. 54. American Society of Civil Engineers, New York.

Vijith, H. and Dodge-Wan, D. (2019). Modelling terrain erosion susceptibility of logged and regenerated forested region in northern Borneo through the Analytical Hierarchy Process (AHP) and GIS techniques. *Geoenvironmental Disasters*, 6(1), pp. 1-18.

Vijith, H., Suma, M., Rekha, V. B., Shiju, C. and Rejith, P. G. (2012). An assessment of soil erosion probability and erosion rate in a tropical mountainous watershed using remote sensing and GIS. *Arabian Journal of Geosciences*, 5, pp. 797-805.

Vojtek, M. and Vojteková, J. (2019). Flood susceptibility mapping on a national scale in Slovakia using the analytical hierarchy process. *Water*, 11(2). 364.

Walling, D. E. (1983). The sediment delivery problem. *Journal of hydrology*, 65(1-3), pp. 209-237.

Wischmeier, W.H. and Smith, D.D. (1978). *Predicting Rainfall Erosion Losses: A Guide to Conservation Planning*. U.S. Department of Agriculture, Agriculture Handbook No. 537.

Wischmeier, W.H., Johnson, C.B. and B.V. Cross. (1971). A soil erodibility nomograph for farmland and construction sites. *Journal of Soil and Water Conservation* .26, pp. 189-193.

Xiaoqing, Y. (2003). *Manual on sediment management and measurement*, World Meteorological Organization, Operational Hydrology Report No. 47, Secretariat of the World Meteorological Organization, Geneva.

Yue-Qing, X., Xiao-Mei, S., Xiang-Bin, K., Jian, P. and Yun-Long, C. (2008). Adapting the RUSLE and GIS to model soil erosion risk in a mountains karst watershed, Guizhou Province, China. *Environmental monitoring and assessment*, 141, pp. 275-286.

Zonunsanga, R. and Rao, Ch.U.B. (2013). Shifting cultivation and land degradation in Teirei watershed, Mizoram. *Geographic*, 8, pp. 64 – 73.

BIO-DATA OF THE CANDIDATE

Name : PC. Lalrindika

Father's name : PC. Vanlalhruaia

Mother's name : Vanlalruali

Gender : Male

Date of Birth : 27th January 1987

Marital Status : Married

Religion : Christian

Address : C-83, Ramthar Veng, Aizawl-796007

Mobile : 9089527354 / 9612328280

Email : rinteapachuau21jan@gmail.com

Academic Profile:

Class	Board of Examination	Year of passing
X	M.B.S.E	2004
XII	M.B.S.E	2006
B.A	Mizoram University	2009
M.Sc	Mizoram University	2012
NET	UGC	2016 & 2018
SLET	SLET Commission (NE Region)	2017
NET-JRF	UGC	2018
PGC Geoinformatics	IGNOU	2022

PRESENTATIONS AND PUBLICATIONS OF RESEARCH PAPER

A. Presentation of Research Papers

1. "Assessment of Soil Fertility Status in parts of Tuirial Watershed, Mizoram," in International Seminar on Recent Advances in Science and Technology (ISRAST), organized by North East (India) Academy of Science and Technology (NEAST), Mizoram University, Aizawl, India, 16th to 18th November, 2020.

2. "A Comparative Analysis of Soil Physical Properties under Different Land Use Systems in Aizawl District, Mizoram," in the XVth DGSI International Geography Online Conference, organized by The Deccan Geographical Society, India, 26th to 28th November, 2020.

3. "Evaluating the Spatio-Temporal Characteristics of Rainfall Erosivity in Aizawl District, Mizoram," in National Seminar on Climate and Development Interface, organized by the Department of Geography, Government Aizawl North College and State Institute of Rural Development & Panchayati Raj, Govt of Mizoram in collaboration with Geography Association of Mizoram (GAM), 24th to 25th March, 2022.

4. "Integrated Analytical Hierarchy Process (AHP) and GIS Technique based Soil Erosion Susceptibility Mapping in Chite Watershed, Mizoram, India," in the International Seminar on Recent Advancement in Geographical Studies: A Multi-dimensional Outlook, organized by Department of Geography, Rampurhat College, and IQAC, Rampurhat College, Birbhum district, West Bengal, India, 1st and 2nd September, 2022.

5. "A geoinformatics and RUSLE model-based soil erosion assessment in a tropical mountainous area of Chite watershed, Mizoram, India," in the three days International Conference on Environmental Hazards in Mountainous Regions: Problems and Prospects, organized by School of Earth Science and Natural Resource Management, Pachhunga University College, Mizoram, India, during 21st to 23rd February, 2024.

B. Publication of Research Papers

Journal Publication

1. Water Quality Assessment of Chite River using Overall Index of Pollution (OIP) in Aizawl, Mizoram, *Geographic*, July 2020, Vol. 15, pp. 56-62, ISSN 0975-4121.

2. Evaluating the spatiotemporal dynamics of Rainfall Erosivity in Aizawl District, Mizoram, *Geographic*, July 2022, Vol. 17, pp. 18-31, ISSN 0975-4121.

3. Vulnerability level of forest degradation in Mizoram: A spatio-temporal density analysis, *Disaster Advances*, October 2022, Vol. 15 (10), pp. 28-34, ISSN 0974-262X.

4. A Comparative Analysis of Soil Physical Properties under different Land use Systems in Aizawl District, Mizoram, *Geographic*, July 2023, Vol. 18, pp. 32-36, ISSN 0975-4121.

5. Assessment of soil fertility status in parts of tuirial watershed, Mizoram, *Journal of Emerging Technologies and Innovative Research*, November 2023, pp. c149-c153, ISSN: 2349-5162.

6. Integrated Analytical Hierarchy Process (AHP) and GIS technique based Soil Erosion Susceptibility Mapping in Chite Watershed, Mizoram, India, *Disaster Advances*, March 2024, Vol. 17 (3), pp. 25-34, ISSN 0974-262X.

7. A geoinformatics and RUSLE model-based soil erosion assessment in tropical mountainous area of Chite watershed, Mizoram, India, *Journal of Degraded and Mining Lands Management*, April 2024, Vol. 11 (3), pp. 5875-5884, ISSN: 2339-076X.

Chapter in Edited Book

1. Assessment of water quality supplied by water vendors in Aizawl city, Mizoram, in Contemporary Issues, Problems and Challenges in India, Research and Publication Cell, Govt Hnahthial College, India, ISBN: 978-81-953777-1-8.

PARTICULARS OF THE CANDIDATE

NAME OF THE CANDIDATE : PC. LALRINDIKA

DEGREE : DOCTOR OF PHILOSOPHY

DEPARTMENT : GEOGRAPHY AND RESOURCE MANAGEMENT

TITLE OF THESIS : ASSESSMENT OF EROSION AND SEDIMENTATION IN CHITE WATERSHED, MIZORAM

DATE OF ADMISSION : 27TH AUGUST 2018

APPROVAL OF RESEARCH PROPOSAL:

1. DRC : 18th MARCH 2019
2. BOS : 3rd APRIL 2019
3. SCHOOL BOARD : 26th APRIL 2019

MZU REGISTRATION NO. : 1074 OF 2006-2007

Ph.D. REGISTRATION NO. & DATE : MZU/Ph.D./1204 of 27.08.2018

EXTENSION : NIL

(PROF. CH. UDAYA BHASKARA RAO)

Head

Department of Geography and Resource Management

ABSTRACT

ASSESSMENT OF EROSION AND SEDIMENTATION IN CHITE WATERSHED, MIZORAM

AN ABSTRACT SUBMITTED IN PARTIAL FULFILLMENT OF THE REQUIREMENTS FOR THE DEGREE OF DOCTOR OF PHILOSOPHY

PC. LALRINDIKA

MZU REGISTRATION NO: 1074 OF 2006-07

PH.D. REGISTRATION NO: MZU/Ph.D./1204 of 27.08.2018

DEPARTMENT OF GEOGRAPHY AND RESOURCE MANAGEMENT

SCHOOL OF EARTH SCIENCE AND NATURAL RESOURCE MANAGEMENT

APRIL, 2024

ABSTRACT

ASSESSMENT OF EROSION AND SEDIMENTATION IN CHITE WATERSHED, MIZORAM

AN ABSTRACT SUBMITTED IN PARTIAL FULFILLMENT OF THE REQUIREMENTS FOR THE DEGREE OF DOCTOR OF PHILOSOPHY

PC. LALRINDIKA

MZU REGISTRATION NO: 1074 OF 2006-07

PH.D. REGISTRATION NO: MZU/Ph.D./1204 of 27.08.2018

DEPARTMENT OF GEOGRAPHY AND RESOURCE MANAGEMENT

SCHOOL OF EARTH SCIENCE AND NATURAL RESOURCE MANAGEMENT

APRIL, 2024

ASSESSMENT OF EROSION AND SEDIMENTATION IN CHITE WATERSHED, MIZORAM

BY

PC. LALRINDIKA

DEPARTMENT OF GEOGRAPHY AND RESOURCE MANAGEMENT

SUPERVISOR

PROF. P. RINAWMA

JOINT SUPERVISOR

DR. R. ZONUNSANGA

SUBMITTED

IN PARTIAL FULFILLMENT OF THE REQUIREMENT OF THE DEGREE OF DOCTOR OF PHILOSOPHY IN GEOGRAPHY OF MIZORAM UNIVERSITY, AIZAWL.

ABSTRACT

Soil erosion and sedimentation are recently recognized as one of the most significant challenges among various global environmental issues. The gravity of soil erosion arises from both on-site and off-site consequences, affecting the economy and the environment. On-site effects are evident in land degradation due to topsoil removal and loss of essential soil nutrients. On the other hand, sedimentation is the main off-site consequences of soil erosion downstream, which causes water pollution, increased flood risks, reduced reservoir lifespan, disruption of riverine ecosystems, etc. The geographical location of India encompassing humid subtropical and tropical areas and its agriculture based economy makes water-induced soil erosion a significant threat. Moreover, mountainous areas in these humid climate experiences severe soil loss. Mizoram, a rugged mountainous region of northeast India faces critical soil erosion issues, primarily due to its vulnerable environmental characteristics coupled with unsustainable human activities. Soil erosion and sedimentation pose significant challenges in the state, impacting sustainable land management, water resource planning, and environmental security. Despite the apparent repercussions, research studies on these issues has been insufficient. Therefore, a timely and precise assessment is crucial to understand their extent and magnitude, enabling effective erosion control and sustainable resource management. However, conventional methods, such as field surveys and measurements, are costly, labour intensive, time-consuming, and spatially limited. In addition to this, data for runoff and sediment flux are not available as river basins in the state have no river gauging station. Given these limitations, this research aims to comprehensively analyse soil erosion and sedimentation in Chite watershed under the following objectives: -

(i) To identify the spatial pattern of soil erosion susceptibility.
(ii) To evaluate soil erosion rate and soil loss.
(iii) To determine the area above the soil loss tolerance limits.
(iv) To estimate the amount of sediment yield.
(v) To prioritized critical areas of sustainable watershed management.

In the present research, several models were developed through Remote sensing and Geographic Information Systems (GIS) technology to produce beneficial insights into the process of soil erosion and sedimentation in Chite watershed. The study area's erosion susceptibility was evaluated using the Analytical Hierarchy Process (AHP) considering ten erosion conditioning factors which were selected through a literature review. Collinearity among these factors was assessed using Variance Inflation Factor (VIF) and Tolerance (T). Erosion susceptibility mapping was then prepared by applying AHP-derived weights to the conditioning factors. Finally, the model's accuracy was validated using Receiver Operating Characteristics (ROC) curves and the area under the ROC curve (AUC). Subsequently, the Revised Universal Soil Loss Equation (RUSLE) model was applied to estimate erosion rates or soil loss potential within the watershed. Additionally, the calculated soil erosion rate was compared with pre-determined Soil Loss Tolerance Limits (T) to identify the possible risk of soil erosion in the watershed. To evaluate sediment yield at the basin outlet, the RUSLE-Sediment Delivery Ratio (RUSLE-SDR) method was employed. This model combines the results obtained from the RUSLE model with the determined sediment delivery ratio (SDR). At the final phase of the research, a comprehensive watershed prioritization scheme was developed using Compound Value (C_V) method, integrating the findings from erosion susceptibility mapping, soil loss estimation, delineated areas exceeding soil loss tolerance limit and sediment yield assessment at sub-watersheds level.

The assessment of erosion susceptibility in Chite watershed reveals that the very high and high susceptibility zone covers an area of about 4.08 and 9.50 km^2, which accounts for 7.83% and 18.21% of the study area respectively. Hence, about one-fourth, i.e., 26.04% of the total geographical area, extending over 13.56 km^2 have higher chances of soil erosion occurrences and are mainly confined to the northern parts as well as along the eastern and western corners of the study area. The results have also unveiled that slope has highest influence on soil erosion, followed by rainfall intensity, normalized difference vegetation index (NDVI) and elevation. Generally, these zones have higher elevation, higher lineament density, higher rainfall intensity, steeper slopes, lesser vegetation, lesser distance to steams and are mostly found in areas where natural landscapes are altered by anthropogenic activities like built-up land, cropland and bare

land. Validation of the predicted model against erosion inventory have shown a remarkable outcome with 81% and 92% accuracy rate for field observed erosion and non-erosion points respectively. Hence, erosion susceptibility assessment based on the AHP method is considered to be a highly dependable approach in the watershed.

Soil loss estimation in Chite watershed produced an average annual soil erosion rate of 6.10 tons ha^{-1} $year^{-1}$, which ranges from a minimum rate of 0 to a maximum rate of 4,928.90 tons ha^{-1} $year^{-1}$. The evaluated amount of the total soil loss within the watershed is approximately 3,57,580.90 tons $year^{-1}$. Those regions experiencing severe (20 – 40 tons ha^{-1} $year^{-1}$) and very severe (above 40 tons ha^{-1} $year^{-1}$) soil loss occupies approximately 1.66 and 1.36 km^2 which accounts to only 3.18 and 2.16 % of the total geographical area respectively. Besides the limited areal extent of these two relatively severe soil erosion classes, they have contributed to about 250,768.31 tons of soil loss every year which is 70.13% of the total soil loss from the watershed. This clearly indicates that most of the soil detachment occurs at a relatively small areas within the study area. These areas are extensively found in the croplands and the relatively higher potential of soil loss can be attributed to the dominant practice of shifting cultivation in the study area. Apart from the croplands, the bare land representing earth spoil dumping sites, constructional sites, and unsurfaced agriculture link roads are also the prominent sources of unconsolidated sediments. Moreover, higher rate of erosion are also confined to the areas along the drainage channels, which may be ascribed to the high erosive power of streams as a result of steep and narrow channels and high runoff produced from impervious built-up areas.

Soil loss tolerance limit (T) obtained from the predetermined value for Chite watershed is 7.5 tons ha^{-1} $year^{-1}$. Based on this threshold value, it was found that about 44.23 km^2, i.e., 84% of the study area has a tolerable soil loss, but the remaining 7.93 km^2 (15.20%) has exceeded the maximum limit of acceptable soil erosion rate. These critically sensitive zone are mostly concentrated in the central parts of the study area where the land use is confined to agriculture. However, they are also unevenly distributed throughout the study area in a varying rate and extent. Their limited distribution in some parts of the northern and southern corners is associated with the major land use confined to settlement and forested land respectively. Since, the soil

loss tolerance limit are exclusively recommended based on agricultural land use, the results has clearly reflected the absence of significant soil conservation measures and management system in the study area.

The calculated sediment delivery ratio (SDR) of the study area is 0.288, which produced an estimated sediment yield (SY) of about 102983.29 tons $year^{-1}$. The total sediment yield or sedimentation rate accounts to 28.80% of the gross soil erosion generated within the watershed. This indicates that about 71.20% of the soil detached from different parts of the watershed were deposited elsewhere within the watershed rather than transported to the basin outlet. High amount of sediment yield from Chite watershed can be linked with the small size and high gradient of the watershed, as more sediments are generally transported from smaller sized watershed with a relatively shorter and steeper slopes. The seasonal pattern of sediment yield shows a substantial resemblance of the annual sediment yield in the watershed. Sediment yield during monsoon season was significantly higher when compared to the other seasons as the region receives abundant rainfall during this season. Sediment yield of this season is about 76135.18 tons $year^{-1}$, which contributed to 55.21% of the annual sediment yield in the study area. On the other hand, the dry months of winter season has recorded the lowest sediment yield of about 10927.75 tons $year^{-1}$, which accounts to only 7.92% of the total annual sediment yield.

The watershed prioritization was conducted based on the aforementioned assessment evaluated in each geographical segments, i.e., the eight sub-watersheds simultaneously. The calculated compound value (C_V) of all the assessment in each geographical unit was used as an index to categorize the sub-watersheds into three priority class as: Low (> 5.67 CV), Medium (3.50 – 5.50 CV) and High (< 3.5 CV) respectively. The low priority class includes SW-7 and SW-8 covering about 25.35% of the study area is considered as a relatively secure and well protected area. These area shows a relatively lower level of natural resource depletion. Only a few anthropogenic activities are observed in these areas and as a result, they have good natural vegetation cover, comprising both open and dense forests. The medium priority class extending to approximately 31.78% of the watershed's area includes SW-2, SW-5 and SW-6. These geographical segments have experienced certain forms of human interventions like

peripheral settlement sites, sporadic agricultural land, unsurfaced agricultural link roads and deforested areas overgrown with grasses, bamboos and scattered bushes. The high priority classes including SW-1, SW-3 and SW-4, are the most critical areas, occupying about 42.89% of the study area. Rapid urbanization is observed in SW-1 and some parts of SW-3 and are located in the upper catchment where there are found numerous unsustainable development activities and extensive deforestation. Just beyond the urban land use, in most parts of SW-3 and SW-4, there is a profound modification of natural landscape in terms of agricultural practice, which mainly comprise of the traditional shifting cultivation from just adjacent to the settlement areas and extending to few kilometres away. The critical sub-watersheds comprising both the medium and high priority class are then proposed for implementing immediate action in terms of erosion control and resource conservation measures.

The findings of this research have a couple of implications relating to erosion control, sustainable natural resource management and environmental conservation. The integration of multiple methodologies in watershed prioritization enhanced a comprehensive understanding of the study area. Subsequently, these prioritized critical areas of soil erosion and sedimentation processes will facilitate the foundation for executing site-specific resource allocation and implementation of conservation measures within the watershed. Furthermore, the incorporation of remote sensing and Geographic Information System (GIS) technologies in this research has provided a robust methodology for erosion and sedimentation assessment, enabling a rapid and precise visual representation of the watershed's status. The research findings may provide a valuable resource to stakeholders, policymakers and researchers involved in soil erosion and sedimentation control, as well as sustainable resource management planning. Ultimately, this research is expected to have a significant contribution to the sphere of knowledge pertaining to sustainable watershed management, encourage further research endeavours as well as conservation initiatives in the future.